伏羲天水

Musa Sapientum Extract (MSE)
Banana Plant Extract (BPE)
Super Green (SG)

相關專利/文獻資訊彙編

第二版 2025

本文所刊載之下列文字為同義字詞
(Synonyms)

Musa Sapientum Extract (MSE)

Banana Plant Extract (BPE)

Super Green (SG)

伏義天水

天綠元素

舒培葛林

修培刻灵®

蕉仙素

目錄

一、專利技術

（一）專利　I584814-芭蕉科植物的萃取方法及其萃取物及其用途

中華民國專利證書

發明第　I584814　號

發明名稱：芭蕉科植物的萃取方法及其萃取物及其用途

專利權人：劉人豪

發明人：劉人豪、鄭詠德、陳哲賢

專利權期間：自2017年6月1日至2036年3月22日止

上開發明業經專利權人依專利法之規定取得專利權

經濟部智慧財產局 局長　洪淑敏

中華民國106年6月1日

【19】中華民國　　【12】專利公報　（B）

【11】證書號數：I863489

【45】公告日：中華民國 113 (2024) 年 11 月 21 日

【51】Int. Cl.：　*A61K36/88　(2006.01)*　　*A61P35/00　(2006.01)*

發明　　全 5 頁

【54】名　　稱：香蕉萃取物在提高癌細胞對抗癌藥物的敏感性上的用途

【21】申請案號：112129719　　【22】申請日：中華民國 112 (2023) 年 08 月 08 日

【72】發 明 人：賴基銘 (TW) LAI, GI-MING；姚智榮 (TW) YAO, CHIH-JUNG；廖建皇 (TW) LIAO, CHIEN-HUANG

【71】申 請 人：臺北醫學大學　TAIPEI MEDICAL UNIVERSITY
臺北市信義區吳興街 250 號

【74】代 理 人：高玉駿；楊祺雄

【56】參考文獻：

TW　I584814B

期刊 Budi HS, et al. "Palmitic acid of Musa Paradisiaca induces apoptosis through caspase-3 in human oral squamous cell carcinoma" Eur Rev Med Pharmacol Sci. 26(19): 2022 Oct; 7099-7114

審查人員：楊婷雅

【57】申請專利範圍

1. 一種香蕉萃取物供應用於製備一用來提高癌細胞對抗癌藥物的敏感性之醫藥品的用途，其中該香蕉萃取物是藉由一包含下列步驟的方法而被製得：
   備備一原料，該原料包含香蕉(　*Musa paradisiaca*)的樹莖、樹葉、樹皮或其組合，並將該原料進行破碎成為待萃物；
   將該待萃物浸泡於體積百分比為 5%至 40%的鹽水，並進行加熱，其中該待萃物與鹽水的體積比為 95：5 至 60：40；
   將浸泡後待萃物以低溫破壁法萃取獲得一粗萃取物，該粗萃取物包含纖維與液體；
   將粗萃取物進行離心，使粗萃取物中的纖維與液體分離，將液體部分進行過濾後於桶中靜置，成為粗萃取液；以及
   將粗萃取液以遠紅外線石進行發酵，得到香蕉萃取物。
2. 如請求項 1 的用途，其中該癌細胞是具抗藥性的癌細胞。
3. 如請求項 1 的用途，其中該癌細胞是選自於由下列所構成的群組：膀胱癌細胞、肺腺癌細胞、以及它們的組合。
4. 一種組合供應用於製備一用來治療具抗藥性的癌症之醫藥品的用途，該組合包含有一抗癌藥物或者它的一藥學上可接受的鹽類，以及一香蕉萃取物，其中該香蕉萃取物是藉由一包含下列步驟的方法而被製得：
   備備一原料，該原料包含香蕉的樹莖、樹葉、樹皮或其組合，並將該原料進行破碎成為待萃物；
   將該待萃物浸泡於體積百分比為 5%至 40%的鹽水，並進行加熱，其中該待萃物與鹽水的體積比為 95：5 至 60：40；
   將浸泡後待萃物以低溫破壁法萃取獲得一粗萃取物，該粗萃取物包含纖維與液體；
   將粗萃取物進行離心，使粗萃取物中的纖維與液體分離，將液體部分進行過濾後於桶中靜置，成為粗萃取液；以及

將粗萃取液以遠紅外線石進行發酵，得到香蕉萃取物。

5. 如請求項4的用途，其中該癌症是選自於由下列所構成的群組：胰臟癌、肺腺癌、以及它們的組合。
6. 如請求項4的用途，其中該香蕉萃取物與該抗癌藥物是呈單一的劑型或分開的劑型。
7. 如請求項4的用途，其中該香蕉萃取物是呈一供非經腸道投藥、口服投藥或局部投藥的劑型。
8. 如請求項4的用途，其中該抗癌藥物是呈一供非經腸道投藥、口服投藥或局部投藥的劑型。
9. 如請求項1或4的用途，其中該抗癌藥物是選自於由下列所構成的群組：Gefitinib、Gemcitabine、Oxaliplatin、5-FU 、以及它們的組合。
10. 如請求項1或4的用途，其中備一原料之步驟中，該樹莖、樹葉與樹皮的重量比為5：3：2至6：2：2。
11. 如請求項1或4的用途，其中將該待萃物浸泡於體積百分比為5%至40%的鹽水並進行加熱之步驟中，該待萃物與鹽水的體積比為70：30。
12. 如請求項1或4的用途，其中將粗萃取物進行離心之步驟中，該粗萃取物以3000轉(RCF)離心1分鐘。
13. 如請求項1或4的用途，其中該粗萃取物經離心且液體部分經過濾後的液體於桶中靜置之步驟中，粗萃取液係桶中80%至90%的上層液體。
14. 如請求項1或4的用途，其中該香蕉萃取物為液體，顏色為深金棕色，比重為1.12±10%、黏度為1.914±10%厘斯、沸點為104±10%℃以及水溶性100%；萃取物其化學性質中，酸鹼值為13、鈉含量55,000±10%(mg/kg)、鉀含量1192±10%(mg/kg)、鈣含量33±10%(mg/kg)、鎂含量26±10%(mg/kg)、鋅含量9±10%(mg/kg)以及鐵含量9±10%(mg/kg)。

圖式簡單說明

本發明的上述以及其它目的，特徵與優點，在參照以下的詳細說明與較佳實施例和隨文檢附的圖式後，將變得明顯，其中：

圖1顯示香蕉萃取物對於各組PANC-1細胞生存率之影響；

圖2顯示香蕉萃取物對於被處理Gemcitabine之各組PANC-1/Gem細胞生存率之影響，其中"**"與"***"分別表示當與抗癌藥物組作比較，$p < 0.01$與$p < 0.001$，以及"##"與"###"分別表示當與對應的萃取物組作比較，$p < 0.01$與$p < 0.001$；

圖3顯示香蕉萃取物對於被處理Oxaliplatin之各組PANC-1/Gem細胞生存率之影響，其中"**"表示當與抗癌藥物組作比較，$p < 0.01$，以及"#"與"###"分別表示當與對應的萃取物組作比較，$p < 0.05$與$p < 0.001$；

圖4顯示香蕉萃取物對於被處理5-FU之各組PANC-1/Gem細胞生存率之影響，其中"*"與"**"分別表示當與抗癌藥物組作比較，$p < 0.05$與$p < 0.01$，以及"###"表示當與對應的萃取物組作比較，$p < 0.001$；

圖5顯示香蕉萃取物對於各組HCC827細胞生存率之影響；以及

圖6顯示香蕉萃取物對於被處理Gefitinib之各組HCC827GR細胞生存率之影響，其中"*"與"**"分別表示當與抗癌藥物組作比較，$p < 0.05$與$p < 0.01$，以及"#"、"##"與"###"分別表示當與對應的萃取物組作比較，$p < 0.05$、$p < 0.01$與$p < 0.01$。

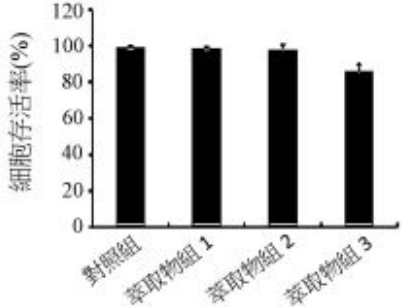
細胞存活率(%)
120
100
80
60
40
20
0
對照組
萃取物組 1
萃取物組 2
萃取物組 3

圖 1

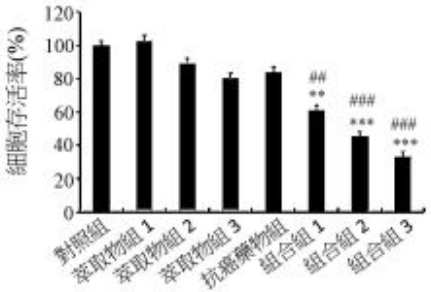
細胞存活率(%)
120
100
80
60
40
20
0
##
**
###
***
###
***
對照組
萃取物組 1
萃取物組 2
萃取物組 3
抗癌藥物組
組合組 1
組合組 2
組合組 3

圖 2

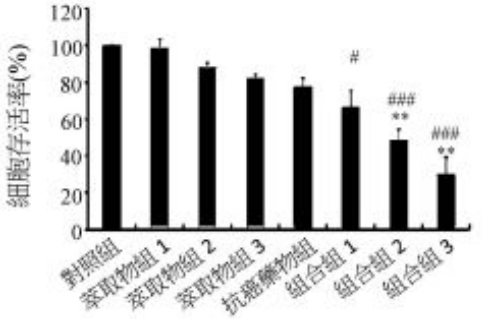
細胞存活率(%)
120
100
80
60
40
20
0
#
###
**
###
**
對照組
萃取物組 1
萃取物組 2
萃取物組 3
抗癌藥物組
組合組 1
組合組 2
組合組 3

圖 3

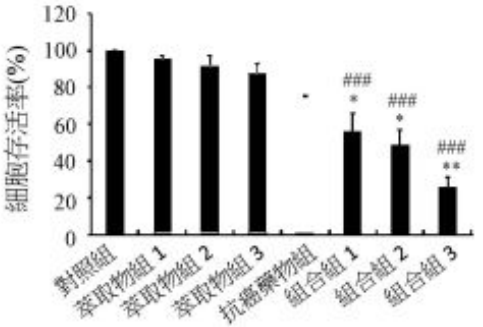
細胞存活率(%)
120
100
80
60
40
20
0
###
*
###
*
###
**
對照組
萃取物組 1
萃取物組 2
萃取物組 3
抗癌藥物組
組合組 1
組合組 2
組合組 3

圖 4

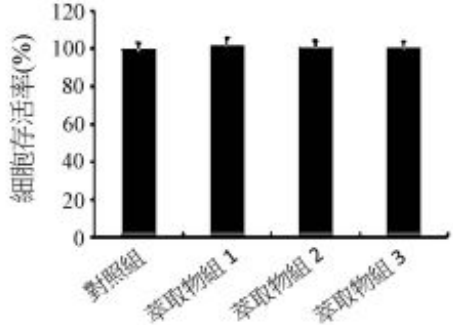
細胞存活率(%)
120
100
80
60
40
20
0
對照組
萃取物組 1
萃取物組 2
萃取物組 3

圖 5

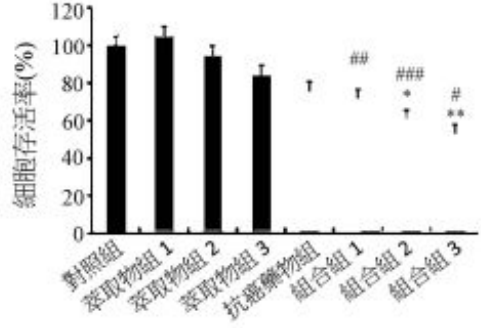
細胞存活率(%)
120
100
80
60
40
20
0
##
###
*
**
#
對照組
萃取物組 1
萃取物組 2
萃取物組 3
抗癌藥物組
組合組 1
組合組 2
組合組 3

圖 6

二、學術論文

（一）糖尿病-香蕉提取物對糖尿病大鼠傷口癒合的促進作用

Experimental research

Wound healing is promoted by *Musa paradisiaca* (banana) extract in diabetic rats

Yung-Ze Cheng[1], I-Min Liu[2], Jiaw-Tang Cheng[3], Bor-Shyh Lin[4], Frank Liu[4]

[1]Department of Medical Research, Chi-Mei Medical Center, Yongkang, Tainan, Taiwan
[2]Department of Pharmacy & Graduate Institute of Pharmaceutical Technology, Tajen University, Yanpu, Pingtung, Taiwan
[3]Institute of Imaging and Biomedical Photonics, National Chiao Tung University, Guiren, Tainan, Taiwan
[4]Department of Research and Development, Natural Well Technical Company Guishan, Taoyuan, Taiwan

Corresponding author:
Prof. Jiaw-Tang Cheng, PhD
Department of Medical Research
Chi-Mei Medical Center
Yongkang
Tainan, Taiwan
E-mail: jtcheng150@gmail.com

Submitted: 8 July 2019
Accepted: 26 November 2019

Arch Med Sci
DOI: https://doi.org/10.5114/aoms.2020.103344
Copyright © 2020 Termedia & Banach

Abstract

Introduction: Impairments in wound healing commonly occur among patients with diabetes. Herbal medicines have a long history of usage in wound care management. Super green (SG) is a newly discovered natural product obtained from *Musa paradisiaca*. This study aimed to investigate the efficacy of the topical application of SG in healing surgical wounds in diabetic rats.

Material and methods: Wistar rats received a one-time intraperitoneal injection of streptozotocin to induce type 1 diabetes. Full-thickness excisional skin wounds were created on the backs of the rats. The relevant groups were topically treated with the indicated concentrations of SG or vehicle dressing throughout the study duration. Histological analysis was performed and the mRNA levels of proinflammatory cytokines were measured to evaluate the improvement of wound closure.

Results: The wound area ratio of the SG (1/6000 dilution)-treated group was greatly reduced compared to that of the vehicle-treated group. The histological analysis showed fewer inflammatory cells, accelerated re-epithelialization, and increased collagen deposition in SG (1/6000)-treated wounds. The gene expression levels of tumor necrosis factor-α, interleukin-1β, and interleukin-6 were decreased and the levels of type I and type III collagen were increased after SG treatment.

Conclusions: These results show that the most therapeutically efficacious concentration of SG (1/6000 dilution) can enhance wound repair in diabetic rats. SG has the potential to be a new treatment strategy for diabetic wounds.

Key words: wound healing, diabetes, *Musa paradisiaca* extract, inflammatory cytokines.

Introduction

Diabetes mellitus (DM) is a metabolic disorder characterized by chronic hyperglycemia that currently affects over 422 million people worldwide [1]. Diabetes is often accompanied by a range of disorders, including obesity [2], atherosclerosis [3], peripheral arterial disease [4], and obstructive sleep apnea [5]. Impaired wound healing is a common complication in patients with diabetes that severely affects life quality

Wound healing analysis

Rat wounds were photographed under isoflurane anesthesia on day 0, day 3, day 7, day 10 and day 15 after induction. A standard ruler was placed on the side of the wounds. The wound areas were measured using ImageJ Software, and the area observed on day 0 was considered 100%.

Histopathological examination

At the end of the experiment, rats were anesthetized with 2% isoflurane, and the wound area was sampled for histological examination. Skin tissue samples were formalin-fixed and embedded in paraffin. The section thickness of skin tissue was 5 µm. After hematoxylin and eosin (HE) staining, wound healing was evaluated in terms of the extent of dermal inflammation, angiogenesis, presence of granulation tissue, and re-epithelialization [21]. The parameters used to assess healing were as follows: for dermal inflammation, "-" – no dermal inflammation, "+" – mild dermal inflammation, "++" – moderate dermal inflammation; and "+++" – marked dermal inflammation; for angiogenesis, "-" – no angiogenesis, "+" – mild angiogenesis (< 5 vessels per high-power field), "++" – moderate angiogenesis (5–10 vessels per high-power field), and "+++" – marked angiogenesis (> 10 vessels per high-power field); for granulation tissue thickness, "-"– none, "+" – scant, "++" – moderate, and "+++" – marked; for re-epithelialization, "-" – no re-epithelialization, "+" – < 50% of the wound, "++" – > 50% of the wound, and "+++" – complete re-epithelialization [22, 23].

Collagen deposition in diabetic wounds was assessed by Masson's trichrome staining [24]. Collagen fibers were stained blue, and muscle and connective tissues were stained red. HE staining or Masson's staining was performed according to the manufacturer's protocol. Samples were observed using optical microscopy. The collagen deposition volume and other parameters were quantified using ImageJ. Five different fields of vision were randomly selected.

Real-time quantitative PCR detection

The expression of collagen I, collagen III, IL-1β, IL-6 and TNF-α in wound tissues in STZ-treated rats was measured using RT-PCR. Total RNA was extracted from tissue samples using the TRIzol method (Thermo Fisher Scientific, Waltham, MA, USA) and processed according to the manufacturer's instructions. Five micrograms of RNA were reverse transcribed to cDNA using the Transcriptor First Strand cDNA Synthesis Kit (Roche, Basel, Switzerland). Amplification and detection were performed with a LightCycler 480 system (Roche). Gene expression was quantified using the relative standard curve method. β-Actin was used to normalize the RT-PCR results. The primer sequences used were as follows:
collagen I(α1) F: 5′-CTGGCAAGAACGGAGATGAT-3′;
collagen I(α1) R: 5′-AATCCACGAGCACCCTGA-3′;
collagen III(α1) F: 5′-CAGGAAACCTAGGAGAAAGG-3′;
collagen III(α1) R: 5′-CCAGCTACTCCTAAGGTCCTG-3′;
TNF-α F: 5′-CAGCCTCTTCTCCTTCCTGAT-3′;
TNF-α R: 5′-GCCAGAGGGCTGATTAGAGA-3′;
IL-6 F: 5′-GATGAGTACAAAAGTCCTGATCCA-3′;
IL-6 R: 5′-CTGCAGCCACTGGTTCTGT-3′;
IL-1β F: 5′-CAGCCAATCTTCATTGCTCA-3′;
IL-1β R: 5′-AGTCATCCTCATTGCCACTGT-3′;
β-actin F: 5′-CTAAGGCCAACCGTGAAAAG-3′;
β-actin R: 5′-GCCTGGATGGCTACGTACA-3′.

Statistical analysis

The data are expressed as the means ± SEM ($n = 6$). Statistical analysis was performed by one-way ANOVA followed by the Bonferroni post hoc test. The statistical analysis software used was SPSS 21. $P < 0.05$ was considered statistically significant.

Results

Effect of SG on wound healing in diabetic rats

To evaluate the effect of SG ointment on lesion area, we compared wound healing in diabetic rats treated with different drugs. In morphological microanalysis, the wounds appeared clean without signs of irritation or bleeding throughout the experiment (Figure 1 A). On day 10, the topical application of SG at various dilutions and Sulfasil significantly decreased wound size compared to that in the vehicle-treated group. On day 15, the wound closure effect of SG at a dilution of 1/6000 was more effective than that of other dilutions of SG and was comparable with the effect of Sulfasil (Figure 1 B). Figure 1 C shows the wound area ratio of each group during the wound healing process. Healing was promoted after SG and Sulfasil treatment, and the wound area ratio of the SG/6000-treated group was more decreased between day 7 and day 10 than that of the other groups. However, CG failed to affect wound contraction compared with that in other groups.

Histopathological examination

Images of HE-stained wound sections of skin on day 15 are shown in Figure 2. Inflammatory cell infiltration (inflammation), epidermal cell regeneration (re-epithelization), granulomas (granulation), and the number of blood vessels (angiogenesis) are presented in Table I. Inflammatory cell infiltration was observed in all diabetic groups; however, SG/6000, SG/3000 and Sulfasil treatment decreased the inflammatory effects.

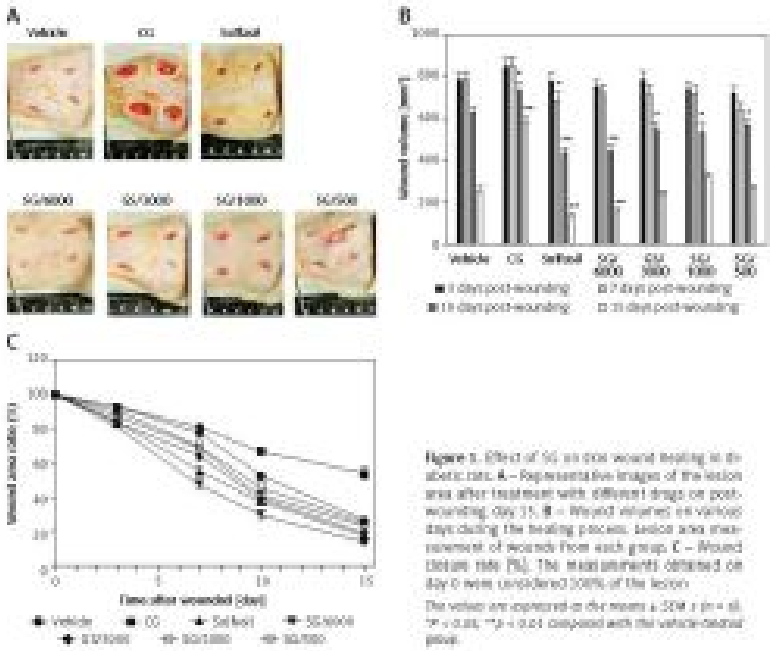

Figure 1. Effect of SG on rat wound healing in diabetic rats. **A** – Representative images of the lesion area after treatment with different drugs on post-wounding day 15. **B** – Wound volumes on various days during the healing process. Lesion area measurement of wounds from each group. **C** – Wound closure rate (%). The measurements obtained on day 0 were considered 100% of the lesion.

The values are expressed as the means ± SEM. n (in = 6). *P < 0.05, **P < 0.01 compared with the vehicle-treated group.

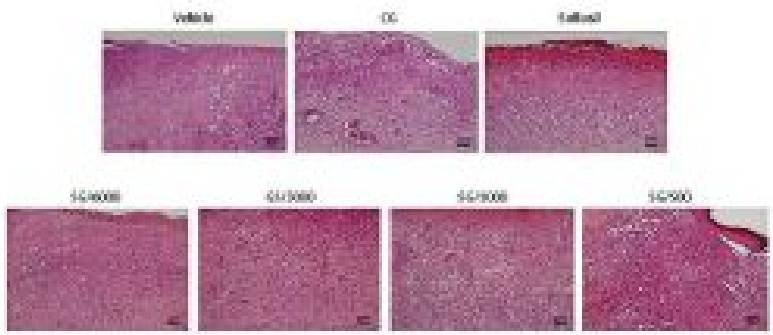

Figure 2. HE-stained skin tissue sections 15 days after induction in diabetic rats treated with different drugs (scale bar: 50 μm). The parameters used to assess the healing of excision wounds in the diabetic rats are shown in Table I.

Among these treatments, SG/6000 was the most effective. The number of new blood vessels in the lesions was increased in the SG/6000–, SG/3000– and Sulfasil-treated groups. To evaluate the kinetics of wound closure, the number of granulomas was measured. The SG/6000- and Sulfasil-treated groups exhibited more granulomas than the other groups. Moreover, the SG/6000-treated group showed higher re-epithelialization levels than those of the other groups. After treatment with CC, the wound size of the STZ-treated diabetic rats was not obviously improved.

Analysis of collagen deposition

Total collagen content was analyzed using Masson's trichrome staining. Our results indicat-

Table 1. Histological comparison of excision wound values per treatment

Treatments	Inflammation	Angiogenesis	Granulation	Re-epithelialization
Vehicle	+++	+	+	–
CG	+++	+	+	–
Soffacid	++	++	++	–
SG/6000	+	+++	++	+
SG/3000	++	++	+	–
SG/1500	+++	++	+	–
SG/750	+++	+	+	–

The parameters used to assess the healing of excision wounds in the diabetic rats were evaluated as follows: absence (inflammation), excessive (granulation (angiogenesis), appearance epithelial cell regeneration and healing (re-epithelialization) and granulation tissue (granulation).

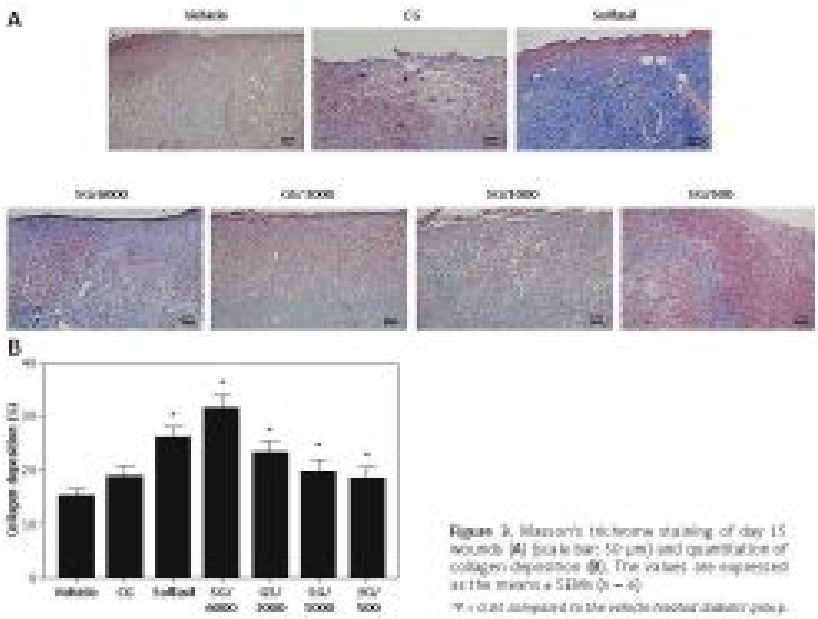

Figure 3. Masson's trichrome staining of day 15 wounds (**A**) (scale bar: 50 µm) and quantification of collagen deposition (**B**). The values are expressed as the means ± SEMs ($n = 6$).

*$P < 0.05$ compared to the vehicle-treated diabetic group.

ed that vehicle- and CG-treated diabetic wounds had poor collagen deposition (Figure 3 A). The SG- and Soffacid-treated type 1 diabetic groups exhibited significantly increased collagen deposition on day 15. Compared with the groups treated with other dilutions of SG, the SG/6000-treated group showed the highest level of collagen deposition (Figure 3 B). Moreover, the gene expression levels of collagen I and collagen III were markedly increased in the SG/6000-treated group compared with the vehicle-treated diabetic group (Figure 4).

Effect of SG on mRNA expression levels of inflammatory cytokines

To investigate the molecular mechanism of SG-induced wound healing activity, the expression levels of related inflammatory cytokines were examined. TNF-α, IL-1β, and IL-6 are the major genes that are generally involved in wound healing. On day 3, a significant decrease in the expression of TNF-α, IL-1β, and IL-6 in the wound tissue of SG/6000-treated rats compared with vehicle-treated rats was noted (Figure 5). Meanwhile,

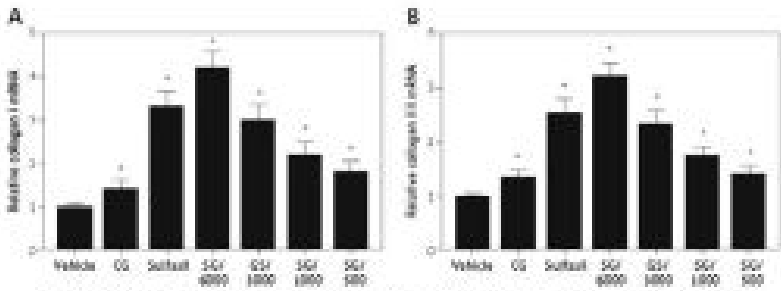

Figure 4. Quantification of collagen I (**A**) and collagen III (**B**) gene expression levels in the wounds of diabetic rats treated with different drugs. The values are expressed as the means ± SEMs ($n = 6$)

*P < 0.01 compared to the vehicle-treated diabetic group

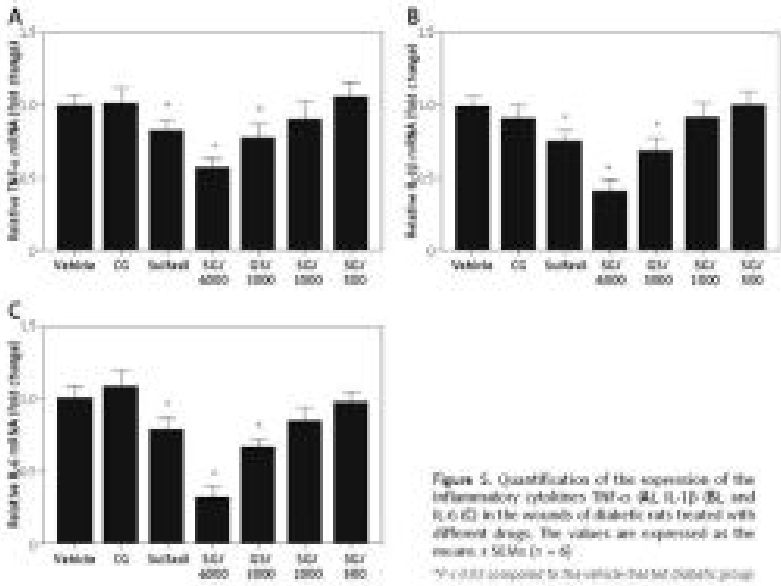

Figure 5. Quantification of the expression of the inflammatory cytokines TNF-α (**A**), IL-1β (**B**), and IL-6 (**C**) in the wounds of diabetic rats treated with different drugs. The values are expressed as the means ± SEMs ($n = 6$)

*P < 0.01 compared to the vehicle-treated diabetic group

SG/3000 and Sulfasil treatment showed modest effects.

Discussion

SG is a water-soluble natural product obtained from *Musa paradisiaca* plants. It has been documented that extracts of *Musa* species have antibacterial and antioxidant activities [25], and promote the healing of burn wounds [19]. Impaired wound healing is a common and potentially serious complication in diabetes [26]. In the present study, we used excisional wound models to investigate the role of SG in diabetic rats [27]. Furthermore, the wound healing effects of SG at a 1:6000 dilution were superior to those of SG at other concentrations in the initial stage of wound healing in STZ-induced diabetic rats. In contrast, the highest dilution of SG had better effectiveness in promoting wound healing in the late stage. However, CG did not promote wound-healing activity in STZ-induced diabetic rats. The findings of the present study indicated that SG/6000 was beneficial in skin wound healing in diabetic rats.

The wounds of diabetic rats in the present investigation showed prolonged inflammation, microvasculature aberrations that result in irreg-

ular circulation and diminished angiogenesis and decreased collagen production, which was similar to the previous study [28]. Many factors, including a hyperglycemic environment, chronic inflammation, wound infection, vascular insufficiency, and hypoxia, have been shown to impair wound healing in diabetes [29]. In the wound tissue of diabetic mice, the absence of the expression of various growth factors delays re-epithelization and granulation tissue formation [30]. In our histopathological studies, SG/6000 significantly decreased inflammation and increased granulation tissue formation and neovascularization of excision wounds in diabetic rats. Moreover, SG/6000 improved collagen deposition compared with that in other groups. Collagen is an essential and main component of granulation tissue that contributes to wound strength and the healing process [31]. It has been reported that collagen deposition in acute wounds is impaired in type 1 diabetes, which might be due to the inhibition of fibroblast proliferation [32]. During the early stages of healing, the levels of type III collagen are increased [33]. In the remodeling phase, collagen III that is produced rapidly in the extracellular matrix is replaced by collagen I, which has a higher tensile strength but takes more time to be deposited [34]. In the current study, SG/6000 significantly increased collagen deposition and elevated the gene expression of collagen type I and collagen type III. Therefore, SG/6000 has been suggested to improve diabetic wound healing in terms of increasing collagen formation.

In the present study, SG/6000 treatment significantly decreased the number of inflammatory cytokines compared with that in other groups. Persistent inflammation in diabetes is associated with delayed wound healing. In diabetes, high glucose promotes inflammation through endothelial cell damage, the release of proinflammatory cytokines, and capillary permeability [35]. In the inflammatory phase, activated macrophages produce growth factors and inflammatory cytokines such as TNF-α, IL-1β, and IL-6 [34]. In the wound healing process, proinflammatory cytokines are involved in cell proliferation and differentiation as well [36]. IL-6 plays a crucial role in many wound healing phases, promoting the migration and proliferation of keratinocytes [37]. In the early stages of wound healing, TNF-α and IL-1β stimulate granulation tissue formation and neovascularization. TNF-α has been reported to regulate vascular endothelial growth factor levels and collagen synthesis in wound healing [38, 39]. IL-1β inhibits type I collagen synthesis during the repair phase of the wound healing response [40]. However, the persistence of inflammatory cytokines impairs the healing of diabetic wounds. SG treatment regulated these mediators by reducing proinflammatory cytokines at the early stage of wound healing and promoting wound repair at the late postinjury stages.

Our results indicated that SG/6000 has more potent anti-inflammatory wound healing stimulating properties than silver sulfadiazine. Silver sulfadiazine has been utilized in advanced wound care to improve the microenvironment of wounds [41]. The application of heparan sulfate can accelerate tissue regeneration in the early phase of tissue repair [42]. Nonetheless, a recent study indicated that silver dressings do not decrease the amount of bacteria in diabetic wounds [43]. A previous study documented that extracts of *Musa paradisiaca* have antibacterial activity against *Pseudomonas aeruginosa* and *Staphylococcus aureus* [44] and can increase the viability of collagen fibrils by increasing the strength of collagen fibers [45]. In addition, *Musa* species show antidiabetic and better ulcer healing effects in diabetic rats with co-occurring gastric ulcers [46]. Therefore, SG might be a target for the treatment of diabetes.

In conclusion, the present study showed that SG improves the healing process in diabetic rats through its anti-inflammatory effect and may help us cure wound injury in the clinic in the future. SG ointment has the potential to be a new alternative therapeutic strategy for wound healing.

Acknowledgments

We thank Natural Well Technical Ltd. Company for providing the sapen green extract.

Conflict of Interest

The authors declare no conflict of interest.

References

1. Dunachie S, Chamnan P. The double burden of diabetes and global infection in low and middle-income countries. Trans R Soc Trop Med Hyg 2019; 113: 56-64.
2. Wang H, Zhang JF, Xing XY, et al. MARCH8 factors associated with weight loss in patients with newly diagnosed type 2 diabetes treated with acarbose or metformin. Arch Med Sci 2018; 15: 209-20.
3. Abwa H, Gad R, Hagazy H, et al. Is subclinical atherosclerosis associated with visceral fat and fatty liver in adolescents with type 1 diabetes? Arch Med Sci 2018; 14: 1553-60.
4. Mejías SG, Rangelvd K. Prevalence of peripheral arterial disease among diabetic patients in Santo Domingo, Dominican Republic and associated risk factors. Arch Med Sci Atheroscler Dis 2018; 3: e15-e40.
5. Teng S, Wang S, Wang M, et al. STOP-Bang questionnaire screening for obstructive sleep apnea among Chinese patients with type 2 diabetes mellitus. Arch Med Sci 2018; 14: 971-8.
6. Spravchikov N, Sizyakov G, Gartsbein M, et al. Glucose effects on skin keratinocytes: implications for diabetes skin complications. Diabetes 2001; 50: 1627-35.

7. Demidova-Rice TN, Hamblin MR, Herman IM. Acute and impaired wound healing: pathophysiology and current methods for drug delivery, part 1: normal and chronic wounds: biology, causes, and approaches to care. Adv Skin Wound Care 2012; 25: 304-14.
8. Grzelak T, Wedrychowicz A, Grupinska J, et al. Neuropeptide B and neuropeptide W as new serum predictors of nutritional status and of clinical outcomes in pediatric patients with type 1 diabetes mellitus treated with the use of pens or insulin pumps. Arch Med Sci 2019; 15: 619-31.
9. Zhao R, Liang H, Clarke E, et al. Inflammation in chronic wounds. Int J Mol Sci 2016; 17: 2085.
10. Ramalho T, Filgueiras L, Silva-Jr IA, et al. Impaired wound healing in type 1 diabetes is dependent on 5-lipoxygenase products. Sci Rep 2018; 8: 14164.
11. Javor J, Ferencik S, Bucova M, et al. Polymorphisms in the genes encoding TGF-beta1, TNF-alpha, and IL-6 show association with type 1 diabetes mellitus in the Slovak population. Arch Immunol Ther Exp 2010; 58: 385-93.
12. Tong M, Tuk B, Shang P, et al. Diabetes-impaired wound healing is improved by matrix therapy with heparan sulfate glycosaminoglycan mimetic OTR4120 in rats. Diabetes 2012; 61: 2633-41.
13. Ibrahim N, Wong SK, Mohamed IN, et al. Wound healing properties of selected natural products. Int J Environ Res Public Health 2018; 15: E2360.
14. Kumar KPS, Bhowmik D, Duraivel S, et al. Traditional and medicinal uses of banana. J Pharmaco Phytochem 2012; 1: 51-63.
15. Imam M, Akter S. Musa paradisiaca L. and Musa sapientum L.: a phytochemical and pharmacological review. J App Pharm Sci 2011; 1: 14-20.
16. Shodehinde SA, Oboh G. Antioxidant properties of aqueous extracts of unripe Musa paradisiaca on sodium nitroprusside induced lipid peroxidation in rat pancreas in vitro. Asian Pac J Trop Biomed 2013; 3: 449-57.
17. Kapadia SP, Pudakalkatti PS, Shivanaikar S. Detection of antimicrobial activity of banana peel (Musa paradisiaca L.) on Porphyromonas gingivalis and Aggregatibacter actinomycetemcomitans: an in vitro study. Contemp Clin Dent 2015; 6: 496-9.
18. Kalita H, Boruah DC, Deori M, et al. Antidiabetic and antilipidemic effect of musa balbisiana root extract: a potent agent for glucose homeostasis in streptozotocin-induced diabetic rat. Front Pharmacol 2016; 7: 102.
19. Amutha K, Selvakumari U. Wound healing activity of methanolic stem extract of Musa paradisiaca Linn. (Banana) in Wistar albino rats. Int Wound J 2016; 13: 763-7.
20. Mohammadimanesh A, Vahedinya AA, Doaei S, et al. The effect of different types of honey on the lipid profile of streptozotocin-induced diabetic rats. Arch Med Sci Atheroscler Dis 2019; 4: e112-6.
21. Chan JK. The wonderful colors of the hematoxylin-eosin stain in diagnostic surgical pathology. Int J Surg Pathol 2014; 22: 12-32.
22. Altavilla D, Saitta A, Cucinotta D, et al. Inhibition of lipid peroxidation restores impaired vascular endothelial growth factor expression and stimulates wound healing and angiogenesis in the genetically diabetic mouse. Diabetes 2001; 50: 667-74.
23. Altavilla D, Galeano M, Bitto A, et al. Lipid peroxidation inhibition by raxofelast improves angiogenesis and wound healing in experimental burn wounds. Shock 2005; 24: 85-91.
24. Kamber M, Papalazarou V, Rouni G, et al. Angiotensin II inhibitor facilitates epidermal wound regeneration in diabetic mice. Front Physiol 2015; 6: 170.
25. Karuppiah P, Mustaffa M. Antibacterial and antioxidant activities of Musa sp. leaf extracts against multidrug resistant clinical pathogens causing nosocomial infection. Asian Pac J Trop Biomed 2013; 3: 737-42.
26. Berlanga-Acosta J, Schultz GS, Lopez-Mola E, et al. Glucose toxic effects on granulation tissue productive cells: the diabetics' impaired healing. Biomed Res Int 2013; 2013: 256043.
27. Cheng KY, Lin ZH, Cheng YP, et al. Wound healing in streptozotocin-induced diabetic rats using atmospheric-pressure argon plasma jet. Sci Rep 2018; 8: 12214.
28. Seitz O, Schurmann C, Hermes N, et al. Wound healing in mice with high-fat diet- or ob gene-induced diabetes-obesity syndromes: a comparative study. Exp Diabetes Res 2010; 2010: 476969.
29. Baltzis D, Eleftheriadou I, Veves A. Pathogenesis and treatment of impaired wound healing in diabetes mellitus: new insights. Adv Ther 2014; 31: 817-36.
30. Pastar I, Stojadinovic O, Yin NC, et al. Epithelialization in wound healing: a comprehensive review. Adv Wound Care (New Rochelle) 2014; 3: 445-64.
31. Ganeshkumar M, Ponrasu T, Krithika R, et al. Topical application of Acalypha indica accelerates rat cutaneous wound healing by up-regulating the expression of type I and III collagen. J Ethnopharmacol 2012; 142: 14-22.
32. Black E, Vibe-Petersen J, Jorgensen LN, et al. Decrease of collagen deposition in wound repair in type 1 diabetes independent of glycemic control. Arch Surg 2003; 138: 34-40.
33. Volk SW, Wang Y, Mauldin EA, et al. Diminished type III collagen promotes myofibroblast differentiation and increases scar deposition in cutaneous wound healing. Cells Tissues Organs 2011; 194: 25-37.
34. Serra MB, Barroso WA, da Silva NN, et al. From inflammation to current and alternative therapies involved in wound healing. Int J Inflam 2017; 2017: 3406215.
35. Kaur R, Kaur M, Singh J. Endothelial dysfunction and platelet hyperactivity in type 2 diabetes mellitus: molecular insights and therapeutic strategies. Cardiovasc Diabetol 2018; 17: 121.
36. Koh TJ, DiPietro LA. Inflammation and wound healing: the role of the macrophage. Expert Rev Mol Med 2011; 13: e23.
37. Werner S, Krieg T, Smola H. Keratinocyte-fibroblast interactions in wound healing. J Invest Dermatol 2007; 127: 998-1008.
38. Totomoch-Serra A, Munoz ML, Burgueno J, et al. Association of common polymorphisms in the VEGFA and SIRT1 genes with type 2 diabetes-related traits in Mexicans. Arch Med Sci 2018; 14: 1361-73.
39. Krzyszczyk P, Schloss R, Palmer A, et al. The role of macrophages in acute and chronic wound healing and interventions to promote pro-wound healing phenotypes. Front Physiol 2018; 9: 419.
40. Chesney J, Metz C, Stavitsky AB, et al. Regulated production of type I collagen and inflammatory cytokines by peripheral blood fibrocytes. J Immunol 1998; 160: 419-25.
41. Murphy PS, Evans GR. Advances in wound healing: a review of current wound healing products. Plast Surg Int 2012; 2012: 190436.
42. Olczyk P, Mencner L, Komosinska-Vassev K. Diverse roles of heparan sulfate and heparin in wound repair. Biomed Res Int 2015; 2015: 549417.

43. Finley PJ, Huckfeldt RE, Walker KD, et al. Silver dressings improve diabetic wound healing without reducing bioburden. Wounds 2013; 25: 293-301.
44. Agarwal PK, Singh A, Gaurav K, et al. Evaluation of wound healing activity of extracts of plantain banana (*Musa sapientum* var. *paradisiaca*) in rats. Indian J Exp Biol 2009; 47: 32-40.
45. Tsuchiya H, Sato M, Miyazaki T, et al. Comparative study on the antibacterial activity of phytochemical flavanones against methicillin-resistant Staphylococcus aureus. J Ethnopharmacol 1996; 50: 27-34.
46. Kumar M, Gautam MK, Singh A, et al. Healing effects of *Musa sapientum* var. *paradisiaca* in diabetic rats with co-occurring gastric ulcer: cytokines and growth factor by PCR amplification. BMC Complement Altern Med 2013; 13: 305.

(二) Banana Plant Extract

Int. J. Med. Sci. 2024, Vol. 21 107

IVYSPRING International Publisher

International Journal of Medical Sciences

2024; 21(1): 107-122. doi: 10.7150/ijms.86748

Research Paper

Inhibition of Polyinosinic-Polycytidylic Acid-Induced Acute Pulmonary Inflammation and NF-κB Activation in Mice by a Banana Plant Extract

Chien-Huang Liao[1,#], Tung-Yuan Lai[2,3,#], Yu-Ying Lin[1], Yi-Chun Liao[4], Gi-Ming Lai[1,5], Tien-Hua Chu[6], Szu-Yao Wu[6], Wei-Lun Tsai[1], Jacqueline Whang-Peng[1,5], Frank Liu[7], Tzeon-Jye Chiou[1,8,✉], Chih-Jung Yao[5,9,✉]

1. Cancer Center, Wan Fang Hospital, Taipei Medical University, Taipei 11696, Taiwan.
2. Department of Chinese Medicine, Hualien Tzu Chi Hospital, Buddhist Tzu Chi Medical Foundation, Hualien 97002, Taiwan.
3. Traditional Chinese Medicine Cancer Center, Hualien Tzu Chi Hospital, Hualien 97002, Taiwan.
4. Institute of Biomedical Sciences, Academia Sinica, Taipei, 11529, Taiwan.
5. Division of Hematology and Medical Oncology, Department of Internal Medicine, Wan Fang Hospital, Taipei Medical University, Taipei 11696, Taiwan.
6. Chimera Bioscience Inc., No. 18 Syuan St., Zhongzheng Dist., Taipei 10097, Taiwan.
7. Department of Research and Development, Natural Well Technical Company, Guishan, Taoyuan 33377, Taiwan.
8. Department of Medical Education and Research, Wan Fang Hospital, Taipei Medical University, Taipei 11696, Taiwan.
9. Department of Internal Medicine, School of Medicine, College of Medicine, Taipei Medical University, Taipei 11031, Taiwan.

#These authors contributed equally to this work.

✉ Corresponding authors: [illegible]

© The author(s). This is an open access article distributed under the terms of the Creative Commons Attribution License (https://creativecommons.org/licenses/by/4.0/). See http://ivyspring.com/terms for full terms and conditions.

Received: 2023.08.02; Accepted: 2023.10.17; Published: 2024.01.01

Abstract

NF-κB activation is pivotal for the excess inflammation causing the critical condition and mortality of respiratory viral infection patients. This study was aimed to evaluate the effect of a banana plant extract (BPE) on suppressing NF-κB activity and acute lung inflammatory responses in mice induced by a synthetic double-stranded RNA viral mimetic, polyinosinic-polycytidylic acid (poly (I:C)). The inflammatory responses were analyzed by immunohistochemistry and HE stains and ELISA. The NF-κB activities were detected by immunohistochemistry *in vivo* and immunofluorescence and Western blot *in vitro*. Results showed that BPE significantly decreased influx of immune cells (neutrophils, lymphocytes, and total WBC), markedly suppressed the elevation of pro-inflammatory cytokines and chemokines (IL-6, RANTES, IFN-γ, MCP-1, keratinocyte-derived chemokine, and IL-17), and restored the diminished anti-inflammatory IL-10 in the bronchoalveolar lavage fluid (BALF) of poly (I:C)-stimulated mice. Accordingly, HE staining revealed that BPE treatment alleviated poly (I:C)-induced inflammatory cell infiltration and histopathologic changes in mice lungs. Moreover, immunohistochemical analysis showed that BPE reduced the pulmonary IL-6, CD11b (macrophage marker), and nuclear NF-κB p65 staining intensities, whilst restored that of IL-10 in poly (I:C)-stimulated mice. *In vitro*, BPE antagonized poly(I:C)-induced elevation of IL-6, nitric oxide, reactive oxygen species, NF-κB p65 signaling, and transient activation of p38 MAPK in human lung epithelial-like A549 cells. Taken together, BPE ameliorated viral mimic poly(I:C)-induced acute pulmonary inflammation in mice, evidenced by reduced inflammatory cell infiltration and regulation of both pro- and anti-inflammatory cytokines. The mechanism of action might closely associate with NF-κB signaling inhibition.

Keywords: banana plant extract, acute pulmonary inflammation, IL-6, NF-κB

Introduction

Viral infections can cause acute pneumonia, resulting in serious morbidity or mortality in patients with pregnancy, obesity, pre-existing chronic diseases or at extremes of age [1]. Viral pneumonia is triggered by exaggerated inflammatory response associated with infiltration of leukocytes into the lung tissue, and

massive production of cytokines, the so-called cytokine storm [2-4]. The exaggerated inflammatory response can diffusely damage lung cells, leading to lung fibrosis and even multi-organ dysfunction [4]. Current antiviral drugs are not effective when treated late after the symptoms onset [5]. At present, no specific treatments are available for curing viral pneumonia [3]. Infections with pneumotropic viruses, such as certain H1N1 and H5N1 influenza virus strains, severe acute respiratory syndrome coronavirus (SARS-CoV), and Middle East respiratory syndrome coronavirus (MERS-CoV) could cause lung injuries and even mortality in patients [5,6]. Recently, the severe acute respiratory syndrome coronavirus 2 (SARS-CoV-2; causative agent of COVID-19) can induce critical pneumonia that may be followed by organ failure, and even death [7], which has imposed serious threats on public health burden worldwide [8]. Further research for therapeutic strategies to improve the treatment outcome of these life-threatening viral pneumonias are still required and ongoing. Among the strategies proposed, the potential of anti-inflammatory therapy in the treatment of SARS-CoV-2 infection becomes a topic of great interest [9]. Drugs with anti-inflammatory activity were repurposed for the treatment of COVID-19 patients although their contemporary clinical efficacy has not been proven to correlate with the current pandemic [10].

Natural products and plant extracts could be considered as a potential source to develop novel antiviral or anti-inflammatory therapeutics for treating or preventing viral pneumonia. A plethora of natural products and plant extracts were reported to exhibit potent activities against various strains of influenza virus like SARS-CoV-2 or druggable targets like angiotensin-converting enzyme 2 (ACE2) receptor [11, 12]. Their potential roles in SARS-CoV-2 treatment have gained public attention recently [11, 12]. In addition, natural products also contain a variety of active compounds possessing anti-inflammatory activities in repressing the crucial driven cytokine and signaling pathway such as IL-6 and NF (nuclear factor)-κB, respectively [13]. Their therapeutic potential against COVID-19 inflammation also has been noticed and studied [14]. *Musa paradisiaca* L., prevalently known as banana, is an herbaceous plant of the Musaceae family and the genus *Musa*. It is one of the most important crops of the world and is the staple food for people living in tropical region. Banana plant is rich in polyphenols, flavonoids, vitamins, potassium, magnesium, and serotonin [15-17]. Compounds contained in *Musa* species had been reported to exert various biological activities, including anti-inflammation, anti-oxidation, anti-diabetes and cardiovascular protection etc. [17]. The anti-inflammatory activities of *Musa* species products had been shown to reduce combined allergic rhinitis and asthma syndrome in mice [17] and attenuate cardiac hypertrophy in rats [16]. Likewise, a banana plant extract (BPE) evaluated in this study was reported to promote wound healing in diabetic rats, accompanied by reduced inflammation [15]. Yet, their effects on viral pneumonia inflammation remain unknown. It is rational and warranted to investigate the effect of *Musa* specie product on the relief of virus-induced acute lung inflammation and NF-κB activation, a key molecular event for eliciting inflammatory responses.

Structurally similar to double stranded RNA, polyinosinic-polycytidylic acid (poly (I:C)) can activate the Toll like receptor 3 (TLR3) pathway to mimic viral infection and induce the subsequent NF-κB activation and cytokines production, leading to pulmonary inflammation and dysfunction [18,19]. This study explores the therapeutic effects of BPE on acute pulmonary inflammation induced by intranasal instillation of RNA viral mimetic poly (I:C) in mice. The impact of BPE treatment on poly (I:C)-induced infiltration of immune cells (neutrophils, lymphocytes, and total WBC), disruption of cytokines and chemokines production (IL-6, regulated on activation, normal T cell expressed and secreted (RANTES), interferon-γ (IFNγ), monocyte chemoattractant protein-1 (MCP-1), vascular endothelial growth factor (VEGF), keratinocyte-derived chemokine (KC), IL-17, and IL-10), and activation of inflammation-associated signaling pathways (NF-κB and MAPK p38) were examined.

Materials and Methods

Reagents

Stock solution of the banana plant extract (BPE) was provided by Natural Well Technical Ltd. Company (Guishan, Taiwan). It was diluted with culture medium for use *in vitro* and double distilled water for use *in vivo* experiments. BPE is a water-soluble substance extracted from the leaves, peels and stems of Musa paradisiaca (Linn) by a patented extraction technology (Invention patent NO. I584814, TW) as described in a previous study [15]. The analyzed components contained in BPE are mainly flavone, polyphenol, polysaccharide, terpenes, and amino acids etc. More details of the components are listed in Table S1. Polyinosinic-polycytidylic acid (poly (I:C) was purchased from InvivoGen (Cat # tlrl-pic, San Diego, CA) and was dissolved in phosphate-buffered saline (PBS) (10 mM phosphate, 138 mM NaCl, pH 7.4) at a concentration of 10

mg/mL and aliquots were stored at -20°C. Pyrrolidine dithiocarbamate (PDTC; an NF-κB inhibitor) was obtained from Sigma-Aldrich (Cat #P8765, St. Louis, MO, USA).

Cell Culture

The type II pulmonary epithelial cell line A549 (BCRC 60074) was purchased from the BCRC (Bioresource Collection and Research Center, Hsin Chu, Taiwan). The human fetal lung fibroblast WI-38 and murine macrophage RAW 264.7 cells were obtained from the American Type Culture Collection (Manassas, VA, USA). A549 cells were maintained in Roswell Park Memorial Institute (RPMI)-1640 medium (Gibco, Carlsbad, CA, USA). WI-38 cells were cultured in Eagle's Minimum Essential Medium (EMEM) (Gibco), and RAW 264.7 cells were cultured in Dulbecco's Modified Eagle's Medium (DMEM) (Gibco). These culture mediums were supplemented with 10% fetal bovine serum (Gibco), 1 × penicillin streptomycin-glutamine (PSG, Gibco). Cells were cultured at 37°C in a water jacketed 5% CO2 incubator. According the effective in vitro concentration (1/6000) of BPE used in a previous study [15], 1/6000, 1/3000, and 1/600 dilutions were chosen as the concentrations of BPE to treat cells in this study.

Western Blotting

After cells were seeded in 6-cm dishes at a density of 5 × 10^5 cells/dish for 24 h, they were then pretreated with BPE for 1 h and then stimulated with poly (I:C) for the time intervals described in the legend of Figure 7. Cell extracts were prepared by resuspending cells in radioimmunoprecipitation assay (RIPA) lysis buffer containing protease inhibitor (Roche, CA, USA). After centrifugation, the supernatants were dissolved in the sample buffer for sodium dodecyl sulfate-polyacrylamide gel electrophoresis (SDS-PAGE). Samples containing equal amounts of protein (50 μg) were separated by SDS-PAGE, and then transferred onto a PVDF membrane. The membrane was blocked with 5% skim milk and probed with primary antibodies at 4°C for overnight. After incubation with horseradish peroxidase-conjugated secondary antibody (Jackson Immunoresearch, PA, USA), the membrane was then observed using Immobilon Western Chemiluminescent HRP Substrate (Millipore, MA, USA). Antibody against NF-κB p65 (sc-8008), phospho-NF-κB p65 (sc-166748), and phospho-IκBα (sc-8404) were purchased from Santa Cruz (Santa Cruz Biotechnology, Inc, CA, USA). Anti-phospho-p38 (ab-178867) and anti-GAPDH (ab-8245) were purchased from Abcam (Abcam, MA, USA). The results of Western blots were quantified by Image J software (ImageJ Version 1.52, National Institutes of Health, Bethesda, MD, USA) downloaded from https://imagej.nih.gov/ij/download.html (accessed on 25 September 2019).

RNA extraction and Quantitative RT-PCR

After cells were seeded in 6-well plate at a density of 2 × 10^5 cells/well for 24 h, Raw 264.7 cells were pretreated with different concentrations of BPE or PBS (Control, CTL) for 1 h, and A549 and WI-38 cells were pretreated with different concentrations of BPE, 10 μM of PDTC or PBS (Control, CTL) for 1 h. Afterward, cells were then stimulated with poly (I:C) (10 μg/mL) for 6 h and then their total RNAs were extracted using RNeasy Mini Kit and treated with an RNase-free DNase I set (Qiagen, Hilden, Germany) according to the manufacturer's protocol. Total RNA (1 μg) was reverse-transcribed using oligo (dT) 15 primers and a reverse transcription system (Promega, Madison, USA). Reactions were carried out using Fast SYBR® Green PCR Master Mix (Applied Biosystems, Warrington, UK) on the StepOne Plus Real-Time PCR System (Applied Biosystems, Foster City, CA, USA) by denaturation at 95°C for 10 min, followed by 40 cycles at 95°C for 15 s and 60°C for 40 s. Melting curve analyses were performed to verify the amplification specificity. Relative quantification of gene expression was performed according to the ΔΔ-CT method using StepOne Software 2.0 (Applied Biosystems). *Glyceraldehyde-3-phosphate dehydrogenase* (GAPDH) or *18S* was used to normalize the RT-PCR results. The primer sequences used were as follows:

Human *IL-6* F: 5'-GGAGAG-GAGACTTCACA GAGGA-3'; Human *IL-6* R: 5'- ATTTCCACGATTTCC CAGAGA-3'; Human *GAPDH* F: 5'-GTGGACCT GACCTGCCGTCT-3'; Human *GAPDH* R: 5'-GGAG GAGTGGGTGTCGCTGT-3'.

Mouse *IL-6* F: 5'-TGGAGTCACAGAAGGAG TGGCTAAG-3'; Mouse *IL-6* R: 5'-TCTGACCACA GTGAGGAATGTCCAC-3'; Mouse *IL-10* F: 5'-GGTTG CCAAGCCTTATCGGA-3'; Mouse *IL-10* R: 5'-ACCTG CTCCACTGCCTTGCT-3'; Mouse *18S* F: 5'-GTAAC CCGTTGAACCCCATT-3'; Mouse *18S* R: 5'-CCATCC AATCGGTAGTAGCG-3'.

Immunofluorescence analysis

For the examination of nuclear translocation of NF-κB p65, A549 cells (1.0 × 10^5 cells/ well) were cultured in a 24-well plate and pretreated with BPE (1/6000 dilution) for 1 h and then poly (I:C) (10 μg/mL) for 4 h. Cells were fixed in 4% paraformaldehyde/PBS for 15 min at room temperature, permeabilized with 0.5% Triton X-100 in PBS for 5 min, and then blocked with 5% bovine serum albumin (BSA)/PBS for 30 min. Plate was incubated at 4 °C

with anti-p65 or anti-phospho-p65 antibody. After overnight incubation, cells were washed and incubated for 1 h at room temperature with 1:2000 dilution of Alexa 488 or 555-labeled donkey anti-rabbit antibody (Life Technologies, Eugene, OR, USA). Cells were then counterstained with 4',6-diamidino-2-phenylindole (DAPI) for cell nuclei and observed by Olympus IX73 inverted fluorescence microscope (Olympus, MA, USA). The images of immunofluorescence were analyzed by SPOT Advanced Imaging software ver5.2 (SPOT imaging, MI, USA).

Measurement of nitrite and intracellular reactive oxygen species (ROS) levels

A549 or WI-38 cells (2×10^5 cells per well in a 24-well plate) were pretreated with RPE for 1 h and then stimulated with poly (I:C) (10 μg/mL) for 24 h. The supernatants of the cultured cells were collected, and the accumulated nitrite (NO_2^-, one of two primary stable and nonvolatile breakdown products of nitric oxide (NO)) was measured using Griess reagent (Promega, Madison, WI, USA). The intracellular accumulation of ROS was measured with DCFDA / H2DCFDA-Cellular ROS Assay Kit (ab113851, Abcam) according to the manufacturer's instructions. In brief, A549 or WI-38 cells were pretreated with RPE for 1 h, then stimulated with poly (I:C) (10 μg/mL) for 24 h, and then stained with 20 mM H2DCF-DA in PBS for 1 h at 37°C. DCF fluorescence intensity was measured at 485-nm excitation and 535-nm emission using a fluorescence plate reader (Molecular Devices, CA, USA).

Mice

Thirty-five female C57BL/6 mice (8-12 weeks old) were purchased from National Laboratory Animal Center and housed in the specific pathogen-free animal facility of Chimera Bioscience (Taipei, Taiwan). All mice experiments were followed the guidelines of the Care and Use of Laboratory Animals [20] and approved by protocol number # CMR-AP1090092001 of the Institutional Animal Care and Use Committee of Chimera Bioscience (Taipei, Taiwan).

Establishment of poly (I:C)-induced lung inflammation model

The poly (I:C)-induced lung inflammation model was established as described in a previous study [18]. High molecular weight polyinosine-polycytidylic acid (HMW poly (I:C), Invivogen, San Diego, CA, USA) was prepared according to vendor's instruction. Since preliminary experiment showed that RPE at dilution of 1/60 (200 μL/mouse) was effective against poly (I:C) (100 μg/mouse)-induced pulmonary inflammation, Female C57BL/6 mice (8-12 weeks old) were equally divided to five groups (control group, poly (I:C) group, and three poly (I:C) + RPE (1/600, 1/200, 1/60 dilutions) groups). In each group, three mice were used for BALF acquisition and four mice were for immunohistochemistry (IHC) study after treatment. Mice were anesthetized with 4% isoflurane for daily intranasal instillation of poly (I:C). HMW poly (I:C) (100 μg/mouse) or PBS with a total volume of 50 μL were administered intranasally (i.n.) for consecutive 3 days with a 24-hour interval between each administration. RPE (at concentrations of 1/600, 1/200, and 1/60 dilutions) were given twice a day by oral gavage (p.o.) (200 μL/mouse) at 1 h before and 6 h after each daily poly (I:C) challenge for 3 days. Control and poly (I:C) groups were administrated with same volume of PBS (i.n.) and double-distilled water (p.o.) as poly (I:C) and RPE, respectively. Mice were then sacrificed with the overdose anesthetics Zoletil and Rompun at 24 h after the last poly (I:C) administration, and the BALF and lung were collected for further analysis.

Collection of bronchoalveolar lavage fluid (BALF)

BALF sample was collected by flushing through the trachea back and forth for 3 times with 1 mL cold PBS. The lung tissues were then harvested and frozen. BALF was centrifuged at 500 × g for 10 min at 4 °C. Cell-free supernatants were collected and stored at -80°C until the measurement of cytokines and chemokines. The BALF cell pellet was resuspended in PBS for immune cell count by an automated hematology analyser ProCyte (IDEXX ProCyte Dx, IDEXX Laboratories, Westbrook, ME, USA).

Histopathological examination

Mice lungs were fixed in 10% neutral buffered formalin for paraffin embedding. The whole lung was then sectioned at 5 μm and stained with hematoxylin and eosin (H&E). Histological analyses were focus on inflammatory cells infiltration and semi-quantitatively graded in a blinded manner on a range of 0 to 5 as described in a previous study [21].

Antibody array detection of cytokines levels in BALF

Murine interleukin-6 (IL-6), IL-10, IL-17, keratinocyte-derived chemokine (KC), monocyte chemoattractant protein-1 (MCP-1), regulated upon activation normal T expressed and secreted (RANTES), vascular endothelial growth factor (VEGF), and interferon-gamma (IFN-γ) in the BALF samples were quantified with Quantibody mouse

cytokine array kit (QAM-CYT-1, RayBiotech, Inc., Norcross, USA). The assay was performed according to the manufacturer's protocol and data were analyzed with the software provided by the company.

Immunohistochemistry Assay

Immunohistochemistry (IHC) was performed as reported by a previous study [22]. At 24 h after the last poly (I:C) administration, the lung tissues of mice were embedded in paraformaldehyde for the IHC staining of CD11b, IL-6, IL-10, and p65. The images of IHC were captured with Olympus BX61 microscope (Olympus, MA, USA).

Statistical analysis

The statistical analysis of data was performed using one-way ANOVA followed by Dunnett's t test. Probability value of $p < 0.05$ was considered statistically significant. Single asterisk (*) indicates $p < 0.05$; double asterisks (**) indicate $p < 0.01$; triple asterisks (***) indicate $p < 0.001$; number sign (#) indicates $p < 0.01$.

Results

BPE decreased the elevated immune cell count in BALF from poly (I:C)-treated mice

To evaluate the anti-inflammatory effects of BPE *in vivo*, acute pulmonary inflammation in mice was generated by intranasal administration of poly (I:C) as described in Materials and Methods section. One day after the last poly (I:C) stimulation, severely increased immune cell number was observed in the bronchoalveolar lavage fluid (BALF) from poly (I:C) alone-treated mice, in comparison with that from PBS-treated control (CTL) (Figure 1). Treatment with BPE significantly reduced the poly (I:C)-induced elevation of total white blood cell (WBC) (Figure 1A), neutrophils (Figure 1B), and lymphocytes (Figure 1C) counts in BALF.

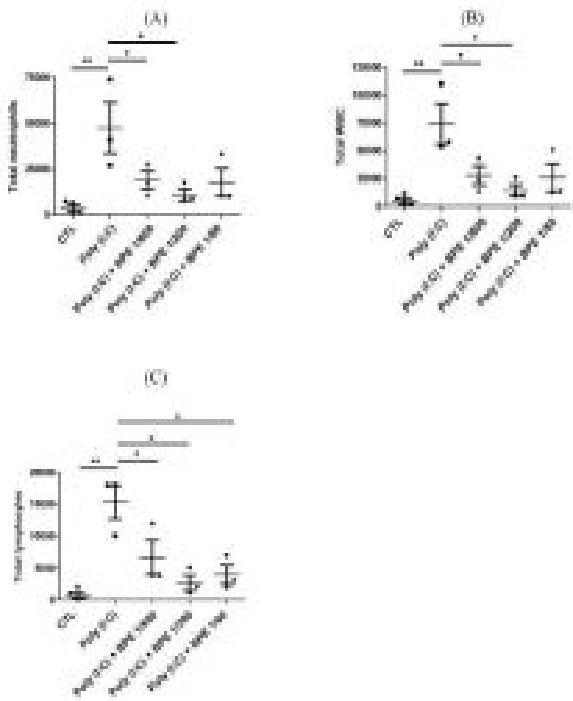

Figure 1. Treatment with BPE prevented the influx of inflammatory cells into the airways of poly (I:C)-treated mice. C57BL/6N mice were treated with BPE (200 μL/mouse at concentration of 1:800, 1:1200, 1:1600 dilution) via oral gavage 1 h prior to and 4 h after an i.n. administration of poly (I:C) (100 μg in 50 μL PBS/mouse) every 24 h for three cycles. Control (CTL) group was administrated with same volume of PBS. One day after the last administration of poly (I:C), mice were euthanized and bronchoalveolar lavages (BAL) were performed. The total numbers of (A) WBC cells, (B) neutrophils, and (C) lymphocytes in the bronchoalveolar lavage fluid (BALF) were measured. The values are expressed as the means ± SD ($n = 3$). The value of poly (I:C)-administrated group was compared with that of PBS-treated control (CTL) or BPE-treated groups. *$p < 0.05$; **$p < 0.01$.

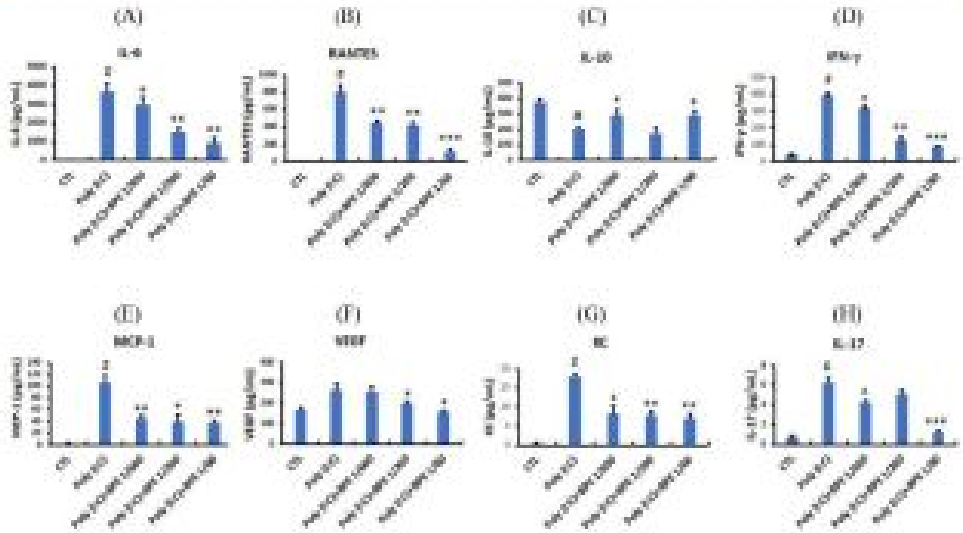

Figure 2. Effects of BPE on the cytokines and chemokines contained in the BALF of Poly (I:C)-stimulated mice. Cytokines and chemokines levels of (A) Interleukin (IL)-6, (B) Chemokine ligand 5 (CCL5, RANTES), (C) IL-10, (D) interferon gamma (IFN-γ), (E) monocyte chemotactic protein (MCP)-1, (F) vascular endothelial growth factor (VEGF), (G) keratinocytes-derived chemokine (KC), and (H) IL-17 in the BALF of treated mice were analyzed at 24 h after the last poly (I:C) administration. Values are means ± SD (n = 5). $^{\#}p < 0.05$, compared with the control (CTL) group. The values of BPE-treated groups were compared with that of poly (I:C) alone-treated group. $^{*}p < 0.05$; $^{**}p < 0.01$; $^{***}p < 0.001$.

Consistent with the elevated immune cell count, enzyme linked immunosorbent assay (ELISA) showed that pro-inflammatory cytokines and chemokines such as IL-6, RANTES, IFN-γ, MCP-1, KC, and IL-17 were drastically increased in the BALF from poly (I:C) alone-treated mice (Figure 2), whereas the anti-inflammatory IL-10 was diminished (Figure 2C). Treatment with BPE counteracted this phenomenon by reducing the above elevated pro-inflammatory cytokines (Figure 2), and restoring the diminished anti-inflammatory IL-10 (Figure 2C). These results show the anti-inflammatory property of BPE and imply the attenuated pulmonary inflammation in BPE-treated mice.

BPE attenuated poly (I:C)-induced lung inflammation and histopathological changes in mice

To confirm the effects of BPE in BALF, hematoxylin-eosin (HE) staining of the mice lung tissues was performed to examine the histopathological change. As shown in Figure 3A, HE staining showed intact bronchial and alveolar structures in the lungs of PBS-treated control mice, and no obvious inflammatory cell infiltration or interstitial hyperemia was displayed. In contrast, inflammation cells permeating into pulmonary alveoli, thickening of the alveolar wall, and pulmonary congestion were found in the lung tissues of poly(I:C) alone-treated mice (Figure 3A). In line with the results shown in BALF, BPE treatment markedly ameliorated the aforementioned poly (I:C)-induced damages, evidenced by less severe alveolar wall collapse and decreased inflammatory cell infiltration (Figure 3A). The degree of cell infiltration was semi-quantitatively scored as shown in Figure 3B. Poly (I:C) stimulation severely increased the score from 0.28 ± 0.07 of control to 4.33 ± 0.44, which could be significantly reduced to 1.66 ± 0.43, 2.66 ± 0.41, and 2.33 ± 0.40 by treatment with BPE at dilution of 1/600, 1/200, and 1/60, respectively (Figure 3B). Although the effect was not in a dose-dependent manner, BPE appeared to exhibit protective effects against the damage produced by poly (I:C) in mice lungs.

BPE suppressed CD11b and IL-6, whilst restored IL-10 levels in poly (I:C)-stimulated mice lungs

Since HE staining showed inhibitory effects of BPE on poly (I:C)-induced inflammatory cell infiltration and pathological change in mice lungs, we examined the pulmonary levels of CD11b (a marker ubiquitously expressed on monocytes and neutrophils and discretely expressed on inflammatory alveolar macrophages in mice [23]), IL-6 (a crucial

pro-inflammatory cytokine), and IL-10 (an important anti-inflammatory cytokine) in mice lung tissues by immunochemistry staining. In agreement with the marked inflammatory cell infiltration shown in HE staining, much higher staining intensity of CD11b, was observed in the lungs of poly (I:C) alone-stimulated mice, in comparison to that of PBS-treated control (Figure 4A). Treatment with BPE obviously reduced the intensity of CD11b staining caused by poly (I:C) stimulation (Figure 4A). In line, poly (I:C) stimulation resulted in marked increase of IL-6 and diminishment of IL-10 staining intensities, when compared with that of PBS-treated control (Figure 4A). BPE treatment reduced the elevated IL-6 whilst restored the diminished IL-10 staining intensities mentioned above (Figure 4A). These results further display the anti-inflammatory activity of BPE in this poly (I:C)-induced acute pulmonary inflammation mouse model.

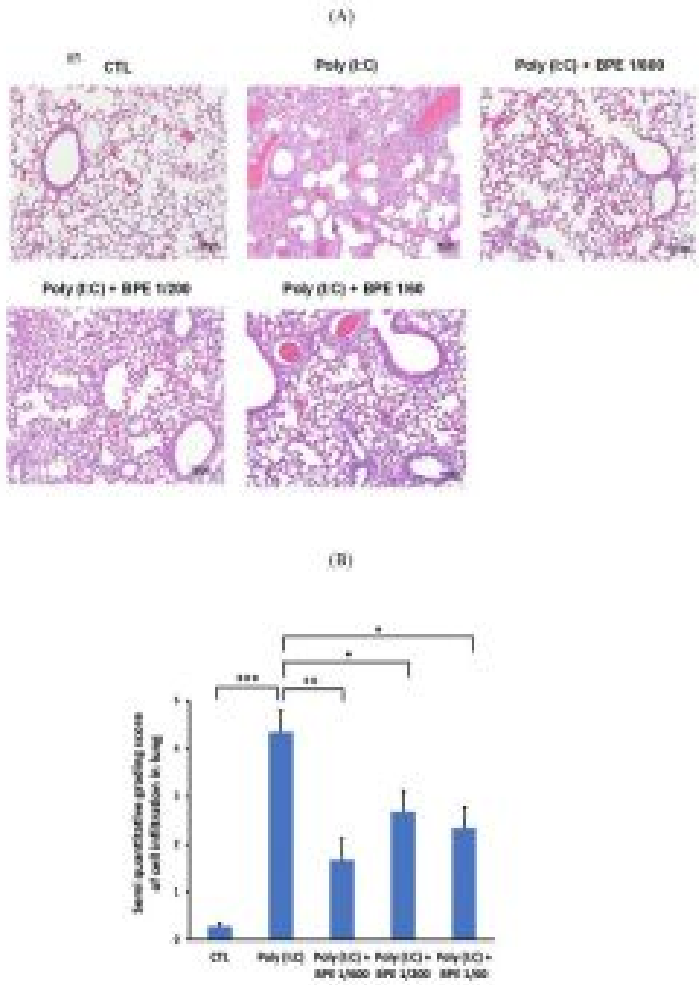

Figure 3. Treatment with BPE reduced poly (I:C)-caused histopathologic changes in mice. (A) Representative hematoxylin-eosin (HE) staining images showing the histopathologic changes in mice lungs of indicated groups. Mice of each group were treated as described in Materials and Methods. Lungs from each experimental group were processed for histological evaluation at 24 h after the last poly (I:C) stimulation. Scale bar = 100 μm. (B) Semi-quantitative grading score of inflammatory cells infiltration in a blinded manner on a range of 0 to 5 as described in Materials and Methods. The data are presented as the mean ± SD (n = 4). The value of poly (I:C) alone-treated group was compared with that of PBS-treated control (CTL) or BPE-treated groups. *p < 0.05, **p < 0.01, ***p < 0.001.

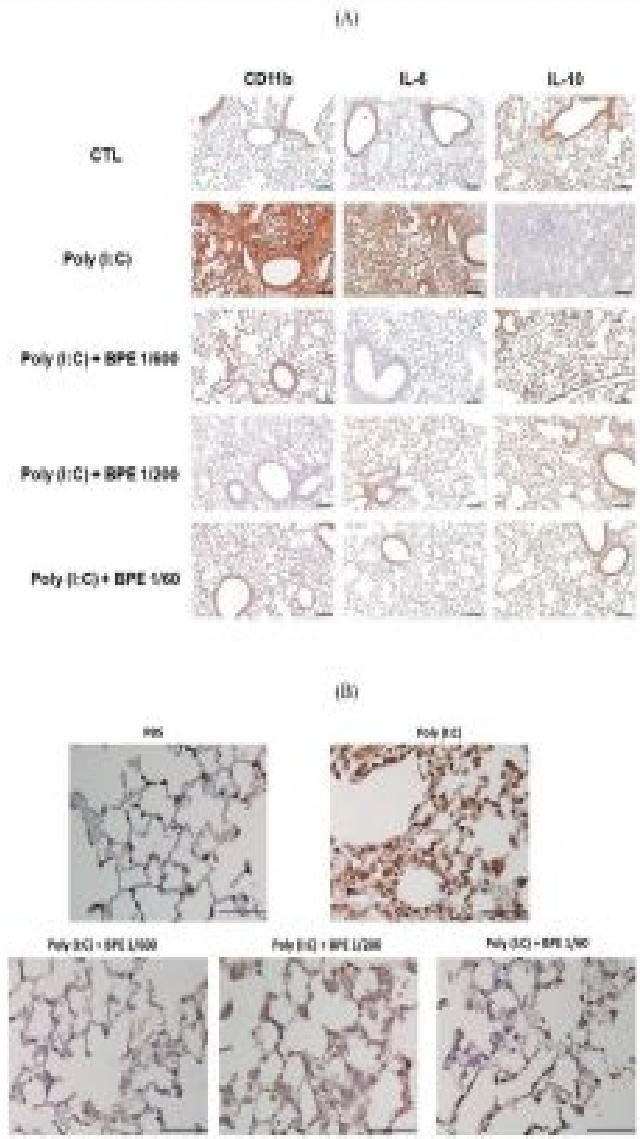

Figure 4. Effect of BPE on poly (I:C)-induced changes in CD11b, IL-4, IL-10, and NF-κB p65 protein levels of mice lungs. Representative immunohistochemistry staining images of (A) CD11b, IL-4, IL-10, and (B) NF-κB p65, respectively, in the lungs of mice treated as indicated. Mice of each group were treated as described in Materials and Methods. The intensity of brown positive staining represents the protein level detected by antibody used for each sample. (A) bar = 100 μm, (B) bar = 50 μm.

BPE suppressed poly (I:C)-induced NF-κB activation in mice lungs

In the progression of acute pulmonary inflammation, nuclear factor κB (NF-κB) activation had been demonstrated as a key event by several studies [24-26]. The critical event for activating NF-κB signaling is nuclear translocation of the p65 subunit of NF-κB (NF-κB p65) [27]. To investigate the mechanism underlying the BPE-exerted anti-inflammatory effects, immunohistochemistry staining was also performed to examine the nuclear translocation of

NF-κB p65 protein. As expected, much higher staining intensity of nuclear NF-κB p65 was found in the lungs of poly (I:C) alone-treated mice, in comparison with that of PBS-treated control (Figure 4B). In support of its effects mentioned above, BPE treatment substantially reduced the staining intensity of nuclear NF-κB p65 protein resulted from challenge of poly (I:C) (Figure 4B). It is very likely that inhibition of NF-κB played a crucial role in the anti-inflammatory property of BPE.

BPE suppressed poly(I:C)-induced inflammation-associated responses in cultured epithelium-like cells, fibroblast, and macrophage

Upon pulmonary viral infection, inflammation was raised by the complex interaction of lung tissues, immune cells (such as macrophages and neutrophils), and the secreted mediators (such as chemokines, cytokines and reactive oxygen species (ROS)) [28,29]. To further characterize the anti-inflammatory property of BPE, we explored its effects in cultured macrophage-like, alveolar type II epithelium-like, and lung fibroblast cells primed with pro-inflammatory stimulator poly (I:C).

RAW 264.7 macrophage-like cells were employed to study the effects of BPE in primed macrophage. As shown in Figure 5A, poly (I:C) (10 μg/mL) significantly increased transcription of the crucial pro-inflammatory cytokine *IL-6* in RAW 264.7 cells. Pretreatment with BPE significantly suppressed the *IL-6* mRNA induction by poly (I:C), although the effect was not statistically significant at the concentration of 1/200 dilution (left panel of Figure 5A). Intriguingly, in contrast to that observed in Figure 2C and 4A, the *IL-10* mRNA level of cultured RAW 264.7 cells was elevated by challenge with poly (I:C), and treatment with BPE at concentration of 1/2000 dilution further enhanced the poly (I:C)-elevated *IL-10* transcription (right panel of Figure 5A).

A549 and WI-38 cells were employed for the experiments to study the effects of BPE in human alveolar type II epithelium-like and lung fibroblast cells, respectively. The transcription of the crucial pro-inflammatory cytokine *IL-6* in A549 and WI-38 cells was significant increased after priming with poly (I:C) (10 μg/mL) for 6 h, and pretreatment with BPE at various diluted concentrations could effectively counteract this induction of *IL-6* mRNA expression (Figure 5B). It is known that poly (I:C) induced IL-6 secretion in bronchial epithelial cells via NF-κB activation [30]. An effective NF-κB inhibitor pyrrolidine dithiocarbamate (PDTC) [31] was used as a positive control to suppress the *IL-6* induction. Notably, the efficacy of BPE was similar to that of PDTC (Figure 5B). This result is in accordance with that shown in Figure 4, which implies the close association between NF-κB inhibition and the anti-inflammatory effects of BPE.

Upon priming with poly (I:C) (10 μg/mL), drastically increased productions of nitric oxide (NO) (Figure 5C) and reactive oxygen species (ROS) (Figure 5D) were detected in these A549 and WI-38 cells. Coincide with its inhibitory effect on the *IL-6* mRNA induction mentioned above, BPE also effectively suppressed poly (I:C)-induced NO and ROS productions in these A549 and WI-38 cells (Figure 5C and 5D).

BPE suppressed poly (I:C)-induced NF-κB activation in A549 cells

Regarding the inhibitory effect of BPE on NF-κB activity shown in Figure 4B, we investigated whether BPE could also inhibit poly (I:C)-induced NF-κB activation in A549 cells. Immunocytofluorescence analysis for nuclear translocation of NF-κB p65 subunit was performed in poly (I:C)-primed A549 cells. As shown in Figure 6A, the green fluorescence-labeled p65 subunit distributed dominantly in the cytoplasm of control A549 cells. Priming with poly (I:C) induced nuclear translocation of p65 protein in A549 cells, as evidenced by the condensed green immunocytofluorescence intensity in nuclear regions (labeled by DAPI) (Figure 6A). As expected, pretreatment with BPE obviously inhibited this nuclear translocation of p65 protein as that done by PDTC (Figure 6A). This phenomenon was more clearly demonstrated by labeling the phosphorylated p65 protein (p-p65, active form of p65) with red fluorescence (Figure 6B). Only very slight red fluorescence could be seen in PBS-treated A549 cells, and priming with poly (I:C) dramatically increased the red fluorescence staining intensity, indicating intense activation of NF-κB signaling (Figure 6B). Pretreatment with BPE or PDTC clearly diminished the increased red fluorescence (Figure 6B), implying the drastic inhibition on NF-κB activity.

Activation of NF-κB signaling requires phosphorylation and subsequent degradation of the inhibitory subunit of NF-κB alpha (IκBα) [32]. Afterward, we examined the phosphorylation of IκBα by Western blot in poly (I:C)-stimulated A549 cells with or without BPE pretreatment. After primed with poly(I:C) for 4 h, an increased phosphorylated IκBα (p-IκBα) level was observed while activation of NF-κB was evidenced by the increased level of phosphorylated p65 subunit (p-p65) (Figure 7A). In agreement with the result of immunocytofluorescence shown in Figure 6, pretreatment with BPE suppressed

the increase of both p-p65 and p-IκBα levels induced by poly(I:C) (Figure 7A). This result further confirmed the inhibitory effect of BPE on poly(I:C)-induced NF-κB activation in A549 cells.

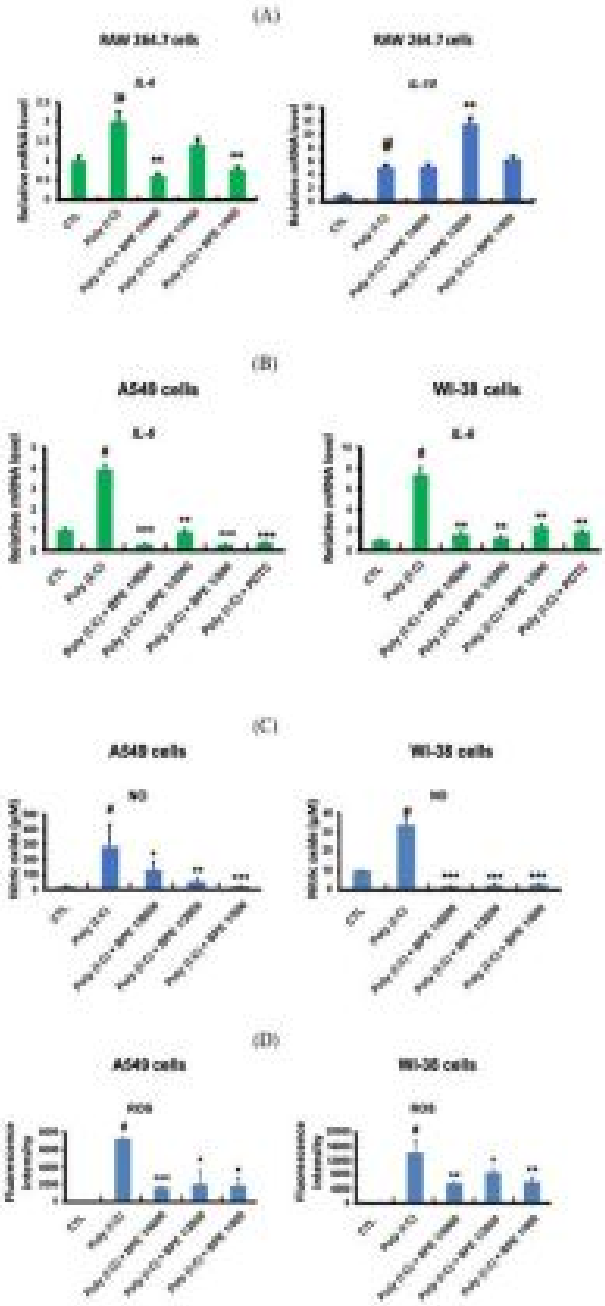

Figure 5. Effects of BPE on poly (I:C)-induced pro-inflammatory mediators in RAW 264.7, A549, and WI-38 cells. (A) Raw 264.7 cells were processed with different concentrations of BPE or PBS (Control, CTL) for 1 h and then stimulated with poly (I:C) (10 μg/mL) for 6 h. The mRNA levels of IL-6 and IL-10 were measured by real-time

reverse-transcription polymerase chain reaction assay and normalized to 18S mRNA level. (B) A549 and WI-38 cells were pretreated with different concentrations of BPE, 80 μM of PDTC or PBS (Control, CTL) for 1 h and then stimulated with poly (I:C) (10 μg/mL) for 4 h. The mRNA level of IL-6 was measured by real-time reverse-transcription polymerase chain reaction assay and normalized to GAPDH mRNA level. (C) A549 and WI-38 cells were pretreated with different concentrations of BPE or PBS (Control, CTL) for 1 h then incubated with poly(I:C) (10 μg/mL) for 24 h. The amount of nitric oxide (NO) released into the media was measured by Griess reagent. (D) The cellular reactive oxygen species (ROS) levels of the cells described in (C) were measured by DCFDA / H2DCFDA - Cellular ROS Assay Kit (ab113851, Abcam). The values represent mean ± SD (n=3). #p < 0.01, compared with control (CTL) group; *p < 0.05, **p < 0.01, ***p < 0.001, compared with poly (I:C) alone-treated group.

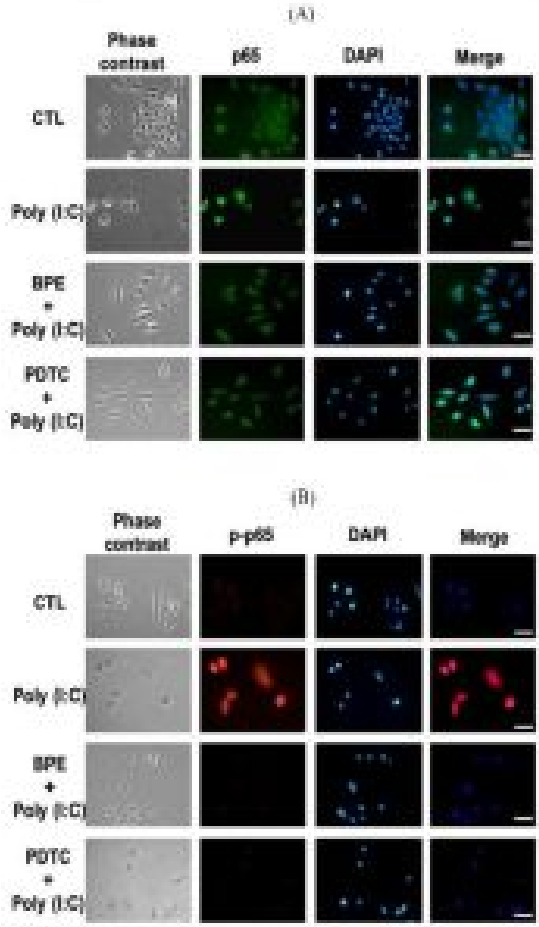

Figure 6. Representative immunofluorescence images showing effect of BPE on the nuclear translocation of NF-κB p65 in poly (I:C)-stimulated A549 cells. A549 cells were pretreated with BPE (1:5000 dilution), PDTC (50 μM) or PBS for 1 h and then incubated with 10 μg/mL of poly (I:C) for 4 h. The cellular localization of NF-κB p65 was then revealed by antibody against (A) p65 and (B) phospho-p65 (p-p65), respectively, and visualized via fluorescent secondary antibody under fluorescence microscope. The nucleus was labeled with 4',6-diamidino-2-phenylindole (DAPI) (blue fluorescence). Scale bar is 50 μm.

It is reported that in pathogen (nontypeable Hemophilus influenza)-infected epithelial cells, p38 MAP kinase signaling mediates NF-κB activation [33]. The phosphorylated (activated) p38 (p-p38) level in A549 cells was thus examined by Western blot at various time points (15, 30, 60, and 120 min) after priming with poly (I:C). As shown in Figure 7B, a transient increase of p-p38 occurred at 15 min after poly (I:C) stimulation, and pretreatment with BPE abrogated this transient increase of p-p38. In addition to suppressing NF-κB activation, this stabilization of p38 MAP kinase activity might also contribute to the inhibitory effect of BPE on poly (I:C)-induced inflammation.

Discussion

From SARS-CoV, MERS-CoV to the recent COVID-19 (SARS-CoV-2), the fight against viral

pneumonia remains continue and the treatment of patients with severe disease is still challenging and evolving. In the management COVID-19 patients, anti-inflammatory therapy plays a pivotal role in preventing further injury and organ damage or failure [10]. According to the reported anti-inflammatory effects of *Musa* species products [15,17], we speculate the effects of a banana plant extract BPE on relieving viral inflammatory response in mice lung. By using the mouse model of pulmonary inflammation induced by RNA viral mimetic poly (I:C) [34], this study presents the anti-inflammatory effects of BPE in the aspects of modulating immune mediators production, suppressing immune cells infiltration, and inhibiting the prominent signaling molecule NF-κB.

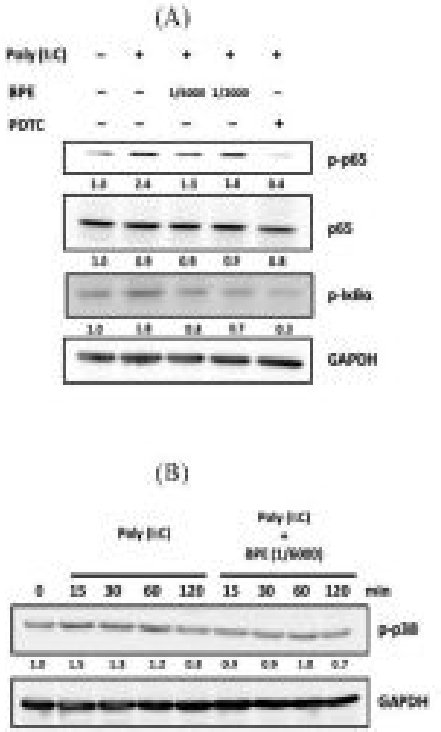

Figure 3. Effects of BPE on poly (I:C)-induced activation of NF-κB and p38 in A549 cells. (A) A549 cells were pretreated with BPE (1/6000 or 1/2000 dilution), PDTC (10 μM) or PBS for 1 h and then incubated with 10 μg/mL of poly (I:C) for 4 h. The protein level of NF-κB p65 (p65), phospho-p65 (p-p65), phospho-IκBα (p-IκBα), and GAPDH were detected by Western blots. After normalization to GAPDH, the fold changes of dense protein levels were indicated below the bands. (B) A549 cells were pretreated with BPE (1/6000 dilution) or PBS for 1 h and then incubated with 10 μg/mL of poly (I:C) for 15, 30, 60, and 120 min, respectively. Western blot analysis of the phospho-p38 (p-p38) protein level was done. Numbers below the corresponding band indicate relative intensity after normalization to GAPDH.

BPE treatment substantially diminished poly (I:C)-induced pro-inflammatory cytokines and chemokines in BALF, implying its potential in attenuating the cytokine storm initiated by viral infection. Exaggerated overproduction of pro-inflammatory cytokines and chemokines (so-called cytokine storm) has been observed in SARS-CoV, MERS-CoV, and the recent COVID-19-induced SARS-CoV-2 [28]. In hospitalized COVID-19 patients, cytokine storm was found to correlate with disease severity and unfavorable outcomes, which thus highlighted the implementation of anti-inflammatory treatment [28]. It is believed that IL-6 play a key role to incite the inflammatory cytokine storm, which may cause eventual pulmonary fibrosis and organ failure [35]. The significantly increased IL-6 level in COVID-19 patients was found to closely correlate with acute respiratory distress syndrome (ARDS) severity and outcome [28]. Moreover, preliminary clinical data showed the effective treatment of severe and critical COVID-19 patients by a recombinant humanized anti-human IL-6 receptor monoclonal antibody tocilizumab, suggesting the potential therapeutic strategy via interfering of IL-6 [35]. Coincide with this IL-6 targeting strategy, the present study demonstrated substantial reducing effect of BPE on poly (I:C)-induced IL-6 production both *in vivo* (BALF and immunohistochemistry staining of lung section) and *in vitro* (A549 epithelial-like, WI-38 fibroblast, and RAW 264.7 macrophage-like cells). These IL-6 suppressing effects further suggest the possibility of BPE to reduce the aforementioned cytokine storm. In addition to the antibody against IL-6, a case series study reported that RANTES (chemokine ligand 5, CCL5)-specific antibody leronlimab clinically improved critically COVID-19 patients and reduced the elevated plasma IL-6 and RANTES [36]. In line with this, BPE suppressed both elevations of RANTES and IL-6 in the BALF from poly (I:C)-treated mice, implying a compelling anti-inflammation effect it exerted.

Musa species products have been shown to suppress pro-inflammatory IL-6 in isoproterenol-induced hypertrophy rat heart, lipopolysaccharide (LPS)-treated embryonic rat heart cell line [16], and the wounds of diabetic rats [15]. Parallelly, other researchers reported that *Musa* species products inhibited pro-inflammatory NF-κB activity in rat oral mucosal wound [37] and in BALF cells from ovalbumin-stimulated mice [17]. Yet, the effects of *Musa* species products on IL-6 level and NF-κB activity were not simultaneously analyzed in these above studies. The present study demonstrated remarkable suppressing effects of BPE against viral mimetic poly(I:C)-induced NF-κB activation and IL-6

production in mice. The crucial role of NF-κB inhibition in reducing highly pro-inflammatory cytokine such as IL-6 has been recently highlighted for treatment of critical stage COVID-19 patients [38]. Inhibition of NF-κB was found to suppress both virus- and LPS-induced cytokine storm, and was proposed as a potential strategy for critical COVID-19 patients' treatment [38]. In contrast to blocking single targets of inflammatory cytokine cascade, inhibition of NF-κB pathway provides the potential to simultaneously inhibit multiple strongly pro-inflammatory cytokines and chemokines, as well as adhesion molecules incressed during acute COVID-19 stages [38]. In accordance with this notion, upon inhibiting NF-κB, BPE markedly suppressed the elevation of multiple pro-inflammatory cytokines and chemokines in the BALF from poly (I:C)-stimulated mice. Of note, impressively decreased mortality has been observed in COVID-19-infected patients treated by various approved medications with implicated NF-κB suppressing activity, such as Aspirin [39], Bruton tyrosine kinase inhibitors (e.g. Ibrutinib, Acalabrutinib) [40,41], Dexamethasone [42], and N-acetyl-cysteine [43]. Nevertheless, treatments by above medications so far could not completely prevent the mortality of COVID-19 patients yet [43,44]. The central role of NF-κB activation in the progression of acute pneumonia inflammation has been demonstrated by several studies [45]. Considering the substantial effect of BPE on NF-κB inhibition, it might hopefully be used as a complimentary for overcoming the limitation of those aforementioned NF-κB therapeutics in the treatment of severe pneumonia inflammation.

A previous study by Panda et al. had showed the antiviral activity of different plant parts of banana (*Musa* spp.) [46]. In addition to aforementioned anti-inflammatory effects, BPE might also exhibit antiviral activity upon treatment of viral pneumonia. Compared to other natural plant extracts with antiviral or anti-inflammatory activity alone, treatment with BPE might exhibit both activities to combat viral pneumonia. It is worthy to investigate the antiviral activities of BPE in the future work for further demonstrating its potential in integrative treatment or prevention of viral pneumonia.

Like that reported in a previous study [47], poly (I:C) elevated the mRNA levels of both IL-6 and IL-10 in RAW 264.7 cells cultured *in vitro*. However, in the mouse model of this study, poly (I:C) challenge elevated pro-inflammatory IL-6 but diminished the anti-inflammatory IL-10 protein levels in lung tissue and BALF evidenced by immunohistochemistry and ELISA analyses, respectively. The mechanism underlying this unexpected result is unclear. Intriguingly, treatment with BPE not only repressed the elevated IL-6 but also restored the diminished IL-10 in the lung tissues and BALFs form poly (I:C)-stimulated mice. Upregulating IL-10 production was reported to ameliorate bacterial outer membrane vesicle-induced sepsis in mice [48], thus raising the possibility that the increased IL-10 contributed to BPE-mediated anti-inflammation effects in this study. However, besides IL-10's classical anti-inflammatory actions, a nonclassical pro-inflammatory effects of IL-10 was also proposed to explain the drastic early increased IL-10 in severe cases of COVID-19 [49]. Further mechanistic studies will be needed to investigate the exact role of BPE-restored IL-10 in treating viral pneumonia inflammation.

On the other hand, repressing the activity of pro-inflammatory cytokines has ameliorated diabetic wound healing in both animal models and humans [50]. Human diabetic foot ulcers have decreased IL-10 level [50,51], and increasing IL-10 was proposed as an interesting option to improve healing of diabetic wounds [50]. A previous study by Cheng et al. demonstrated that wound healing in diabetic rats was promoted by this water-soluble extract of *Musa paradisiaca* (Linn), BPE [15]. The restored IL-10 by BPE found in this study might also occur in Cheng et al.'s study and participate in promoting wound healing in diabetic rats. The IL-10 restoring effect of BPE might be useful for maintaining physiological balance of host inflammatory response. Nevertheless, like the aforementioned paradoxical role of IL-10 in viral pneumonia inflammation, a recent study showed that IL-10 level was increased in diabetic wound during the acute phase of healing, and blocking IL-10 signaling during this phase stimulated healing, accompanied by increased scarring [52]. Given these conflict views of IL-10 in anti-inflammation [49] and wound healing [52], a more nuanced appreciation of BPE-restored IL-10 is needed for its application to adequately manipulate IL-10 in a contextualized manner.

Conclusions

For the first time, the remedial effect of *Musa* species product, BPE, was demonstrated in viral mimetic poly(I:C)-induced acute pulmonary inflammation in mice. The possible underlying mechanisms were proposed as shown in scheme 1. Experimental results of this study unveil the capability of BPE to suppress poly(I:C)-induced activation of NF-κB and p38 MAPK signaling as well as the subsequent productions of IL-6 and pro-inflammatory mediators. Some effects of BPE observed in this study were not dose-dependent. This phenomenon was also shown in a previous study

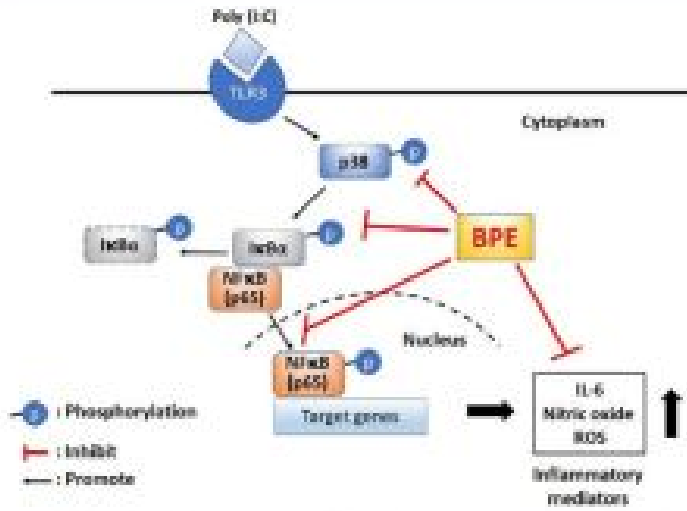

Scheme 1. Proposed positive molecular mechanisms of BPE to suppress poly (I:C)-induced inflammatory responses. BPE: banana plant extract; TLR3: Toll-like receptor 3; ROS: reactive oxygen species.

describing the wound healing promoting effect of BPE in diabetic rats [15]. It might due to the complex components contented in BPE and the uncertain interactions between the components at various diluted concentrations. Further studies are under way to address this issue. As such, further satisfactory preclinical assessment to optimize the dosage, start, and duration of BPE treatment is required to evaluate its safety and efficacy as an integrative adjuvant for improving the management of viral pulmonary inflammation.

Supplementary Material

Supplementary table.
https://www.medsci.org/v21p0107s1.pdf

Acknowledgments

This research was supported by a research grant from Wan Fang Hospital, Taipei Medical University, Taipei, Taiwan (110-eva-03) and a joint grant of Wan Fang Hospital and Cody and Brody Co., Ltd., Taipei, Taiwan (W475).

Institutional Review Board Statement

All mice experiments were approved by protocol number # CMR-AP109092901 and followed the guidelines of the Care and Use of Laboratory animals and the Institutional Animal Care and Use Committee of Chimera Bioscience.

Author Contributions

Conceptualization, C.-H.L. and T.-Y.L.; methodology, C.-H.L., Y.-Y.L., T.-H.C. and S.-Y.W.; investigation, Y.-C.L., T.-J.C., T.-Y.L., Y.-Y.L., W.-L.T. and C.-J.Y.; execution of experiments, C.-H.L., Y.-Y.L., T.-H.C. and S.-Y.W.; resources, F.L.; writing—review and editing, G.-M.L., T.-J.C. and C.-J.Y.; supervision, T.-J.C. and J.W.-P.; project administration, Y.-Y.L. and C.-J.Y.; funding acquisition, G.-M.L. and C.-J.Y. All authors have read and agreed to the published version of the manuscript.

Competing Interests

This work was partially supported by a joint grant from Wan Fang Hospital, Taipei Medical University and Cody and Brody Co., Ltd., Taipei, Taiwan (W475). Ci-Ming Lai and Chih-Jung Yao are the Principal Investigator and Co-Principal Investigator of the Grant W475, respectively. Frank Liu owns the patent for the extract technology of BPE. The funders had no role in the design, interpretation of data, writing of the manuscript, or decision to publish the results.

References

1. Gao L, Wei D, Zhang X, Wu Y, Li Q, Zhou M, et al. Clinical Features Predicting Mortality Risk in Patients With Viral Pneumonia: The MuLBSTA Score. Front Microbiol. 2019; 10: 2752.
2. Pandey P, Kanapuli G. Targeting tumour necrosis factor to ameliorate viral pneumonia. FEBS J. 2022; 289: 885-900.
3. Pandey P, Al Rumaih Z, Kale MT, Ng E, Ke R, Chaudhri G, et al. Targeting avirulent virus and TNF/NF-kappaB or STAT3 signaling for effective treatment of viral pneumonia. Proc Natl Acad Sci U S A. 2022; 119: e2122725119.
4. Li Q, Zhang T, Wang Y, Yang S, Luo J, Tang T, et al. Qing-Wen-Bu-Fei Mixture Ameliorates Poly (I:C)-Induced Viral Pneumonia Through

Regulating the Inflammatory Response and Serum Metabolism. Front Pharmacol. 2022; 13: 891871.
5. Alon R, Sportiello M, Kozlovski S, Kumar A, Reilly EC, Zarbock A, et al. Leukocyte trafficking to the lungs and beyond: lessons from influenza for COVID-19. Nat Rev Immunol. 2021; 21: 49-64.
6. Cai J, Gao L, Li Y, Fan T, Qu L, Sun Y, et al. Andrographolide sulfate inhibited NF-kappaB activation and alleviated pneumonia induced by poly I:C in mice. J Pharmacol Sci. 2020; 144: 189-96.
7. Huang C, Wang Y, Li X, Ren L, Zhao J, Hu Y, et al. Clinical features of patients infected with 2019 novel coronavirus in Wuhan, China. Lancet. 2020; 395: 497-506.
8. Dadhwal K, Stonham R, Breen H, Poole S, Saeed K, Dushianthan A. Severe COVID-19 pneumonia in an intensive care setting and comparisons with historic severe viral pneumonia due to other viruses. Clin Respir J. 2022; 16: 801-8.
9. Hojyo S, Uchida M, Tanaka K, Hasebe R, Tanaka Y, Murakami M, et al. ... [illegible] ...
9. Heimfarth L, Serafini MR, Martins-Filho PR, Quintans JSS, Quintans-Junior LJ. Drug repurposing and cytokine management in response to COVID-19: A review. Int Immunopharmacol. 2020; 88: 106947.
10. Heimfarth L, Serafini MR, Martins-Filho PR, Quintans JSS, Quintans-Junior LJ. Drug repurposing and cytokine management in response to COVID-19: A review. Int Immunopharmacol. 2020; 88: 106947.
11. Thomas E, Stewart LE, Darley BA, Pham AM, Esteban I, Panda SS. Plant-Based Natural Products and Extracts: Potential Source to Develop New Antiviral Drug Candidates. Molecules. 2021; 26: 6197.
12. Giordano D, Facchiano A, Carbone V. Food Plant Secondary Metabolites Antiviral Activity and Their Possible Roles in SARS-CoV-2 Treatment: An Overview. Molecules. 2023; 28: 2470.
13. Azab A, Nassar A, Azab AN. Anti-Inflammatory Activity of Natural Products. Molecules. 2016; 21: 1321.
14. Lopes SM, de Medeiros HIR, Scotti MT, Scotti L. Natural Products Against COVID-19 Inflammation: A Mini-Review. Comb Chem High Throughput Screen. 2022; 25: 2358-69.
15. Cheng Y-Z, Liu I-M, Cheng J-T, Lin B-S, Liu F. Wound healing is promoted by Musa paradisiaca (banana) extract in diabetic rats. Archives of Medical Science. 2020; 1-9.
16. Kumari S, Katare PB, Elancheran R, Nizami HL, Paramesha B, Arava S, et al. Musa balbisiana Fruit Rich in Polyphenols Attenuates Isoproterenol-Induced Cardiac Hypertrophy in Rats via Inhibition of Inflammation and Oxidative Stress. Oxid Med Cell Longev. 2020; 2020: 7147498.
17. Gadelha FAAF, Cavalcanti RFP, Vieira GC, Ferreira LKDP, de Sousa GR, Filho JMB, et al. Immunomodulatory properties of Musa paradisiaca L. inflorescence in Combined Allergic Rhinitis and Asthma Syndrome (CARAS) model towards NFκB pathway inhibition. Journal of Functional Foods. 2021; 83: 104540.
18. Stowell NC, Seideman J, Raymond HA, Smalley KA, Lamb RJ, Egenolf DD, et al. Long-term activation of TLR3 by poly(I:C) induces inflammation and impairs lung function in mice. Respir Res. 2009; 10: 43.
19. Harris P, Sridhar S, Peng R, Phillips JE, Cohn RG, Burns L, et al. Double-stranded RNA induces molecular and inflammatory signatures that are directly relevant to COPD. Mucosal Immunol. 2013; 6: 474-84.
20. Guide for the Care and Use of Laboratory Animals. 8th ed. Washington (DC); 2011.
21. Starkhammar M, Kumlien Georén S, Swedin L, Dahlén SE, Adner M, Cardell LO. Intranasal administration of poly(I:C) and LPS in BALB/c mice induces airway hyperresponsiveness and inflammation via different pathways. PLoS One. 2012; 7: e32110.
22. Huang JS, Yao CJ, Chuang SE, Yeh CT, Lee LM, Chen RM, et al. Honokiol inhibits sphere formation and xenograft growth of oral cancer side population cells accompanied with JAK/STAT signaling pathway suppression and apoptosis induction. BMC Cancer. 2016; 16: 245.
23. Duan M, Steinfort DP, Smallwood D, Hew M, Chen W, Ernst M, et al. CD11b immunophenotyping identifies inflammatory profiles in the mouse and human lungs. Mucosal Immunol. 2016; 9: 550-63.
24. Feng G, Jiang ZY, Sun B, Fu J, Li TZ. Fisetin Alleviates Lipopolysaccharide-Induced Acute Lung Injury via TLR4-Mediated NF-kappaB Signaling Pathway in Rats. Inflammation. 2016; 39: 148-57.
25. Wu G, Zhu Q, Zeng J, Gu X, Miao Y, Xu W, et al. Extracellular mitochondrial DNA promote NLRP3 inflammasome activation and induce acute lung injury through TLR9 and NF-kappaB. J Thorac Dis. 2019; 11: 4816-28.
26. Li HT, Ye C, Zhou M, Yang Y, Jin Q, Pan CF. Moxifloxacin suppresses airway inflammation and modulates expression of caveolin-1 and flotillin-1 in airway smooth muscle cells of asthmatic rats. Ann Transl Med. 2019; 7: 649.
27. Giridharan S, Srinivasan M. Mechanisms of NF-kappaB p65 and strategies for therapeutic manipulation. J Inflamm Res. 2018; 11: 407-19.
28. Huang Q, Wu X, Zheng X, Luo S, Xu S, Weng J. Targeting inflammation and cytokine storm in COVID-19. Pharmacol Res. 2020; 159: 105051.
29. Liu Z, Ying Y. The Inhibitory Effect of Curcumin on Virus-Induced Cytokine Storm and Its Potential Use in the Associated Severe Pneumonia. Front Cell Dev Biol. 2020; 8: 479.
30. Mulkeen T, Kita H, O'Grady SM. TLR3-activation evokes IL-6 secretion, autocrine regulation of Stat3 signaling and TLR2 expression in human bronchial epithelial cells. J Cell Commun Signal. 2013; 7: 109-18.
31. Liu SF, Ye X, Malik AB. Inhibition of NF-kappaB activation by pyrrolidine dithiocarbamate prevents In vivo expression of proinflammatory genes. Circulation. 1999; 100: 1330-7.
32. DiDonato JA, Mercurio F, Karin M. Phosphorylation of I kappa B alpha precedes but is not sufficient for its dissociation from NF-kappa B. Mol Cell Biol. 1995; 15: 1302-11.
33. Shuto T, Xu H, Wang B, Han J, Kai H, Gu XX, et al. Activation of NF-kappa B by nontypeable Hemophilus influenzae is mediated by toll-like receptor 2-TAK1-dependent NIK-IKK alpha /beta-I kappa B alpha and MKK3/6-p38 MAP kinase signaling pathways in epithelial cells. Proc Natl Acad Sci U S A. 2001; 98: 8774-9.
34. Gao X, Chan PKS, Lui GCY, Hui DSC, Chu IM, Sun X, et al. Interleukin-38 ameliorates poly(I:C) induced lung inflammation: therapeutic implications in respiratory viral infections. Cell Death Dis. 2021; 12: 53.
35. Xu X, Han M, Li T, Sun W, Wang D, Fu B, et al. Effective treatment of severe COVID-19 patients with tocilizumab. Proc Natl Acad Sci U S A. 2020; 117: 10970-5.
36. Agresti N, Lalezari JP, Amodeo PP, Mody K, Mosher SF, Seethamraju H, et al. Disruption of CCR5 signaling to treat COVID-19-associated cytokine storm: Case series of four critically ill patients treated with leronlimab. J Transl Autoimmun. 2021; 4: 100083.
37. Apriasari ML, Pramitha SR, Puspitasari D, Ernawati DS. Anti-Inflammatory Effect of Musa acuminata Stem. Eur J Dent. 2020; 14: 294-8.
38. Kircheis R, Haasbach E, Lueftenegger D, Heyken WT, Ocker M, Planz O. NF-kappaB Pathway as a Potential Target for Treatment of Critical Stage COVID-19 Patients. Front Immunol. 2020; 11: 598444.
39. Chow JH, Khanna AK, Kethireddy S, Yamane D, Levine A, Jackson AM, et al. Aspirin Use Is Associated With Decreased Mechanical Ventilation, Intensive Care Unit Admission, and In-Hospital Mortality in Hospitalized Patients With Coronavirus Disease 2019. Anesth Analg. 2021; 132: 930-41.
40. Treon SP, Castillo JJ, Skarbnik AP, Soumerai JD, Ghobrial IM, Guerrera ML, et al. The BTK inhibitor ibrutinib may protect against pulmonary injury in COVID-19-infected patients. Blood. 2020; 135: 1912-5.
41. Roschewski M, Lionakis MS, Sharman JP, Roswarski J, Goy A, Monticelli MA, et al. Inhibition of Bruton tyrosine kinase in patients with severe COVID-19. Sci Immunol. 2020; 5: eabd0110.
42. Group RC, Horby P, Lim WS, Emberson JR, Mafham M, Bell JL, et al. Dexamethasone in Hospitalized Patients with Covid-19. N Engl J Med. 2021; 384: 693-704.
43. Assimakopoulos SF, Aretha D, Komninos D, Dimitropoulou D, Lagadinou M, Leonidou L, et al. N-acetyl-cysteine reduces the risk for mechanical ventilation and mortality in patients with COVID-19 pneumonia: a two-center retrospective cohort study. Infect Dis (Lond). 2021; 53: 847-54.
44. Kircheis R, Haasbach E, Lueftenegger D, Heyken WT, Ocker M, Planz O. NF-κB Pathway as a Potential Target for Treatment of Critical Stage COVID-19 Patients. Front Immunol. 2020; 11: 598444.
45. Liu H, Wang W, Shen W, Wang L, Zuo Y. ARHGAP18 ameliorates inflammatory response through inactivating Rac1/Akt/NF-kappaB pathway in acute pneumonia model of rat. Ann Transl Med. 2020; 8: 1209.
46. Panda SK, Castro AHF, Jouneghani RS, Leyssen P, Neyts J, Swennen R, et al. Antiviral and Cytotoxic Activity of Different Plant Parts of Banana (Musa spp.). Viruses. 2020; 12: 549.
47. Ko R, Park JH, Ha H, Choi Y, Lee SY. Glycogen synthase kinase 3beta ubiquitination by TRAF6 regulates TLR3-mediated pro-inflammatory cytokine production. Nat Commun. 2015; 6: 6765.
48. Park KS, Svennerholm K, Shelke GV, Bandeira E, Lässer C, Jang SC, et al. Mesenchymal stromal cell-derived nanovesicles ameliorate bacterial outer membrane vesicle-induced sepsis via IL-10. Stem Cell Res Ther. 2019; 10: 231.
49. Mars H, Chamberlain TC, Mui AL, Little JP. Elevated Interleukin-10 Levels in COVID-19: Potentiation of Pro-Inflammatory Responses or Impaired Anti-Inflammatory Action? Front Immunol. 2021; 12: 677008.
50. Decker C, Sherwick LP. The cytokine milieu of diabetic wounds. Diabetes management. 2015; 5: 525-37.

51. Nanda R, Patel S, Ghosh A, Asha HS, Mohapatra E. A study of apolipoproteins A1(ApoA1) and interleukin 1RL-1R) in diabetes with foot ulcers. Biomedicine (Taipei). 2022; 12: 10-8.
52. Roy S, Zeyen J, Mohamed MF, Aboonabi A, Delgado K, Wallace L, et al. IL-1R Dysregulation Underlies Chemokine Insufficiency, Delayed Macrophage Response, and Impaired Healing in Diabetic Wounds. J Invest Dermatol. 2022; 142: 690-700 e10.

（三）開發BPE應用於癌症整合療法

天然物萃取物 BPE 生物效应的开发应用

前言：

先期研究已表明 BPE 可抑制病毒相似物 Poly (I:C)在小鼠诱导之急性肺炎，其分子机转为抑制 Poly (I:C) 引起之 NFκB 活化与 IL-6 (白介素-6)、Chemokine ligand 5 (CCL5; RANTES)和 monocyte chemotactic protein (MCP)-1、Plasminogen activator inhibitor-1 (PAI-1, 胞浆素原活化抑制剂-1) 等发炎因子，并提升抗发炎因子 IL-10(白介素-10) 的表现。PAI-1 的失调与癌症、发炎、老化、糖尿病及心血管疾病关系密切 (Int J Mol Sci 22(5): 2721, 2021)。已有許多 PAI-1 抑制劑正被合成研發中，因此值得开发 BPE 应用于防治这些疾病的生物效应。

主要研究方向

1. BPE 倍增维生素 D3 对急性骨髓性白血病 (acute myeloid leukemia, AML) 之分化诱导效用。

急性骨髓性白血病 (AML) 是一种成人急性白血病，即使透过标准治疗后，56 岁以上的患者仅有 20%超过 2 年以上的存活率 (Semin Hematol 43: 89 - 95, 2006)。分化诱导的治疗方式已可有效地治疗 acute promyelocytic leukemia (APL) 类型的白血病，但仍无法用於 AML 白血病的治疗 (Cancer Res 76(9): 2743–2753, 2016)。维生素 D3 (1,25-dihydroxyvitamin D3, Vit D3) 可诱导 AML 白血病细胞分化，但其剂量受限于高血钙症的副作用，临床效果大為受限 (Cancer Lett 319: 8–22, 2012)。最近文献表明，并用 glycogen synthase kinase 3 (肝醣合成酶激酶 3, GSK-3) 抑制剂可显著增强维生素 D3 对 AML 白血病细胞之分化诱导作用，展现了分化治疗 (differentiation-based therapy) 應用於 AML 白血病的新希望 (Cancer Res 76(9): 2743–2753, 2016)。有许多化学合成 GSK-3 抑制剂已进入临床试验，然而皆未被 FDA 核准使用 (Sci. Transl. Med 10: eaam8460, 2018)。我们的研究发现，萃取自可食用之天然物的 BPE 可诱导 AML 细胞株 (THP-1) 之分化标记 CD14 和 CD11b 蛋白的表现 (图一) 以及朝向分化的细胞形态 (图二)。

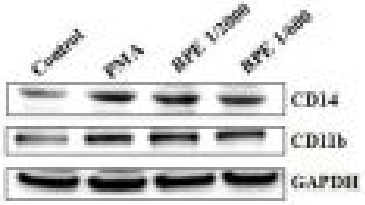

* CD14 which is upregulated primarily during monocytic differentiation
* CD11b, which is upregulated during myelomonocytic differentiation

图一：在作用 96 小时后，利用西方墨点法发现 PMA (5 ng/mL)与 BPE 皆能增加 AML 细胞(THP-1)之分化指标 CD14 与 CD11b 的蛋白表现。

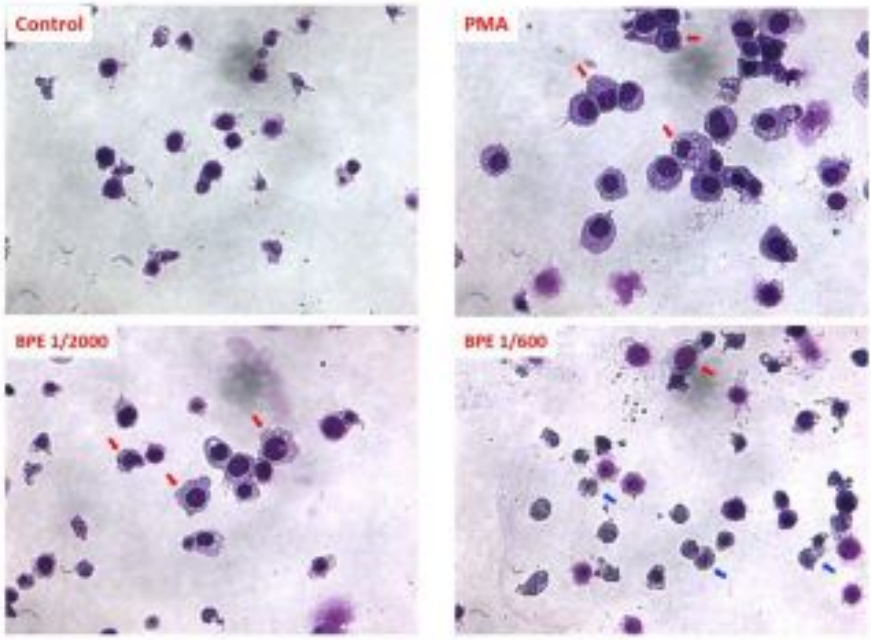

图二: BPE 诱导 AML 细胞株 (THP-1) 的细胞形态变化。正对照组 (phorbol-12-myristate-13-acetate, PMA 处理组) 或不同稀释浓度的 BPE 处理 THP-1 细胞 144 小时后。透过 Diff-Quick staining 染色发现，PMA 能使 THP-1 细胞型态改变，如细胞质变多和产生空泡状 (红色箭头标示)。同时也发现 1/2000 稀释的 BPE 使细胞产生细胞质变多和产生空泡状 (红色箭头标示)，而 1/600 的 BPE 使部分细胞产生细胞质变多和产生空泡状 (红色箭头标示)，也发现此浓度造成细胞破损有死亡的现象 (蓝色箭头标示)。

更值得注意的是，BPE 能显著地倍增维生素 D3 对 THP-1 AML 细胞的分化诱导作用，低剂量维生素 D3 (25 nM) 可增加分化标记 CD14 基因的表现 43.4 倍，并用 BPE 之后则增加为 971.7 倍 (图三)。这结果显示了 BPE 并用低剂量维生素 D3 应用于 AML 白血病之分化治疗的应用潜力。

AML 的市场评估

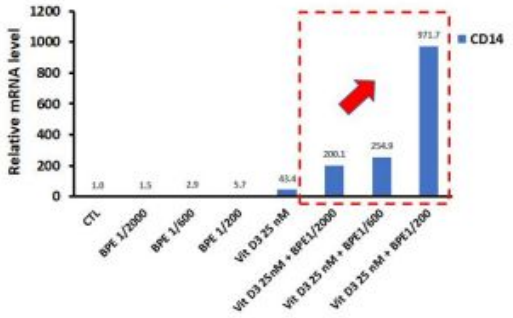

图三: BPE 能显著地倍增维生素 D3 对 THP-1 AML 细胞的分化诱导作用，低剂量维生素 D3 (25 nM)可增加分化标记 CD14 基因的表现 43.4 倍，并用 BPE 之后则增加为 971.7 倍。

2. BPE 降低化疗药在癌细胞引起之老化效应 (Therapy-induced senescence, TIS)。

近期文献表明，化疗药物在治疗过程中会使癌细胞产生老化现象，称为 Therapy-induced senescence (TIS)。老化的癌细胞会分泌 IL-6, PAI-1 等 senescence associated secretory phenotype (SASP, 衰老相关的分泌性蛋白) 相关的介质 (EMBO Reports 19: e44722, 2018)，进而促进转移、复发、抗药性与癌干细胞表征而使癌症更趋恶性 (aggressiveness) (Front Cell Dev Biol 9:722205, 2021; Cell Metab 27(4): 710-711, 2018)。因此，如何在不影响化疗药效用的前提下，防止 TIS 现象产生的危害，是当今癌症化学治疗急待克服的一大瓶颈。我们的研究发现，BPE 不仅能增强化疗药物 gemcitabine 与 oxaliplatin 对胰脏癌抗药细胞株的生长抑制作用 (图四，专利申请中)，亦能减低上述化疗药在胰脏癌抗药细胞株诱导的细胞老化 (cellular senescence) (图五)。再者，NFκB 是引起 SASP 的关键转录因子 (Front Cell Dev Biol 9:722205, 2021; Cell Metab 27(4): 710-711, 2018)，而 PAI-1 是已知的促进 senescence (老化) 因子 (EMBO Reports 19: e44722, 2018)，因此图五的实验结果亦和我们先前发现之 BPE 抑制 Poly (I:C) 诱升 NF κ B 活性与 PAI-1 的效用相互吻合与呼应。

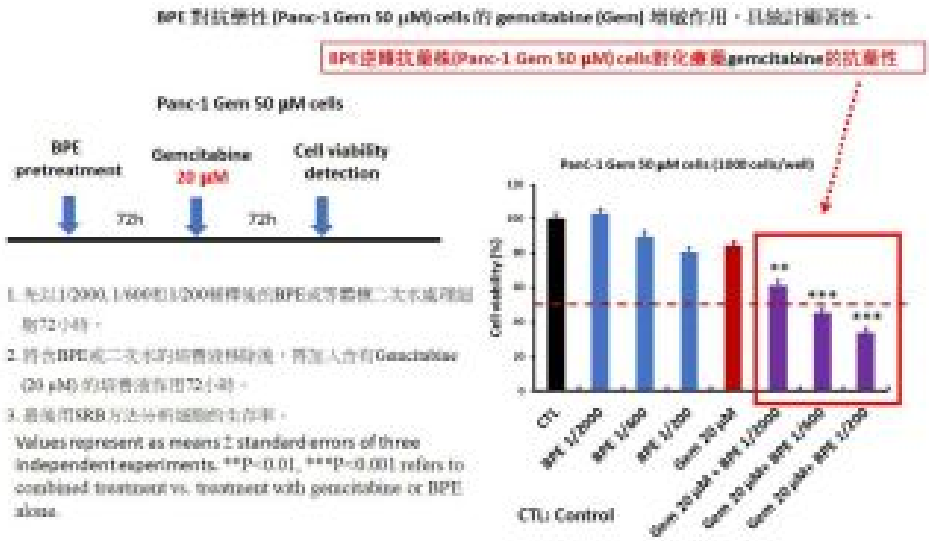

图四: BPE 增强化疗药物 gemcitabine 与 oxaliplatin 对胰脏癌抗药细胞株的生长抑制作用。

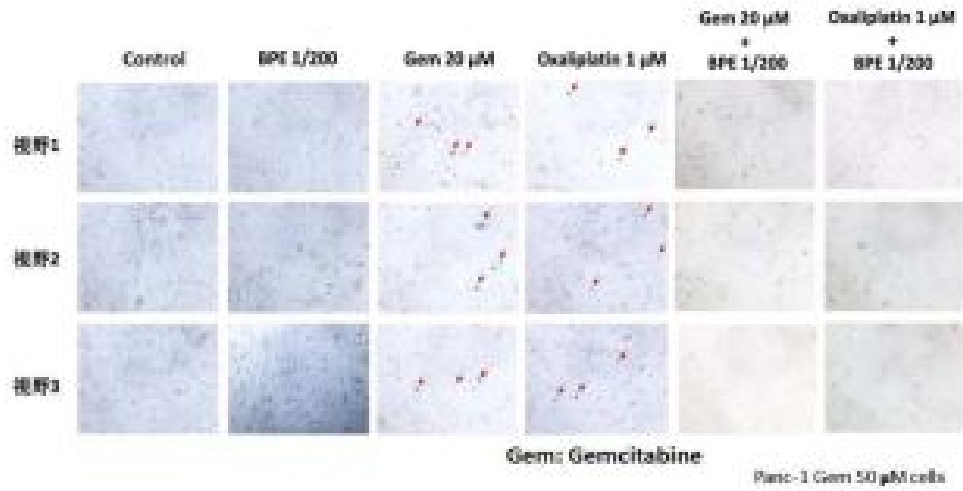

圖五: BPE 抑制化疗药引起胰脏癌抗药性细胞(Panc-1 Gem 50 μM cells) 的细胞老化 (cellular senescence)。化疗药物 Gemcitabine 与 Oxaliplatin 于胰脏癌抗药性细胞株(Panc-1 Gem 50 μM cells)作用 72 小时后，以 SA-β-galactosidase 试剂染色后，发现呈现蓝色反应的衰老癌细胞 (红色箭头指示)。而有前处理 BPE 72 小时后再分别处理 Gemcitabine 或 Oxaliplatin 的组别经 SA-β-galactosidase 试剂染色后，并无发现呈现蓝色反应的衰老癌细胞。显示 BPE 能抑制上述化疗药物引起的癌细胞老化反应。

3. BPE 之 GSK-3 抑制效应开发 (抗发炎、抗癌、免疫调控、防止神经退化)。

Glycogen synthase kinase 3 (GSK-3, 肝醣合成酶激酶 3) 调控着许多的生理机能，失控的 GSK-3 与发生癌症、发炎、神经退化、心血管病变、糖尿病等许多疾病相关 (Pharmacology & Therapeutics 148: 114-131, 2015)。已有文献表明 GSK-3 抑制剂可显著增强维生素 D3 对 AML 白血病细胞之分化诱导作用 (Cancer Res 76(9): 2743–53, 2016)，也有文献指出 GSK-3 抑制剂可降低细菌内毒素 (lipopolysaccharides, LPS) 诱导之发炎因子 IL-6，并同时提升抗发炎因子 IL-10 (Nat Immunol 6(8): 777-784, 2005)。呼应以上 GSK-3 抑制剂之特质，我们的研究发现 BPE 能显著地倍增维生素 D3 对 THP-1 AML 细胞的分化诱导作用 (图三)，且发现 BPE 可抑制 LPS 在肝细胞株 (L02 cells) 诱发的 IL-6 基因表现，并同时促进抗发炎因子 IL-10 的基因表现 (图六)。这些结果显示 BPE 作为天然 GSK-3 抑制剂的应用潜力。因 GSK-3 抑制剂的应用范围广大，许多化学合成 GSK-3 抑制剂被研发合成，有数个已进入临床试验阶段，然而皆未被 FDA 核准使用 (Sci. Transl. Med. 10, eaam8460, 2018)。BPE 萃取自可食用之天然物，相对于上述化学合成 GSK-3 抑制剂，将有更大的临床应用价值，值得进一步研究开发。

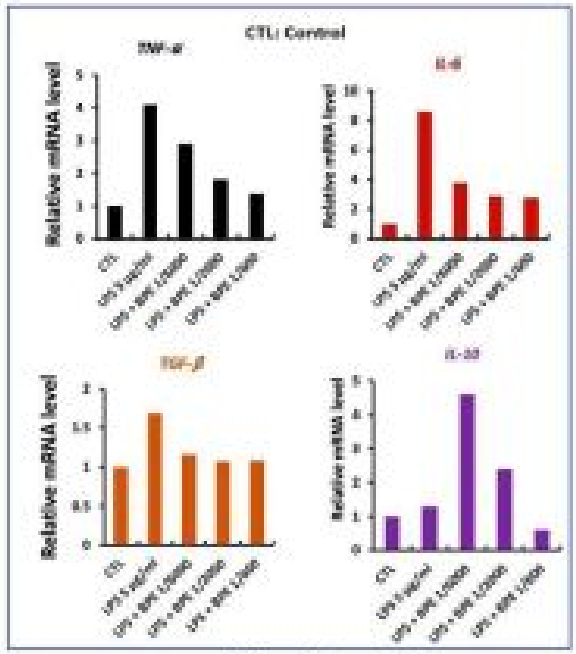

图六: BPE 抑制 LPS 在肝细胞株 (L02 cells) 诱发的发炎因子 IL-6 基因表现，并同时促进抗发炎因子 IL-10 的基因表现。

（四）修培刻灵蕉仙素初步药效学实验结果

修培刻灵蕉仙素初步药效学实验结果

一、修培刻灵蕉仙素冻干粉的制备

17mL修培刻灵蕉仙素溶液冷冻干燥24h，得冻干粉302.0mg粉末**(易吸潮)。**

图 1修培刻灵蕉仙素冻干粉

二、修培刻灵蕉仙素药效学初步研究

1.修培刻灵蕉仙素显著抑制肿瘤细胞的增殖

采用 MTT 方法观察修培刻灵蕉仙素对结肠癌细胞(HCT116 和 Caco2)和肝癌细胞(Hepg2)增殖的影响。修培刻灵蕉仙素浓度梯度为 0.0005、0.0015、0.0046、0.0137、0.0412 、 0.1235 、0.3704 、1.1111 、3.3333 、10 、20 mg/mL，结果发现：**修培刻灵蕉仙素对结肠癌 细胞(**HCT116 **和** Caco2**) 和肝癌细胞(**HEPG2**)增殖有显著的抑制作用，**其 对结肠癌 HCT116 细胞 IC_{50}=1.085 ± 0.024 mg/mL ；对结肠癌 Caco2 细胞 IC_{50}=1.021±0.014 mg/mL；对肝癌 Hepg2 细胞 IC_{50}=1.981±0.028 mg/mL；(见图 2)

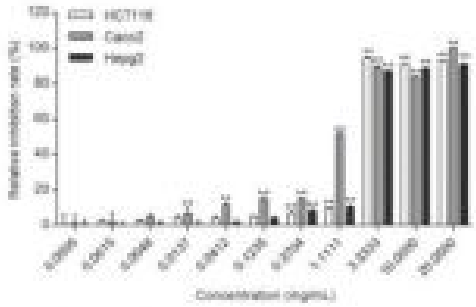

图 2 修培刻灵蕉仙素显著抑制肿瘤细胞的增殖

**P<0.01 vs. Control

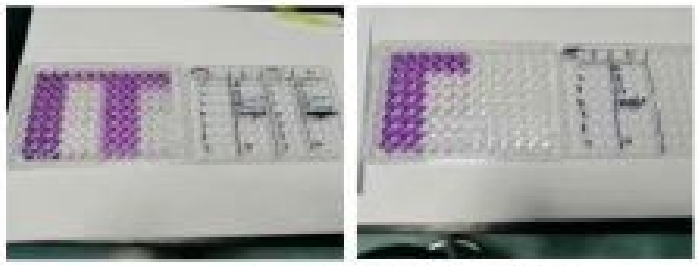

图 3 修培刻灵蕈仙素 MTT 实验照片

2.修培刻灵蕈仙素显著抑制结肠癌 HCT116 细胞的迁移

采用 Transwell 小室实验，观察修培刻灵蕈仙素对结肠癌 HCT116 细胞迁移的影响。依据 MTT 结果，采用 1 、0.5 、0.25 mg/mL 浓度修培刻灵蕈仙素处理结肠癌 HCT116 细胞 24 h 和 48 h 后，观察结肠癌 HCT116 细胞迁移的变化。结果表明：**修培刻灵蕈仙素对结 肠癌** HCT116 **细胞迁移有显著的抑制作用(见图4)。**

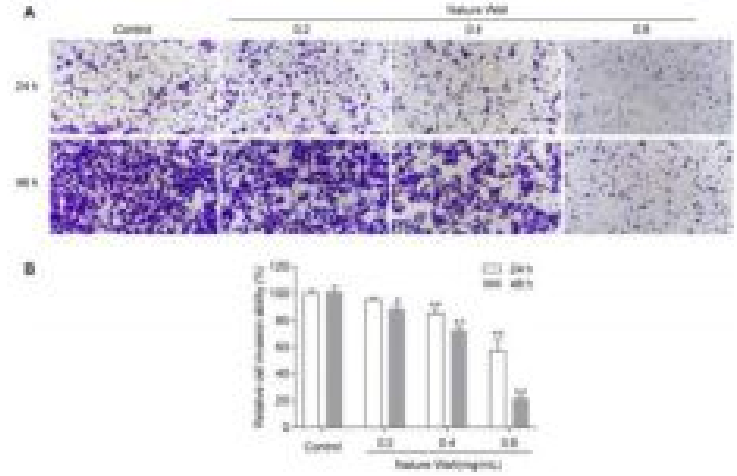

图 4 修培刻灵蕈仙素显著抑制结肠癌 HCT116 细胞迁移能力

A：细胞迁移实验，紫色为迁移的细胞；B：迁移能力数据统计；*P<0.05 vs Control ；**P<0.01 vs Control

（五）一种量子化大蕉（MUSA SAPIENTUM）果提取物抗流感病毒 药效学研究

一种量子化大蕉（MUSA SAPIENTUM）果提取物抗流感病毒药效学研究

范祥翠[1]　重庆医科大学 刘人豪[2]　美国斯坦福大学

秦银艺[3]　郑华[4]　广西修塔刻灵生物科技有限公司　广西南宁 530000

【摘要】目的：检测大蕉（MUSA SAPIENTUM）果提取物对流感病毒的抑制作 用。**方法：**采用组织细胞培养法和建立流感动物模型，对不同浓度的大蕉（MUSA SAPIENTUM）果提取物进行体内、体外抗流感病毒药效学研究。**结果：**大蕉（MUSA SAPIENTUM）果提取物体外对流感病毒一定抑制作用，可维持病毒感染后 48h。体内抗病毒试验结果显示，该提取物可有效的改善流感病毒所致的病毒性肺炎，与病毒对照组有显著差异。**结论：**大蕉（MUSA SAPIENTUM）果提取物在体内、外对流感病毒都具有一定的抑制作用，还能有效改善流感病毒所致小鼠病毒性肺炎。

【关键词】 大蕉（MUSA SAPIENTUM）果提取物；体内、体外；流感病毒；病毒性肺炎

中图文分类号：R285.5　文献标识码：A

Pharmacodynamic Study of a Quantumized Banana (MUSA SAPIENTUM) Fruit Extract as an Anti-Influenza Virus Agent

Xiangcui Fan[1], Chongqing Medical University

Renhao Liu[2], Stanford University, USA

Yinyi Qin[3], Hua Zheng[4], Guangxi Xiupaike Ling Biotechnology Co., Ltd., Nanning, Guangxi 530000

[Abstract] **Objective:** To detect the inhibitory effect of banana (MUSA SAPIENTUM) fruit extract on influenza virus. **Methods:** Tissue cell culture and the establishment of an influenza animal model were used to study the pharmacodynamics of different concentrations of banana (MUSA SAPIENTUM) fruit extract in vitro and in vivo. **Results:** The banana (MUSA SAPIENTUM) fruit extract showed a certain inhibitory effect on influenza virus in vitro, maintaining the effect for 48 hours after viral infection. The results of the in vivo antiviral tests showed that the extract could effectively improve viral pneumonia caused by influenza virus, with significant differences compared to the virus control group. **Conclusion:** The banana (MUSA SAPIENTUM) fruit extract has a certain inhibitory effect on influenza virus both in vitro and in vivo, and can effectively improve viral pneumonia caused by influenza virus in mice.

[**Keywords**] Banana (MUSA SAPIENTUM) fruit extract; in vitro and in vivo; influenza virus; viral pneumonia

Chinese Library Classification Number: R285.5　Document Identification Code: A

天然植物中含有抑菌或抗病毒成分，如锦灯笼[1]、黄芩、石韦、大青叶千金藤[2]、夏枯草、广西地不容[3]、鱼腥草、甘草、连翘、紫花地丁[4]、毛蕊花、叉唇石斛[5]等，通过其独特的药理作用，能够有效地调节人体的免疫功能，增强机体对病毒的抵抗力，在预防和治疗病毒性传染病方面具有独特的疗效和广泛的应用。本研究以特殊的大蕉果提取物为研究对象，构建流感病毒细胞及动物模型，考察该提取物对流感病毒的治疗作用，以期为后期的临床试验提供数据支撑。

（一）体外抗流感病毒试验 1. 材料与方法

1.1 材料与试剂

大蕉（MUSA SAPIENTUM）果提取物，广西修培刻灵生物科技有限公司提供；双黄连口服液，哈药集团三精制药有限公司；Vero（非洲绿猴肾细胞），上海酶联生物技术有限公司，用于流感病毒的培养；甲型流感病毒 FM1，中医科学院武汉病毒研究所；培养基，DMEM Gibco 公司；胎牛血清 Gibco 公司；0.25%胰蛋白酶-EDTA Gibco 公司。

1.2 实验方法

1.2.1 细胞准备

Vero 传代细胞培养 3-5d，达到试验标准时，加入 1ml 胰蛋白酶使其均匀分面在整个细胞层，37℃孵育细胞培养瓶直至细胞从培养瓶表面分离，弃消化液，取数毫升细胞培养液吹散细胞，计数，用培养液稀释至约 3×10^5/ml 后，接种于 96 孔培养板内，待细胞长成单层。

1.2.2 大蕉（MUSA SAPIENTUM）果提取物细胞毒性测定

用细胞维持液将大蕉（ MUSA SAPIENTUM）果提取物原液进行 2 倍递比稀释为 1g/ml、0.5g/ml、0.25g/ml、0.125g/ml、0.0625g/ml、0.03125g/ml、0.015625g/ml、0.0078g/ml；将双黄连口服液稀释为 1.5g/ml、0.75g/ml、0.375g/ml、0.1875g/ml、0.0938g/ml、0.0469g/ml，将上述不同浓度的药物分别加于 Vero 单层细胞上，每孔 0.2 ml，每个浓度 8 复孔，同时设正常细胞对照(不加药物)，37℃、5% CO_2 培养箱培养 72h，每天镜下观察细胞病变(CPE)，培养结束前 4h，吸弃培养板中液体，PBS 冲洗 3 次，每孔加入 MTT(5mg/ml)20 μl，于 37℃培养箱中培养 4h，去上清后每孔加 DMSO 100μl，微量振荡器振荡 5min，酶标读数仪比色(波长 492nm)测吸光度值，计算药物对细胞毒性浓 度，即最大无毒浓度(TC_0)。

1.2.3 大蕉（MUSA SAPIENTUM）果提取物病毒 $TCID_{50}$ 的测定

将流感病毒进行 10 倍递减稀释为 10^{-1}, 10^{-2}, 10^{-3}.....10^{-8} 不同稀释度，感染 MDCK 细胞，用 96 孔板单层培养，每个稀释度 8 个复孔，同时设正常对照(不加病毒)，观察细胞病变，用 Reed-Muench 法计算出 50%细胞感染量($TCID_{50}$)。

“-”细胞生长正常，无病变出现；“+”细胞病变占 25%以下；“++”细胞病变占 50%以下；“+++”细胞病变占 75%以下；“++++”细胞病变占 75%以上。以“++”细胞病变判定为阳性病变孔。

Reed-Muench 公式：距离比例 =（高于 50%病变率的百分 - 50%）/（高于 50%病变率的百分数 - 低于 50%病变率的百分数）

lgTCID50=距离比例 × 稀释度对数之间的差 + 高于 50%病变率的稀释度的对数

1.2.4 大蕉（MUSA SAPIENTUM）果提取物对病毒致细胞病变作用的影响

取已长满单层细胞的培养板，吸弃培养液，以 100TCID50 的流感 病毒攻击量接种细胞，37° C ,5 % CO2 培养箱吸附 2 h ,弃去病毒液，加入各药物最大无毒浓度药液 200 μ L / 孔和待测药物最大无毒浓度连续两个 2 倍递比稀释浓度，每个浓度 8 个复孔培养。同时设阳性对照药物组、细胞对照组（不加病毒不加药）、病毒对照组（加病毒但不加药物的对照组）和空白对照组（无细胞，不加病毒不加药）。 置 37° C,5% CO2 培养箱中培养 5d,每日倒置显微镜观察 CPE 并记录。

2. 结果与分析

2.1 大蕉（MUSA SAPIENTUM）果提取物细胞毒性测定结果

根据 MTT 试验结果，待测大蕉（MUSA SAPIENTUM）果提取物对 Vero 细胞最大无毒浓度（ TC_0）为 0.0625g/ml；双黄连口服液对 Vero 细胞的最大无毒浓度 TC_0为 0.0469g/ml。

2.2 大蕉（MUSA SAPIENTUM）果提取物病毒 $TCID_{50}$的测定结果

$$\text{甲型流感病毒 FM1:} \lg TCID_{50} = (-5) + \left(\frac{100-50}{100-37.5}\right) = -5.8$$

即每孔接种 0. 1ml 滴度为 $10^{-5.8}$的流感病毒可使 50%的 Vero 细胞产生明显病变。

2.3 大蕉（MUSA SAPIENTUM）果提取物对病毒致细胞病变保护作用

与病毒对照组相比，大蕉（MUSA SAPIENTUM）果提取物浓度为 0.0625g/ml 对流感病毒感染宿主细胞 24h,有很好的抑制细胞致病变效应，可维持病毒感染后 48h,但感染 72h,则没有抑制作用，具体结果见表 2。

表 2 大蕉（MUSA SAPIENTUM）果提取物对流感病毒致细胞病变作用的保护作用

病毒感染天数	双黄连口服液 g/ml	大蕉（MUSA SAPIENTUM）果提取物 g/ml			病毒对照	细胞对照
	0.0469	0.0625g	0.03125	0.015625		
1d	-	+	++++	++++	++++	-
2d	-	+++	++++	++++	++++	-
3d	-	++++	++++	++++	++++	-

备注： - 示无细胞病变； ±示有延缓细胞病变作用；+ 示 1/ 4 以下的细胞病变；＋＋示 1/4~1/2 的细胞有病变；+++示 1/2~3/4 的细胞有病变；＋＋＋＋示 3/4 以上的细胞有病变。

说明大蕉（MUSA SAPIENTUM）果提取物体外对流感病毒一定抑制作用，可维持病毒感染后 48h。

（二）体内抗流感病毒试验 1．材料与方法

1.1.1 材料与试剂：同前。

1.1.2 动物：健康 ICR 级小鼠雌雄各半，体重 18-20g 左右，雌雄分别分组，由长春市亿斯实验动物技术有限责任公司提供。

1.2 实验方法

1.2.1 测定流感病毒对小鼠半数致死量(LD_{50})

ICR 小鼠 50 只，体重 18-20g,随机平分成 5 组，流感病毒为 10^{-1}、10^{-2}、10^{-3}、10^{-4}、10^{-5} 个稀释度。小鼠经异氟烷轻度麻醉后，滴鼻感染不同稀释度的病毒液 0.mlL,正常对照组鼻腔滴入等量不含病毒的生理盐水以死亡和生存为观察指标，观察直至感染后第 14 天为止，计算出病毒的半数致死量(LD50) 。

1.2.2 体内抗病毒试验动物分组与给药方式和剂量

60 只小鼠随机平分成 6 组：正常组、病毒模型组、双黄连口服液组和大蕉（MUSA SAPIENTUM）果提取物高、中、低剂量组。于感染前一天灌胃给药，连续 7d，病毒模型组和正常对照组灌服相同体积的生理盐水。待测药大蕉（MUSA SAPIENTUM）果提取物体内高剂量 6g/kg/d，中剂量 3g/kg/d，低剂量

1.5g/kd/d；对照药双黄连口服液根据成人体内用量（按体重 60kg)折算小鼠体内用量为 13.65g/kg/d。

1.2.3 大蕉（MUSA SAPIENTUM）果提取物对流感病毒致小鼠肺炎的治疗作用

在异氟烷浅麻醉下滴鼻感染流感病毒鼠肺适应株 FM1，$15LD_{50}$，在感染后第 6d 解剖，取肺称重，逐个算出肺指数和肺指数抑制率，与病毒模型组比较，进行组间 t 检验，分别计算实验组与病毒对照组 X 的平均值、t 值和 P 值，根据统计学意义判断效果。

肺指数=小鼠肺重 / 小鼠体重×100% 肺指数抑制率=（感染模型组平均肺指数-实验组平均肺指数）/ 感染模型组平均肺指数×100%。

1.2.4 肺病变组织学和病理学检测

2，结果与分析

2.1 流感病毒小鼠的 LD50 为 $10^{-4.33}$。

2.2大蕉（MUSA SAPIENTUM）果提取物对甲型流感病毒 FM1 致小鼠肺炎的影响

采用 SPSS19.0 统计软件分别对治疗组小鼠肺指数与病毒对照组进行均值 t 检验，结果见表 3,剂量为 6g/kg 对流感病毒致小鼠肺炎有一定治疗作用。

表 3 大蕉（MUSA SAPIENTUM）果提取物对小鼠流感病毒性肺炎的作用

组别	剂量（g/kg）	动物（只）	肺指数（%）（ ±SD）	肺指数抑制率（%）	P 值
病毒对照	-	10	1.237±0.139		
正常对照	-	10	0.734±0.068		
双黄连口服液	13.65	10	0.864±0.067	30.2	<0.01
大蕉（MUSA SAPIENTUM）果提取物	6	10	1.084±0.091	36.5	<0.05
	3	10	1.229±0.159	0.65	>0.05
	1.5	10	1.232±0.078	0.40	>0.05

2.3 肺病变组织学和病理学检测结果

模型组肺脏病变主要表现为间质性肺炎，肺泡壁增厚，部分肺泡融合且充有大量炎性细胞，肺泡间隔血管充血，肺泡腔内有浆液性渗出物；支气管上皮细胞脱落到腔内，腔内充有炎性细胞和浆液性渗出物，管壁增厚，周围大量的炎性细胞浸润；与模型组肺脏相比，大蕉（MUSA SAPIENTUM）果提取物高剂量组肺脏结构有一定程度的改善，而低剂量、中剂量组肺脏组织结构无改善，见病理附图。

附：病理切片图

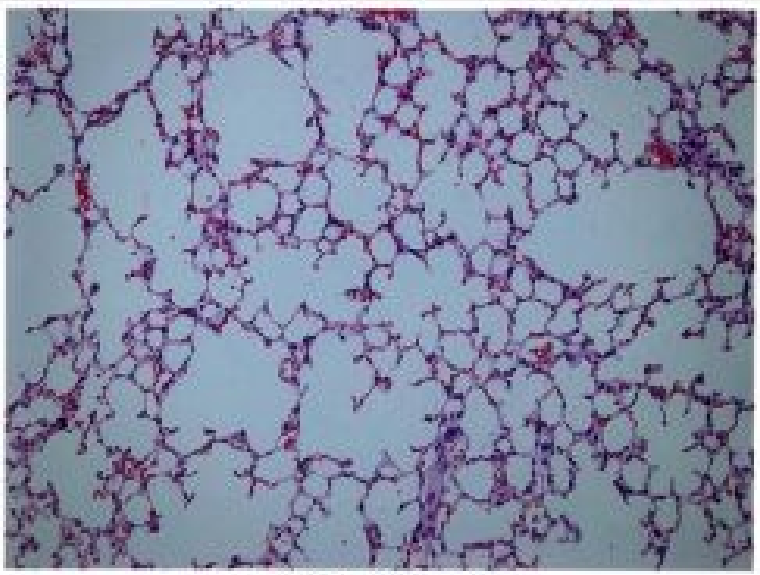

附图 1 正常组 x200

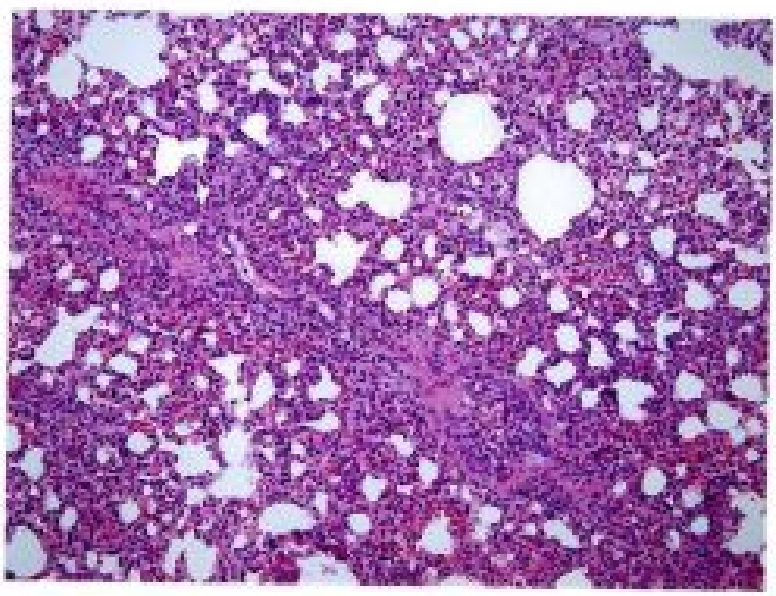

附图 2 病毒组 x200

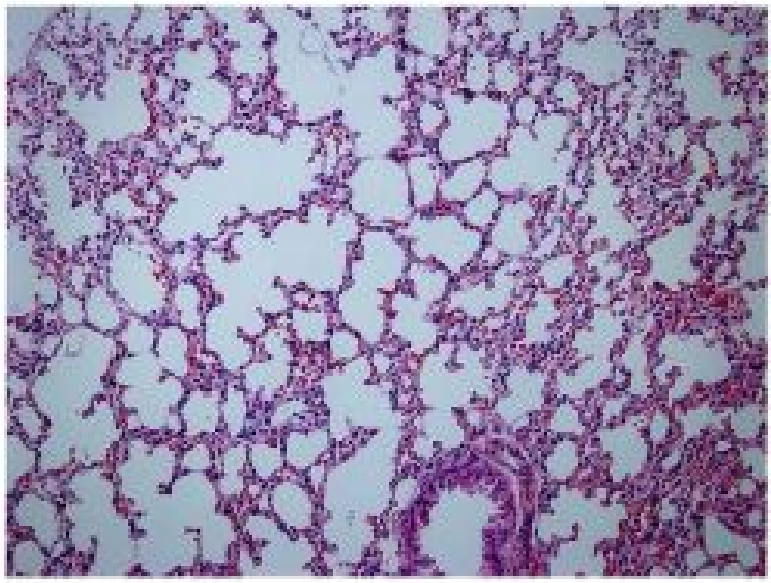

附图 3 双黄连口服液组 x200

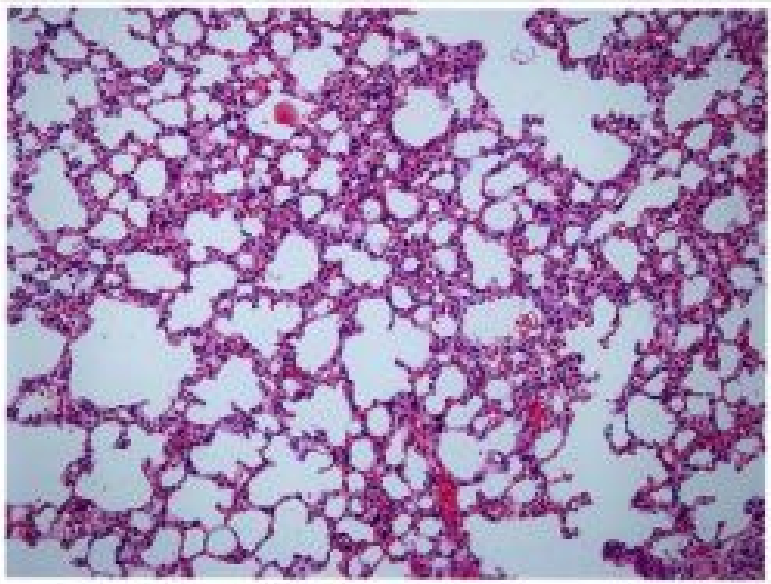

附图 4 大蕉（MUSA SAPIENTUM）果提取物高剂量组 x200

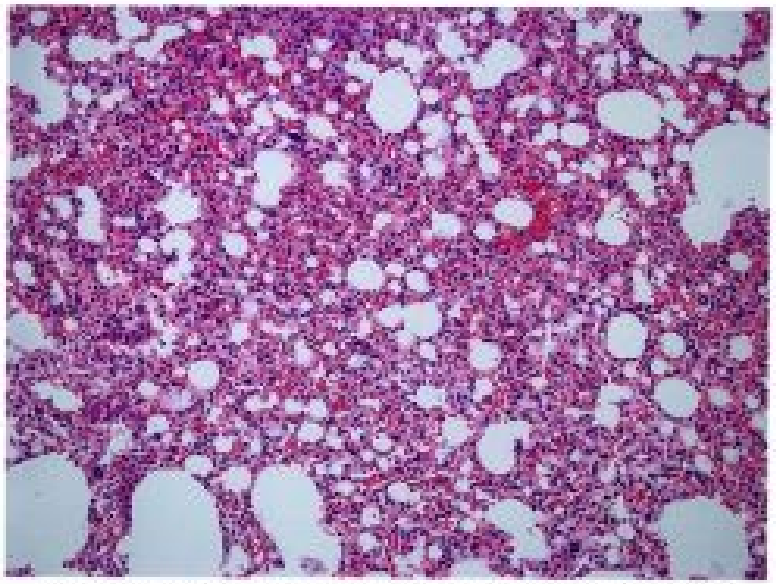

附图 5 大蕉（MUSA SAPIENTUM）果提取物中剂量组 x200

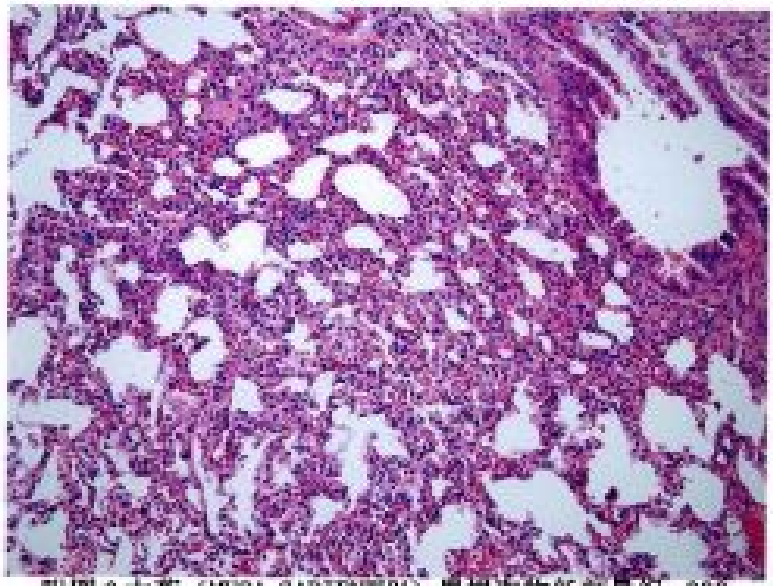

附图 6 大蕉（MUSA SAPIENTUM）果提取物低剂量组 x200

动物体内抗病毒试验结果显示，大蕉（MUSA SAPIENTUM）果提取物 6g/kg 可有效的抑制甲型流感病毒 FM1 所致的病毒性肺炎，与病毒对照组比较差异显著。

（三）讨论与结论

甲型流感病毒 FM1 是一种具有高度传染性的病毒，其症状通常包括发热、咳嗽、喉咙痛、流鼻涕、肌肉疼痛、乏力、肺炎等。甲型流感病毒 FM1 引起的严重肺炎与其诱导微血管内皮细胞通透性增加[6]，影响人肺上皮细胞 BEAS-2B 中的 TLR4、MyD88 和 p-NF-κB 过度表达有关[7]，病情进展较快，容易导致呼吸困难、缺氧，甚至危及生命。

本研究中的大蕉（MUSA SAPIENTUM）果提取物，在稀释到 3‰时 PH 值＞9.5；-300mv 左右的负电位；能长效、稳定地将大分子团簇水活化小分子团 簇；富含植物活性硒、羟脯豆酮、黄酮、氨基酸、多糖、二萜、三萜等，且这 些活性成分的纳米颗粒半径小于 100nm，呈现出植物外泌体的显著特征。以往 的实验结果显示该提取物对大肠杆菌、痤疮丙酸杆菌、金黄色葡萄球菌、白色 念珠菌、大肠杆菌、铜绿假单胞菌、鲍曼不动杆菌均有很强的抑制作用。台北 医科大学万方医院癌症中心、花莲慈济医院中医肿瘤中心等联合试验研究证明 此种提取物能显著抑制促炎细胞因子和趋化因子（IL-6， RANTES，IFN-γ，MCP-1，角质形成细胞衍生趋化因子， IL-17），其对于炎症细胞浸润和促炎及抗炎细胞因子的调节机制可能与 NF-κB 信号抑制密切相关[8]。

本试验显示大蕉（MUSA SAPIENTUM）果提取物对甲型流感病毒具有显著的抑制作用，能有效改善流感病毒性肺炎，其良好的应用潜力，值得进一步深入研究和临床应用，本试验为接下来进一步的研究和应用提供了参考。

参考文献

[1] 孙旭.锦灯笼宿萼醇提物生物活性初步研究及颗粒剂制备[D].吉林农业大学,2022.DOI:10.27163/d.cnki.gjlnu.2022.000598.

[2] 桑会婷，千金藤素抗甲型流感病毒的作用研究[D].南方医科大学,2022.DOI:10.27003/d.cnki.gojyu.2022.000622.

[3] 张汝胜，李霞，黄永林，等.广西地不容非药用部位化学成分研究[J].广西植物,2023,43(01):103-110.

[4] 袁会成，紫花地丁多糖的提取及抗肿瘤活性初步研究.甘肃省，甘肃省武威肿瘤医院,2020-09-02.

[5] 秦泽敏.具有抗菌活性的 Indiacen A 的全合成和叉唇石斛化学成分研究[D].

大理大学,2019.DOI:10.27811/d.cnki.gdixy.2019.000158.

[6] 王祎,曲书焱,姜琪琦,等.苦杏仁苷对流感病毒FM1诱导的微血管内皮细胞通透性的影响[J].中国临床药理学杂志,2024,40(06):820-824.DOI:10.13699/j.cnki.1001-6821.2024.06.008.

[7] 曹媚,耿子涵,包蕾,等.甲型流感病毒对人肺上皮细胞BEAS-2B的影响及疏风解毒胶囊含药血清的干预作用[J/OL].中国实验方剂学杂志,1-11[2024-10-21].https://doi.org/10.13422/j.cnki.syfjx.20241505.

[8] Chien-Huang Liao, Tung-Yuan Lai, Frank Liu, et al., Inhibition of polyinosinic-polycytidylic acid-induced acute pulmonary inflammation and NF-κB activation in mice by a banana plant extract , International Journal of Medical Sciences.2024; 21(1): 107-122

（六）一种量子化大蕉（MUSASAPIENTUM）果提取物抗氧化作用的研究

一种量子化大蕉（MUSASAPIENTUM）果提取物抗氧化作用的研究

范祥翠[1]　重庆医科大学

刘人豪[2]　美国斯坦福大学

秦银艺[3]　郑华[4]　广西修培刻灵生物科技有限公司　广西南宁 530000

姚艺晨[5]　武汉轻工大学食品科学与工程学院　湖北武汉 430048

【摘要】目的：通过检测大蕉（MUSASAPIENTUM）果提取物对羟自由基清除率来 评估样品的抗氧化能力。**方法：**参考 Q/WP-SHACDDTW -WIF-1054 羟自由基清除率测试规范，将样品配制成相应浓度的待测液，根据羟自由基测定试剂盒说明书，按照表 2 中各试剂添加量配制反应体系，混匀，维生素 C 作为阳性对照。在 550 nm 波长下测定各管吸光度值。按照下式计算样品对羟自由基的清除率。**结果：**大蕉（MUSASAPIENTUM）果提取物在样品浓度 为 0.05-3（%，V/V）时，具有对羟自由基的清除能力，且与对照组相比具有统 计学差异（$p<0.01$）。**结论：**大蕉（MUSASAPIENTUM）果提取物具有抗氧化能 力。

【关键词】 大蕉（MUSASAPIENTUM）果提取物；抗氧化 ；羟自由基 中图文分类号：R285.5　文献标识码：A

地球上有很多珍贵的植物具有抗氧化活性，如：藏雪莲、红果枸杞、黑果枸杞、藏红花等[1]。植物抗氧化的研究现状已经取得了显著的进展，科学家们通过对各种植物成分的深入分析，揭示了许多具有抗氧化特性的天然化合物。这些成分不仅在实验室条件下表现出强大的抗氧化能力，而且在动物实验和临床试验中也显示出良好的应用前景。这些抗氧化剂能够有效地清除自由基，延缓细胞老化，预防多种慢性疾病的发生。

本研究中的大蕉（MUSASAPIENTUM）果提取物，PH>12，在稀释到千分之3浓度时PH值>9.5）；-300mv左右的负电位；稀释到极低浓度时仍能使80赫兹以上的大分子团簇水被长效、稳定地活化成低于60赫兹的小分子团簇水；富含植物活性硒、羽扇豆酮、黄酮、氨基酸、多糖、二萜、三萜、多酚、香豆素等，且这些活性成分的纳米颗粒半径小于100nm，呈现出植物外泌体的显著特征。台北医科大学万方医院癌症中心、花莲慈济医院中医肿瘤中心、台湾中医中央研究院生物医学科学研究所等联合试验研究证明此种提取物能显著抑制促炎细胞因子和趋化因子（IL-6， RANTES，IFN-γ， MCP-1，角质形成细胞衍生趋化因子， IL-17），其对于炎症细胞浸润和促炎及抗炎细胞因子的调节机制可能与NF-κB信号抑制密切相关[2]。台湾奇美医疗中心医学研究部和台湾大仁科技大学药学系及药学科技研究所研究证明此种提取物能显著促进糖尿病大鼠中伤口愈合[3]。台湾大仁科技大学在小鼠抗凝血实验中与阿司匹林作对照，研究证明此种提取物能通过抑制血栓素的生成干扰血小板凝集，达到显著的抗凝血的效果。本实验旨在探讨此种提取物在抗氧化上的作用效果。探索植物成分在抗氧化领域的应用前景。

一 测试材料

1 主要试剂

PBS（Gibco）、无水乙醇（国药试剂）、羟自由基测试试剂盒（南京建成）。

2 主要设备

酶标仪（Tecan，Spark）。

3 样品信息

样品信息如下所示：

表1 样品信息

样品名称	样品编号	保存条件
大蕉（MUSASAPIENTUM）果提取物	240402002-1	常温

二 **测试方法** 将样品配制成相应浓度的待测液，根据羟自由基测定试剂盒说明书，按照

表 2 中各试剂添加量配制反应体系，混匀，每个浓度设置 3 个复孔，0.3mg/mL 维生素 C 作为阳性对照。

表 2 实验设计

试剂	对照管	测定管
双蒸水(mL)	0.2	/
底物应用液(mL)	0.2	0.2
样品(mL)	/	0.2
试剂三应用液(mL)	0.4	0.4
混匀，37℃反应 1 分钟，立即加入显色剂终止反应。		
显色剂(mL)	2	2

混匀，室温放置 20 分钟后，每管取 200 μL 转移至 96 孔板，在 550 nm 波长下测定各管吸光度值。按照下式计算样品对羟自由基的清除率。

$$\text{样品对羟自由基的清除率} = \frac{\text{对照 OD 值} - \text{测定 OD 值}}{\text{对照 OD 值}} \times 100\%$$

三 **测试结果与分析** 结果分析

见表 3 和图 1。

表 3 羟自由基清除测试结果分析

组别	样品浓度（%，V/V）	羟自由基清除率（%）	SD	*p*-value
对照组	/	0.00	1.60	/
阳性组/维生素 C	0.3mg/mL	71.02	0.24	0.000**
大蕉（MUSASAPIENTUM）果提取物	0.05	13.37	0.57	0.008**
	0.1	26.97	1.06	0.002**
	0.5	31.26	0.57	0.001**
	1	47.78	1.15	0.000**
	3	62.62	0.89	0.001**

备注：用 t-test 双尾检验方法进行统计分析时，样品组与对照组相比，显著性以*表示，p-value<0.05 表示为*，p-value<0.01 表示为**。

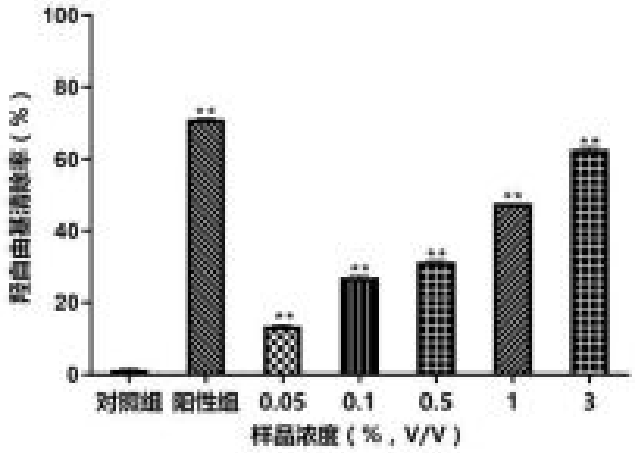

图 1 羟自由基的清除率柱状图

四 讨论

蕉科植物作为一种具有丰富药用价值的植物科属，其独特的生理活性成 分，为治疗各种疾病提供了天然的药物资源。蕉科植物中含有的抗氧化成分主 要包括多酚[1-4]、总黄酮[5]、植物活性硒、多糖[7,8]、β-胡萝卜素和叶黄 素、挥发油、维生素C和维生素E等。这些抗氧化物质能够清除体内的有害自由基，减少氧化应激，从而保护细胞膜和DNA免受损伤。研究表明，定期摄富含抗氧化物质的蕉科食物，有助于降低心血管疾病、某些癌症以及神经退行 性疾病的风险。此外，蕉科植物中的抗氧化成分还具有抗炎作用[9]，能够减轻 体内的炎症反应，进一步促进整体健康。

五　总结

样品大蕉（MUSA SAPIENTUM）果提取物在样品浓度为 0.1%、0.5%、1%、3%时，对应的羟自由基清除率为26.97%、31.26%、47.78%、62.62%，与对照组相比具有统计学差异（$p<0.01$），样品浓度对羟基自由基清除能力呈现正相关 性。试验说明样品大蕉（MUSA SAPIENTUM）果提取物具有对羟自由基的清除能 力，具有抗氧化能力，可作为抗氧化剂。

参考文献

[1] Chien-Huang Liao, Tung-Yuan Lai, Frank Liu, et al., Inhibition of polyinosinic-polycytidylic acid-induced acute pulmonary inflammation and NF-κB activation in mice by a banana plant extract , International Journal of Medical Sciences.2024; 21(1): 107-122

[2] Cheng Y-Z, Liu I-M, Liu F, et al., Wound healing is promoted by musa paradisiaca (banana) extract in diabetic rats. Archives of Medical Science. 2020; 1-9.

[3] 韩明冲,周旭红,李南,等.超声波辅助提取地涌金莲多酚及其抗氧化活性分析[J].南方农业学报,2023,54(11):3302-3313.

[4] 陈文娟,陈建福,林艳,等.超声波辅助提取美人蕉叶多酚工艺及其抗氧化活

性研究[J].南京师范大学学报(工程技术版),2023,23(03):75-83.

[5] 冉静风,陈小爱,易翠平,等.5种香蕉果肉多酚的抗氧化活性和抑制α-葡萄糖苷酶活性[J].食品与机械,2023,39(12):153-161.DOI:10.13652/j.spjx.1003.5788.2023.80536.

[6] 林宝妹,张帅,吴水金,等.香蕉果皮总黄酮提取工艺优化及抗氧化研究[J].粮食与油脂,2023,36(08):95-100.

[7] 唐雅园,王雪峰,韦珍,等.香蕉花多糖抗氧化活性及稳定性研究[J].食品工业科技,2024,45(07):100-107.DOI:10.13386/j.issn1002-0306.2023050330.

[8] 贲锦华、郭诗、郭佳妮、彭馨睿、朱慧楠、缪园欣，响应面法优化香蕉皮多糖提取工艺及其抗氧化活性研究[J]，北方农业学报，2023，51（03）：104-112.

[9] Xu F, Yang L B, Huang X L, et al. Lupenone is a good antiinfammatory compound based on the network pharmacology. Mol Divers, 2020, 24(1): 21-30

（七）一种量子化大蕉（MUSA SAPIENTUM）果提取物抑制人体细胞活性氧自由基ROS的研究

一种量子化大蕉（MUSA SAPIENTUM）果提取物抑制人体细胞活性氧自由基ROS的研究

范祥翠[1] 重庆医科大学

刘人豪[2] 美国斯坦福大学

秦银艺[3] 郑华[4] 广西修培刻灵生物科技有限公司 广西南宁 530000

姚艺晨[5] 武汉轻工大学食品科学与工程学院 湖北武汉 430048

【摘要】目的：基于角质形成细胞，UVB照射诱导产生活性氧自由基（Reactive Oxygen Species，ROS）建立体外氧化损伤细胞模型，通过检测大蕉（MUSASAPIENTUM）果提取物对ROS的抑制能力来评估其抗皱紧致能力。**方法：**实验基于UVB刺激人永生化角质形成细胞（HaCaT）模型，参考Q/WP-SHACDDTW-WIF-1055 UVB刺激角质形成细胞ROS测试规范，细胞接种、配液、UVB辐射、给药后检测细胞ROS含量。**结果：**基于UVB刺激角质形成细胞（HaCaT）模型，样品大蕉（MUSA SAPIENTUM）果提取物在0.625%、1.250%和2.500%（V/V）浓度下，角质形成细胞的ROS含量明显降低，且与NC组相比具有显著差异（$p<0.01$）。**结论：**大蕉（MUSA SAPIENTUM）果提取物能显著的抑制人体细胞活性氧自由基ROS的产生，具有抗皱、紧致功效。

【关键词】大蕉（MUSA SAPIENTUM）果提取物；HaCaT；活性氧自由基ROS；抗皱、紧致

中图文分类号：R285.5 文献标识码：A

活性氧自由基ROS是一类具有高反应性的化学物质，通常在细胞代谢过程中产生，它与细胞信号转导、细胞周期、细胞增殖等生命活动有关，它能造成：对核酸的损伤、对蛋白质的损伤、使肽链断裂、形成蛋白质交联聚合物、改变免疫原性、损伤生物膜、导致能量代谢障碍。ROS含量主要来自线粒体呼

吸过程中的生化反应，约占90%。在ROS相关的疾病状态下，由于ROS的高活泼性，细胞产生氧化应激，导致功能障碍，ROS含量可以高达100 μM，这一病理变化与癌症[1,2]、炎症[3,4,5]、以及阿尔茨海默氏病[6]和帕金森氏病等神经退行性疾病有关。细胞的ROS含量是细胞正常代谢和应对环境变化的重要指标，其水平的测定对于理解细胞功能和疾病机制具有重要意义。

植物的天然成分如多酚、黄酮类化合物和维生素C等，通过其抗氧化机制如直接清除ROS、激活抗氧化酶系统或抑制ROS生成的酶，从而保护细胞免受氧化应激的损害，能够有效地中和并减少ROS的生成[7]。

本研究中的大蕉（MUSASAPIENTUM）果提取物，PH>12，在稀释到千分之3浓度时PH值>9.5），-300mv左右的负电位；稀释到极低浓度时仍能使80赫兹以上的大分子团簇水被长效、稳定地活化成低于60赫兹的小分子团簇水；富含植物活性硒、羽扇豆酮、黄酮、氨基酸、多糖、二萜、三萜、多酚、香豆素等，且这些活性成分的纳米颗粒半径小于100nm，呈现出植物外泌体的显著特征。台北医科大学万方医院癌症中心、花莲慈济医院中医肿瘤中心、台湾中国中央研究院生物医学科学研究所等联合试验研究证明此种提取物能显著抑制促炎细胞因子和趋化因子（IL-6， RANTES，IFN-γ， MCP-1，角质形成细胞衍生趋化因子， IL-17），其对于炎症细胞浸润和促炎及抗炎细胞因子的调节机制可能与NF-κB信号抑制密切相关[8]。台湾奇美医疗中心医学研究部和台湾大仁科技大学药学系及药学科技研究所研究证明此种提取物能显著促进糖尿病大鼠中伤口愈合[9]。台湾大仁科技大学在小鼠抗凝血实验中与阿司匹林作对照，研究证明此种提取物能通过抑制血栓素的生成干扰血小板凝集，达到显著的抗凝血的效果。本实验旨在探讨此种提取物在抑制ROS上的作用效果。探索植物成分在抑制活性氧自由基ROS领域的应用前景。

一 测试材料

1 测试系统

人永生化角质形成细胞（HaCaT）。

2 主要试剂

高糖 DMEM 培养液（VivaCell）、胎牛血清（Gibco）、PBS（VivaCell）、胰蛋白酶（Gibco）、MTT（sigma）、DMSO（国药）、活性氧检测试剂盒（碧云天）。

3 主要设备

CO2 培养箱（Thermo，160i）、生物安全柜（苏净安泰，BSC-1604 II A2）、倒置荧光显微镜（基恩士 BZ-X810）、酶标仪（Tecan，Spark）。

4 样品信息

样品信息如下所示：

表 1 样品信息

样品名称	样品编号	保存条件
大蕉（MUSASAPIENTUM）果提取物	2404003002-1	常温

二 测试方法

1 细胞毒性

1.1 细胞接种：按 1×10⁴个/孔的接种密度接种细胞至 96 孔板，培养箱（37℃、5%CO2）中孵育过夜。

1.2 测试分组：测试设置调零组、对照组、阳性对照组与样品组。样品组中，每个样品设置 8 个浓度梯度，每个浓度梯度下设置 3 个重复孔。

1.3 配液：按测试浓度设定表配制不同浓度的样品工作液。

表 2 测试浓度设定表

样品名称	浓度设置（%，V/V）							
	1	2	3	4	5	6	7	8
大蕉（MUSA SAPIENTUM）果提取物	10.000	5.000	2.500	1.250	0.625	0.313	0.156	0.078

1.4 给药：待 96 孔板中细胞铺板率达到 40%~60%时进行给药。对照组每孔加入 200 μL 含 10%PBS 的培养液；阳性对照组每孔加入 200 μL 含 10%DMSO 的培养液；样品组每孔加入 200 μL 含有相应浓度样品的培养液；调零组无细

胞接种，仅加入 200 μL 细胞培养液。给药完成后将 96 孔板放置在培养箱（37℃、5%CO2）中培养。

1.5 检测：细胞孵育培养 24 h 后，弃掉上清，加入 MTT 工作液（0.5 mg/mL），37℃避光孵育 4 h，孵育结束后，弃掉上清，每孔加 100 μL DMSO，在 490 nm 处读取 OD 值。

1.6 细胞活力计算：根据公式计算

$$\text{细胞活力} = \frac{\text{样品孔 OD} - \text{调零孔 OD}}{\text{溶剂对照孔 OD} - \text{调零孔 OD}} * 100\%$$

2 ROS 含量测试

测试分组具体设置如表 3 所示。

组别	样品浓度（V/V）	造模条件	检测模型	检测指标	检测方法
空白对照（BC）	/	/	人永生化角质形成细胞（HaCaT）	ROS	荧光成像
阴性对照（NC）	/	UVB 300 mJ/cm²			
阳性对照（PC）	100 μg/mL VC+7 μg/mL VE				
大蕉（MUSA SAPIENTUM）果提取物	0.625%				
	1.250%				
	2.500%				

表 3　实验设计

2.1　细胞接种：按 5×10 4 个/孔的接种密度接种细胞至 24 孔板，培养箱（37℃、5%CO2）中孵育过夜。

2.2　配液：按测试浓度设定表（表 3）配制不同浓度的样品工作液。

2.3　待 24 孔板中细胞铺板率达到 40%~60%时进行辐照，阴性对照组、阳性对照组及样品组接受剂量为 300 mJ/cm2 的 UVB 辐射，与此同时，空白对照组放置于相同的环境（UVB 辐射剂量为 0 J/cm2）。

2.4　给药：待辐照结束后进行给药，空白对照组、阴性对照组每孔加入 1 mL 的细胞培养液；阳性对照组每孔加入 1 mL 含有 100 μg/mL VC 和 7 μg/mL VE 的培养液；样品组每孔加入 1 mL 含有相应浓度受试物的培养液，继续培养 24 h。

2.5　ROS 含量检测:DCFH-DA 探针母液按照 1:1000 的比例，用无血清培养液稀释，使其终浓度为 10 μmol/L。每孔分别加入稀释后的 DCFH-DA 探针 500 μL，于 37℃细胞培养箱内孵育。30 min 后，用无血清 DMEM 培养液洗涤细胞 4 次，以充分地去除未进入细胞内的探针。使用荧光显微镜，在激发波长 488 nm 的条件下观察并拍照。

三　测试结果

1 细胞毒性测试结果

样品设定 8 个给药浓度，开展细胞毒性检测实验，MTT 检测结果见表 4。

表 4　MTT 检测结果

细胞活力	对照	PC	浓度设置（%，V/V）							
(%)	/	10%DMSO	10.000	5.000	2.5000	1.250	0.625	0.313	0.156	0.078
Mean	100.00	7.86	7.97	9.47	95.96	98.23	97.19	96.56	98.78	98.67
SD	6.96	0.24	0.15	0.17	2.71	5.92	0.62	1.31	2.36	1.23

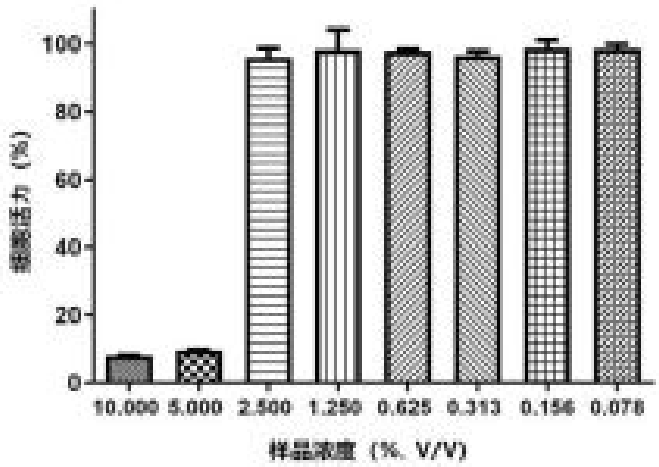

图 1 细胞活力图

以样品所选 8 个浓度为横坐标，细胞活力值为纵坐标，绘制细胞活力图（见图 1）。

故根据 MTT 结果，样品大蕉（MUSA SAPIENTUM）果提取物在 2.500%（V/V）浓度范围内未表现出角质形成细胞毒性。

2 ROS 含量测试结果

根据具体测试方法，进行 ROS 含量检测，检测结果如图 2、表 5 和图 3 所示。

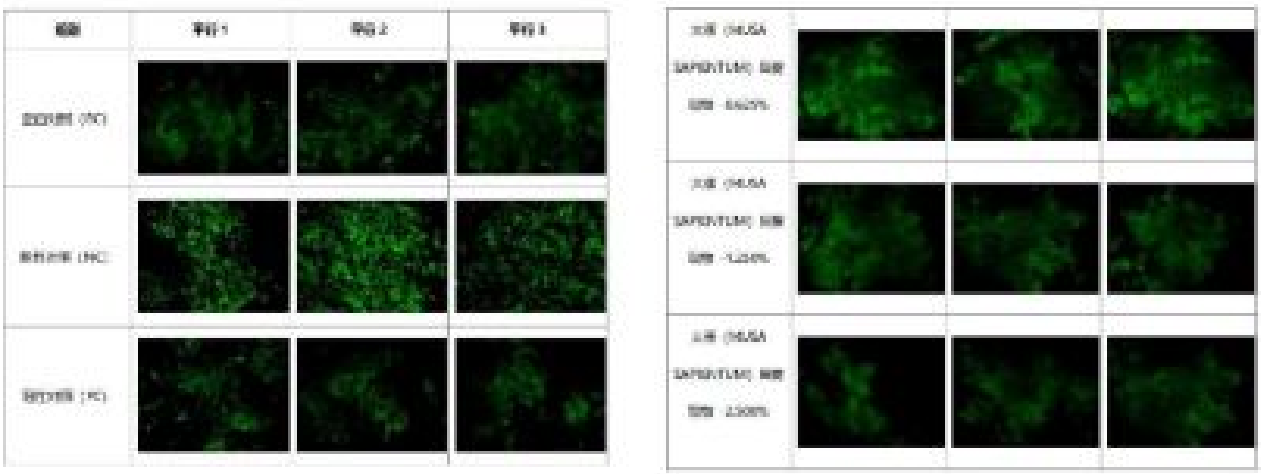

图 2 ROS 含量汇总图

表 5 ROS 数据分析汇总表

组别	Mean（ng/mL）	SD	*p*-value
空白对照（BC）	1.00	0.03	/
阴性对照（NC）	2.09	0.08	0.000##
阳性对照（PC）	1.46	0.09	0.001**
大蕉（MUSA SAPIENTUM）果提取物 -0.625%	1.73	0.04	0.002**
大蕉（MUSA SAPIENTUM）果提取物 -1.250%	1.60	0.08	0.001**
大蕉（MUSA SAPIENTUM）果提取物 -2.500%	1.51	0.02	0.000**

备注：用 *t*-test 双尾检验方法进行统计分析时，NC 组与 BC 组相比，显著性以#表示，*p*-value<0.05 表示为#，*p*-value<0.01 表示为##；样品组、PC 组与 NC 组相比，显著性以*表示，*p*-value<0.05 表示为*，*p*-value<0.01 表示为**。

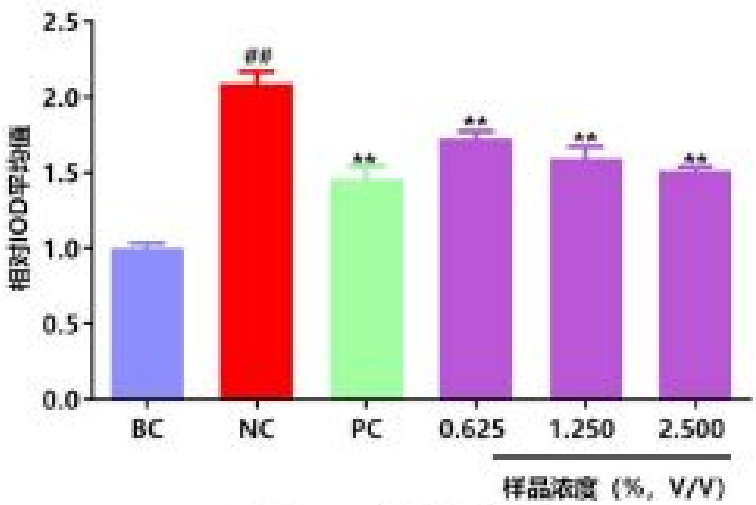

图 3 ROS 相对含量柱状图

与 BC 组相比，NC 组 ROS 荧光信号显著升高（$p<0.01$），表明本次测试 UVB 刺激造模成功。

与 NC 组相比，PC 组 ROS 荧光信号显著降低（$p<0.01$），表明本次阳性对照检测有效。

与 NC 组相比，样品大蕉（MUSA SAPIENTUM）果提取物在 0.625%、1.250%和 2.500% （V/V）浓度下 ROS 荧光信号显著降低（$p<0.01$）。

四 总结

基于 UVB 刺激角质形成细胞（HaCaT）模型，样品大蕉（MUSA SAPIENTUM）果提取物在 0.625%、1.250%和 2.500%（V/V）浓度下，角质形成 细胞的 ROS 含量明显降低，且与 NC 组相比具有显著差异 （$p<0.01$），说明 大蕉（MUSA SAPIENTUM）果提取物能显著的抑制人体细胞活性氧自由基 ROS 的 产生，具有抗皱、紧致功效，在抑制 ROS 领域的应用具有一定的意义。

参考文献 [1]冉遥、冷湛旭、郑凯凯、辛贵忠、濮社班，血根碱在癌症治疗中的抗肿瘤机 制研究进展[J]，中南药学，2024，22（07）:1845-1850. [2]张昕彤、吴昊、胡艳芬、张文桃、畅靖嘉，CYP27A1 对肝细胞癌预后的影响 及生物学作用[J]，解放军医学杂志，2024，49（04）:387-395. [3]罗静,朱华,张淼,等.蝙蝠草醇提物对脂多糖所致 RAW264.7 细胞炎症反应的 抑制作用[J].中成药,2024,46(08):2763-2768.

[4]张之弘,李秀娟,王宇馨,等.中药干预氧化应激防治糖尿病肾病的研究进展[J/OL].实用中医内科杂志,1-5[2024-09-08]http://kns.cnki.net/kcms/detail/21.1187.R.20240813.1451.007.html.

[5]林丽、陆滢、李空飞、王甜甜、于朱若涵，人参皂苷 Rg1 治疗多发性骨髓瘤的网络药理学预测与验证[J]，温州医科大学学报，，2024，54（08）:650-656+663.

[6]沈畅、尹秋媛、孟明耀、孙建伟，溶酶体半乳糖脑苷酯酶的作用机制及疾病[J]，中国生物化学与分子生物学报，2024 ,40 (04):493-503.DOI:10.13865/j.cnki.cjbmb.2024.01.1402.

[7]周宏丹,罗晓萍,涂米雪,等.植物褪黑素：植物应答非生物胁迫的新兴信号分子[J].生物技术通报,2024,40(03):41-51.DOI:10.13560/j.cnki.biotech.bull.1985.2023-0880.

[8]Chien-Huang Liao, Tung-Yuan Lai, Frank Liu, et al., Inhibition of polyinosinic-polycytidylic acid-induced acute pulmonary inflammation and NF-κB activation in mice by a banana plant extract , International Journal of Medical Sciences.2024; 21(1): 107-122

[9]Cheng Y-Z, Liu I-M, Liu F, et al., Wound healing is promoted by musa paradisiaca (banana) extract in diabetic rats. Archives of Medical Science. 2020; 1-9.

（八）一种量子化大蕉（MUSASAPIENTUM）果提取物对人体细胞 作用的研究

一种量子化大蕉（MUSASAPIENTUM）果提取物对人体细胞作用的研究

范祥翠[1]　重庆医科大学 刘

人豪[2]　美国斯坦福大学

秦银艺[3]　郑华[4]　广西修培刻灵生物科技有限公司 广西南宁 530000

姚艺晨[5]　武汉轻工大学食品科学与工程学院 湖北武汉 430048

摘要：专利技术量子化大蕉（MUSASAPIENTUM）果提取物取材于赤道环境生长的特殊品种蕉科植物，运用了十分特殊的萃取技术，使提取物呈现出超高植物碱性、负电位、稳定的离子态小分子团簇、富含多种植物营养素、优异的抗氧化性等5大理化特性。本文阐述了5大理化特征与人体细胞的关联。讨论了现代量子化生物科技在提高植物生物利用度方面的作用，以及如何通过技术优化满足现健康需求。

关键词：量子化；大蕉（MUSASAPIENTUM）果提取物；细胞；健康

中图文分类号：R285.5　文献标识码：A

引言 珍贵植物或具有神奇的药用价值，或富含丰富的营养元素。细胞构成了人

体的基本框架，它们的状态直接决定了个体的整体健康水平。人体并非患有千万种疾病，而是只存在一种根本的疾病，那就是细胞疾病。本文阐述了特殊的量子化大蕉（MUSASAPIENTUM）果提取物如何维护人体细胞健康。

1　赤道蕉科与技术沿革

1.1　赤道蕉科

在赤道地区，存在着一种独特的蕉科植物，这种植物拥有着与众不同的特 性

。

1.2　技术沿革

美国斯坦福大学博士后研究员刘人豪博士团队运用量子化的生物萃取技术研发出了一款特殊的大蕉（MUSASAPIENTUM）果提取物。台北医科大学万方医院癌症中心、花莲慈济医院中医肿瘤中心、台湾中国中央研究院生物医学科学研究所等联合试验研究证明此种大蕉（MUSASAPIENTUM）果提取物能显著抑制促炎细胞因子和趋化因子（IL-6，RANTES，IFN-γ，MCP-1，角质形成细胞衍生趋化因子，IL-17），其对于炎症细胞浸润和促炎及抗炎细胞因子的调节机制可能与NF-κB信号抑制密切相关[1]。台湾奇美医疗中心医学研究部和台湾大仁科技大学药学系及药学科技研究所研究证明此种大蕉（MUSASAPIENTUM）果提取物能显著促进糖尿病大鼠中伤口愈合[2]。台湾大仁科技大学在小鼠抗凝血实验中将此种大蕉（MUSASAPIENTUM）果提取物与阿司匹林作对照，研究证明此种大蕉（MUSASAPIENTUM）果提取物能通过抑制血栓素的生成干扰血小板凝集，达到显著的抗凝血的效果。广西修培刻灵生物科技公司对此种大蕉（MUSASAPIENTUM）果提取物进行的抗氧化、去自由基、抗过敏、抑菌杀菌、促渗透、抗炎、抗肿瘤等实验均取得了正向的结论。

2　核心技术大蕉（MUSASAPIENTUM）果提取物

2.1　大蕉（MUSASAPIENTUM）果提取物具备稳定的离子态，只需把少许提取物直接加入水中即可快速并且长效地活化饮用水。经中国广西、中国台湾多处水源地采集，分批次实验，均显示可以：即时、稳定、长效、耐高温的将分子团簇80赫兹以上的水活化为低于60赫兹的小分子团簇水（见表一）。目前，通常以核磁共振测定的水震动频率的半幅宽度来表示水分子团簇的大小，半幅宽越大水分子团簇越大，半幅宽越小水分子团簇越小[3]。小分子团水，也被称作活化水或是高频水，是一种具有特定结构和功能的水。这种水分子因为其较小的分子大小和独特的运动状态，相较于普通水，对人体细胞有着更多的益处。

2.1.1　更轻易地穿过细胞膜，为细胞带来更多的氧气和养分，同时也帮助细胞更有效地排除废物[4]。

2.1.2　具有一定的抗氧化作用[4]。小分子水中的负电荷可以与体内的自由基结合，从而帮助减少自由基对人体细胞的损害。

2.1.3 具有优良的渗透性和溶解性[5]，更容易进入细胞和细胞发生相互作用，进而影响细胞高级结构，提高酶的活性及酶对热、酸碱的耐受性，促进细胞的生长和生命体的新陈代谢[6]。

2.1.4 呈弱碱性，可以中和体内酸性毒素，调节体液的酸碱度，还可以活化细胞，提高机体的抗病能力[7]。

表一 小分子水实验

样品编码	样品名称	测试项目	测试结果	单位	参考标准
2307001129-3-1	容草山泉	核磁氧谱半峰宽	84.9	Hz	JY/T 0578-2020
		pH	8.36	/	实验室内部方法
2307001129-3-2	容草山泉+大蕉果提取液	核磁氧谱半峰宽	59.4	Hz	JY/T 0578-2020
		pH	10.35	/	实验室内部方法
2307001129-3-3	容草山泉+大蕉果提取液	核磁氧谱半峰宽	59.11	Hz	JY/T 0578-2020
		pH	10 .33	/	实验室内部方法
2307001129-3-4	容草山泉+大蕉果提取液	核磁氧谱半峰宽	58.67	Hz	JY/T 0578-2020
		pH	10.51	/	实验室内部方法
2307001129-3-5	容草山泉+大蕉果提取液	核磁氧谱半峰宽	62.01	Hz	JY/T 0578-2020
		pH	8.44	/	实验室内部方法

注解：

1.NMR 溶剂：氘代水。

2.“2307001129-3-1”：容草山泉直接测试核磁半峰宽和 pH.

3.“2307001129-3-2”：每瓶容草山泉放入定量大蕉果提取液之后尽快测核磁半峰宽和 pH

4.“2307001129-3-3”：每瓶容草山泉放入定量大蕉果提取液后加热到 100℃冷却了尽快测 核磁半峰宽和 pH

5.“2307001129-3-4”：每瓶容草山泉放入定量大蕉果提取液之后放置一个月之后测核磁 半峰宽和 pH

6.“2307001129-3-5”：每瓶容草山泉放入定量大蕉果提取液后加热到 100℃冷却了放置一 个月之后测核磁半峰宽和 pH

2.2 大蕉（MUSASAPIENTUM）果提取物具有很高的植物碱性，其 PH 值高达 12 以上（见表二），在稀释到千分之 3 浓度时 PH 值仍能维持在 9.5 以上。

2.2.1 酶是人体内进行各种生化反应的重要催化剂，碱性环境酶可以更高效地发挥作用。

2.2.2 肿瘤微环境（ME）特指肿瘤细胞所处并影响其行为的内环境，它包括营养供应不足、缺氧以及酸性环境，这些条件为肿瘤细胞提供了一个适应性生长的微环境，促进其增殖、逃避程序性死亡，并维持炎症状态[1]。而碱性环境有助于减少酸性环境对身体的损害，降低肿瘤的发生风险。

2.2.3 在碱性环境中，钙、镁、钾等矿物质可以更有效地被细胞吸收和利用，从而保证骨骼、牙齿、神经、肌肉等方面的健康。

2.2.4 碱性环境可以促进免疫细胞的正常功能，提高身体对各种病原体的抵抗力。

2.3 大蕉（MUSASAPIENTUM）果提取物拥有超高的负电位，达到-300mv（见表二），这一独特的性质使其具备卓越的生物活性。 负电位，这一概念在生物电学和健康科学中逐渐受到重视。所谓负电位，是指生物体在自然状态下，通过生物电的作用，使得体表产生的一种相对于地线的电位负值。这种负电位被认为对身体有诸多益处。

2.3.1 调节人体的生物电活动，更有效地进行能量转换和物质代谢，提高免疫力，增强抵抗力，减少疾病的发生。

2.3.2 调节人体的生物电平衡，提高睡眠质量，提高生活和工作效率。

表二 PH及电位

序号	测试项目	测试单位	测试结果	测试方法
1	pH 值	/	13.06	pH 及电位计
2	电位	mV	-365	
备注	仪器信息：pH 及电位计：奥豪斯 FB20			

2.4 大蕉（MUSASAPIENTUM）果提取物具备优异的抗氧化、抗老化作用（见表三、图一）。该抗氧化抗老化作用可能与其富含抗氧化和抗衰老成分如黄酮、植物活性硒、氨基酸、香豆素、β-谷甾醇、多糖等物质有关；也可能与

其独特的离子态、负电位、植物碱性等理化特性有关联：或者是多种因素的协同作用。这些高效的成分和理化特性能够有效地减缓衰老的过程。

依据Q/WP-SHKJDTW-WIF-1064 羟自由基清除率测试规范，检测此种大蕉（MUSASAPIENTUM）果提取物羟自由基清除率。结论：在样品浓度为 0.05-3（%，V/V）时，具有对羟自由基的清除能力，且与对照组相比具有统计学差异（$p<0.01$），说明样品大蕉果提取物具有抗氧化作用。

表三　羟自由基清除测试结果分析

组别	样品浓度（%，V/V）	羟自由基清除率（%）	SD	*p*-value
对照组	/	0.00	1.60	/
阳性组/维生素 C	0.3mg/mL	71.02	0.24	0.000**
大蕉（MUSA SAPIENTUM）果提取物	0.05	13.37	0.57	0.008**
	0.1	26.97	1.06	0.002**
	0.5	31.26	0.57	0.001**
	1	47.78	1.15	0.000**
	3	62.62	0.89	0.001**

备注：用 t-test 双尾检验方法进行统计分析时，样品组与对照组相比，显著性以*表示，p-value<0.05 表示为*，p-value<0.01 表示为。**

图一　羟自由基的清除率柱状图

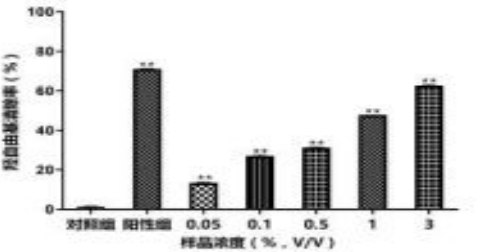

2.5 大蕉（MUSASAPIENTUM）果提取物富含植物干细胞、外泌体和多种营养 素，如硒、羽扇豆酮、黄酮、氨基酸、多糖、二萜、三萜、多酚、香豆素等

（表四），这些营养素的纳米颗粒半径在100nm左右（见表五，图二、三、四）。

黄酮（抽样检测 177ng/100ml）是一种广泛存在于植物中的天然有机化合物。黄酮具有抗氧化、抗炎、抗肿瘤和抗病毒等多种生物效应[9]。它们通过调节细胞周期和促进肿瘤细胞凋亡来展现抗肿瘤特性。黄酮类化合物可以调节血管内皮细胞的功能、改善血管弹性和减少炎症反应，从而能够改善心血管系统的功能，降低心血管疾病的风险。

植物活性硒（抽样检测 6500ug/100ml），具有高度的生物活性，在人体内发挥着诸多重要功能，包括：增强免疫系统、抗氧化[10]、促进新陈代谢、参与甲状腺激素的合成、防治糖尿病、预防上呼吸道感染、预防循环系统疾病、预防神经系统疾病、抵抗有毒害重金属、减轻放化疗副作用、防癌抗癌、抵抗锡对生殖腺和中枢神经的毒害、防治肝病。

二萜（抽样检测 17ng/100ml），普遍存在于自然界中，二萜类化合物因其独特的化学结构和生物活性，被广泛应用于药物研发领域[11]。二萜类化合物常常被研究作为潜在的抗炎、抗癌、抗菌、抗病毒、免疫抑制、降低血压、防止血栓形成等治疗药物。

植物多糖（抽样检测 433mg/100ml），是一种广泛存在于植物细胞壁中的生物大分子，具有多种生物活性，例如抗炎、抗氧化、抗肿瘤、免疫调节等[12]。近年来，随着科学技术的不断发展，人们对植物多糖的研究越来越深入，已经从传统的提取、分离和纯化技术，发展到了基因工程、细胞工程和组织工程等现代生物技术领域。

三萜（抽样检测 22ng/100ml），也被称作灵芝酸，是一种天然存在的有机化合物，广泛分布于植物、动物和真菌等生物体中。三萜复杂的结构赋予了它们多样化的生物活性[13]，如溶血、抗癌、抗炎、抗菌、抗病毒、降低胆固醇、解热镇痛、降血压、护肝调节肝功能等，对身体健康产生积极影响。

皂苷（抽样检测 41ng/100ml），是一种广泛存在于植物中的天然有机化合物，它们通常具有多种生物活性，例如：抗菌、解热镇静、抗癌、调节神经系

统、改善心血管功能[14]、调节肾脏功能、降血糖、降胆固醇、降血压、增强机体免疫力、抗脂质氧化。

β-谷甾醇（抽样检测 3.5mg/100ml），是一种常见的植物甾醇。它能够降低血液中的胆固醇水平，从而有助于预防心血管疾病，具有抗炎、抗肿瘤、保护神经系统等潜在健康效益。还能治疗皮肤溃疡和皮肤肿瘤，抗氧化[15]，治疗皮肤的角质化。

香豆素（抽样检测 61mg/100ml）是一种天然存在于多种植物中的有机化合物，能够抗凝血、抗肿瘤、抗菌抗炎、抗氧化、降血糖、抗骨质疏松、抗高血压、松弛平滑肌、吸收紫外线抗辐射、神经保护、抗抑郁以及抗 HIV 等[16]。

氨基酸（抽样检测 355mg/100ml）是生物体内不可或缺的有机化合物，在许多生物化学过程中扮演重要角色，如代谢调节、信号传递和细胞结构维持等。它具有以下作用：提高免疫力、为身体提供能量、增强肌肉骨骼系统、调节消化、调理情绪、提高睡眠质量、产生荷尔蒙、产生神经递质、刺激健康皮肤、指甲和头发生长[17]。

羽扇豆酮（抽样检测 100mg/100ml）主要存在于多种植物的果实、叶子和树皮中。这种化合物具有多种生物活性，研究表明，可以抑制多种炎症因子的释放、抑制肿瘤细胞的生长和扩散[18]、促进创面愈合，防治老年痴呆，改善恰加斯病，治疗黑色素减退，降低血糖血脂，保护及修复肾脏。

多酚（抽样检测 60mg/100ml），是一类在植物界广泛存在的生物活性物质，主要包括黄酮类、花青素类、儿茶素类等。多酚类物质具有很强的抗氧化性能[19]，能够清除体内的自由基，减缓由自由基引起的脂质过氧化反应，从而保护细胞不受损伤，延缓衰老过程。多酚还具有抗炎、抗病毒、抗细菌和抗癌特性，是未来药物研发的重要方向之一。

薏酯（抽样检测 76mg/100ml），具有以下作用：抗肿瘤、抗炎、抗菌、止血、降血糖、降胆固醇、利尿通便、抗氧化、益智和抗衰老。其显著的抑制 cAMP 磷酸二酯酶、强烈的抑制异常高的免疫反应，广泛应用于肝癌、肺癌、鳞癌、胰腺炎、结肠炎等疾病的治疗[20]。

表四　成分分析

序号	测试项目	测试单位	测试结果	检出限
1	黄酮	mg/100mL	177.5	0.05
2	多酚	mg/100mL	60.5	0.10
3	多糖	mg/100mL	433.2	0.05
4	艾诺酮	mg/100mL	10.0	0.05
5	羟基蒽醌酮	mg/100mL	13.3	0.50
6	三萜类	mg/100mL	22.5	0.50
7	二萜类	mg/100mL	17.7	0.50
8	甾体类	mg/100mL	6.5	0.10
9	钾	mg/100mL	55.2	1.0
10	钠	mg/100mL	507.7	1.0
11	羽扇豆酮	mg/100mL	100.5	0.5
12	硒	mg/100mL	6.7	1.0
13	蒽醌	mg/100mL	76.4	0.05
14	棕榈酸	mg/100mL	88.6	1.0
15	β-谷甾醇	mg/100mL	3.5	1.0
16	氨基酸	mg/100mL	355.8	0.1
17	香豆素	mg/100mL	61.0	1.0
18	皂苷	mg/100mL	41.3	1.0
备注	1. 检测依据： JIS K0133-2007 高频等离子体质谱分析通则；JY/T 007-1996 超导脉冲傅里叶变换核磁共振波谱方法通则 ； GB/T 35959-2018 液相色谱-质谱联用分析方法通则；GB/T 16631-2008 高效液相色谱法通则。 2. 检测仪器 布鲁克 AVANCE NEO 400M 核磁共振波谱仪；超高液相色谱-离子淌度-四级杆飞行时间质谱仪； 赛默飞世尔 Evolution201 紫外-可见光分光光度计；珀金埃尔默 Nexion 300D 等离子体质谱仪；赛默飞世尔 Ultimate3000 高效液相色谱仪。			

在纳米颗粒跟踪分析技术 NTA 下的观察，大蕉（MUSASAPIENTUM）果提取物显示出植物外泌体的显著特征，Mean（平均值）277nm，Mode（most often） 222.8nm，D10 105.8nm，D50 234.1nm。

表五　納米顆粒跟踪分析技术 NTA 下数据

Included Files

20230309 2023-03-09 14-29-26
20230309 2023-03-09 14-30-51
20230309 2023-03-09 14-32-04

Details

NTA Version:	NTA 3.2 Dev Build 3.2.16
Script Used:	SOP Standard Measurement 02-20-20PM 09-
Time Captured:	14:29:26 09/03/2023
Operator:	
Pre-treatment:	
Sample Name:	
Diluent:	
Remarks:	

Capture Settings

Camera Type:	sCMOS
Laser Type:	Blue488
Camera Level:	11
Slider Shutter:	800
Slider Gain:	148
FPS:	25.0
Number of Frames:	1498
Temperature:	25.1 °C
Viscosity:	(Water) 0.888 - 0.890 cP
Dilution factor:	Dilution not recorded

Analysis Settings

Detect Threshold:	3
Blur Size:	Auto
Max Jump Distance:	Auto: 7.2 - 16.1 pix

Results

Stats: Merged Data

Mean:	277.0 nm
Mode:	222.0 nm
SD:	158.5 nm
D10:	105.6 nm
D50:	234.1 nm
D90:	480.3 nm

Bulk: Mean +/- Standard Error

Mean:	280.0 +/- 31.4 nm
Mode:	130.2 +/- 36.6 nm
SD:	148.7 +/- 10.0 nm
D10:	129.3 +/- 34.0 nm
D50:	251.1 +/- 35.5 nm
D90:	441.2 +/- 20.9 nm
Concentration:	1.84e+008 +/- 3.71e+007 particles/ml 9.3 +/- 1.9 particles/frame 12.2 +/- 2.2 centres/frame

图二　納米颗粒跟踪分析技术 NTA 下的观察

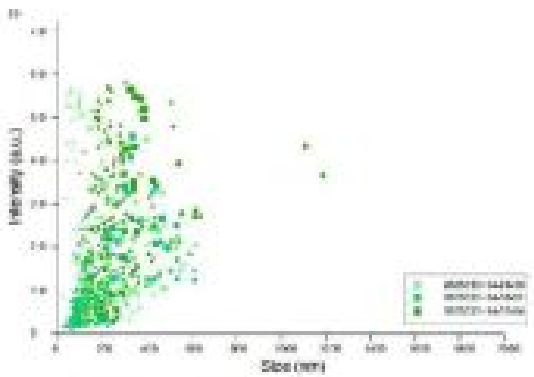

Intensity / Size graph for Experiment
20230309 2023-03-09 14-29-26

图三　纳米颗粒跟踪分析技术 NTA 下的观察

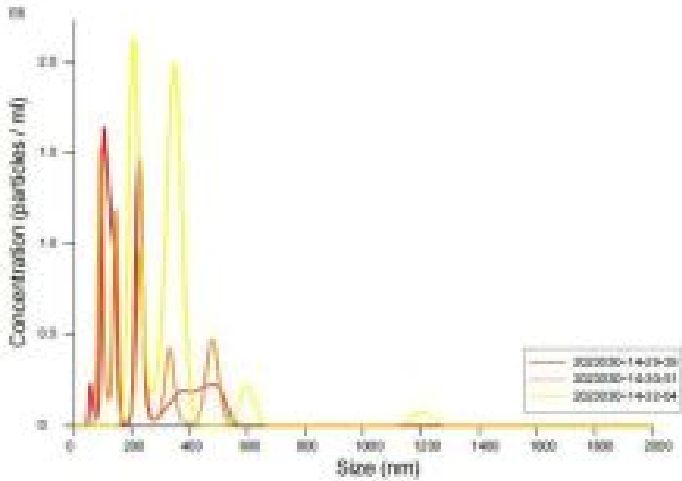

FTLA Concentration / Size graph for Experiment:
20230309 2023-03-09 14-29-26

图四　纳米颗粒跟踪分析技术 NTA 下的观察

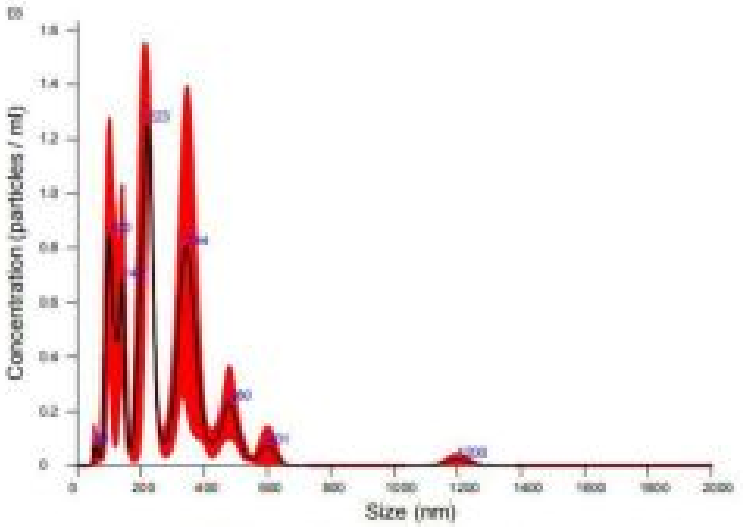

Averaged FTLA Concentration / Size for Experiment:
20230309 2023-03-09 14-29-26
Error bars indicate + / -1 standard error of the mean

3. 现代生物科技在植物萃取中的应用

量子化萃取技术主要是利用量子力学原理，通过调控物质的量子态，实现对目标成分的高效提取。这种量子化萃取技术高效且环保，在植物油脂、植物精油、植物蛋白、天然色素、精细化工、中草药等领域中，都有着广泛的应用。

量子化萃取技术在大蕉（MUSASAPIENTUM）果提取物中的应用显著提升了植物利用度，这种提升不仅意味着更少的原料可以获得更高的提取率，也使得最终产品的效用得到了加强，从而为医药、食品和化妆品等行业提供了更为优质的原材料。萃取过程中用到的如超声辅助提取、微波辅助提取、超临界流体提取、远古特殊菌群生物发酵等先进技术，可以更精确地从芭蕉中提取出所需的活性成分，避免了热敏性成分的破坏。此外，还通过纳米化处理和脂质体包裹等手段，增强了成分的溶解性和稳定性，提高了在体内的吸收率和生物利用 度，使得植物植化素成分能够更快速、更有效地发挥作用，为系统健康提供了 科学的保障。

4 大蕉（MUSASAPIENTUM）果提取物的社会价值及产业价值

在现代社会，中医养生文化面临着诸多挑战和机遇，大蕉（MUSASAPIENTUM）果提取物的成功实践为中医中药的传承和发展提供了新的思路和方向。随着全球化的加速推进，这种蕴含着独特辩证思维的植物提取方 式，其国际化发展潜力无可限量。通过对大蕉（MUSASAPIENTUM）果提取物的深入研究，我们可以发现，中药材与现代生物技术的结合将开创全新的局面。

5 总 结

量子化萃取技术的产物大蕉（MUSASAPIENTUM）果提取物展示了现代生物科技如何赋能植物，通过提取出其独特的化学成分和生理活性，影响人体细胞内的信号通路、调节细胞生长、保持细胞内环境的稳定，使之成为人类健康管理的有力工具。这种现代科技的应用，源于自然生长的植物，无需经过化学合 成，这种方式是在深入研究和科学实验的基础上，结合先进的技术创新成果而 形成，经过了长期的实践验证，确保了其科学性和可靠性。

参考文献

[1] Chien-Huang Liao、 Tung-Yuan Lai、 Yu-Ying Lin、 Yi-Chun Liao、 Gi-Ming Lai、 Tien-Hua Chu、 Szu-Yao Wu、 Wei-Lun Tsai、Jacqueline Whang-Peng、 Frank Liu、 Tzeon-Jye Chiou、Chih-Jung Yao, Inhibition of Polyinosinic-Polycytidylic Acid-Induced Acute Pulmonary Inflammation and NF-κB Activation in Mice by a Banana Plant Extract , International Journal of Medical Sciences.2024; 21(1): 107- 122

[2] Cheng Y-Z, Liu I-M, Cheng J-T, Lin B-S, Liu F. Wound healing is promoted by Musa paradisiaca (banana) extract in diabetic rats. Archives of Medical Science. 2020; 1-9.

[3] 认识活水及活水生态（一）[J].江西水产科技,2021,(01):47-48.

[4] 陈志南,边愚洁,杨向民.肿瘤微环境稳态重塑可阻抑肿瘤进展[J].空军军医大学学报,2024,45(07):723-731.DOI:10.13276/j.issn.2097-1656.2024.07.002.

[5] 李宁,杨媛媛,曲彤,等.异戊烯基黄酮类化合物药理作用研究进展[J].中成药,2024,46(04):1255-1262.

[6] 付嘉,刘楠,颜晓晖.植物来源大环二萜类化合物的研究进展[J].中南药学,2023,21(10):2680-2689.

[7] 姚安妮,汤燕,罗大英,等.药用植物资源多糖类成分相对分子质量与其功效关联性的分析与展望[J].中国中药杂志,2024,49(05):1186-1195.DOI:10.19540/j.cnki.cjcmm.20231221.601.

[8] 张璐,肖瑶,刘姿之,等.乌苏烷型五环三萜的生物合成研究进展[J].中国医药生物技术,2024,19(03):223-230.

[9] 李佩娟,王春梅,赵茜.三七总皂苷预防血栓的机制[J].基础医学与临 床,2024,44(07):912-915.DOI:10.16352/j.issn.1001-6325.2024.07.0912.

[10] 李卓远,史佳慧,刘楠,等.香豆素衍生物的生物活性研究进展[J].精细与专用化学品,2024,32(06):23-30.DOI:10.19482/j.cn11-3237.2024.06.04.

[11] 赵源,刘红波,唐志书,等.大黄蒽醌类物质药理作用研究进展[J].陕西中医,2024,45(06):863-865.

三、產學合作計畫

BPE第一季成果報告

1. BPE能抑制病毒相似物Poly (I:C)誘發肺部細胞的發炎因子TNF-α、 IL-1β和IL-6的表現。

2. BPE能抑制Poly (I:C)發炎所誘發的細胞傷害 (一氧化氮及氧化壓力)

3. BPE抑制Poly (I:C)發炎的分子機轉為抑制p38/NFκB訊號通路，阻止NFκB進入細胞核活化發炎因子基因表現

BPE第二季成果報告

1. BPE抑制M1促發炎型巨噬細胞的發炎作用例如抑制TNF-α和IL-1β的表現及相關機轉為阻止NFκB進入細胞核。

2. BPE抑制Poly (I:C)誘發小鼠肺炎的動物實驗(前導實驗如小鼠肺部沖洗液內的免疫細胞總數，肺組織染色(H&E stain)及免疫組織化學染色)，完整結果於第三跟第四季成果報告。

3. 評估BPE抗肺纖維化能力：建立TGF-β誘發纖維化模式，完整結果於第四季成果報告。

BPE第三季成果報告: BPE抑制Poly (I:C)誘發小鼠肺炎的動物實驗

1. 肺部沖洗液的免疫細胞

在小鼠的肺部沖洗液中發現，Poly (I:C)在作用 3 天後免疫細胞如白血球，嗜中性球細胞和淋巴球細胞的數目明顯增加，而處理不同濃度BPE的組別後，小鼠肺部沖洗液中的白血球，嗜中性球細胞和淋巴球細胞的數目明顯減少，尤其在600倍與200倍稀釋濃度的BPE組別都有統計上的差異。

2. 肺部沖洗液的細胞激素表現

利用ELISA微矩陣晶片分析小鼠肺部沖洗液中細胞激素的差異。結果發現，Poly (I:C)在誘發的20個細胞激素中IL-6表現量最高(增加4000倍)。而抗發炎因子IL-10則下降2倍。而在BPE作用後，IL-6的表現量隨著BPE的濃度增加而下降，呈現劑量依賴關係。另外，BPE會增加IL-10的表現，顯示BPE處理後能有效降低Poly (I:C)所誘發的急性肺部的發炎。

3. 小鼠肺部病理切片

以H&E染色(hematoxylin and eosin stain) 及半定量分析後發現，Poly (I:C)明顯地增加免疫細胞浸潤到肺泡周圍，而在不同濃度的BPE作用下，明顯地阻止免疫細胞浸潤到肺泡，以600倍稀釋濃度的效果最好。利用組織免疫染色法發現，Poly (I:C)會增加CD11b(巨噬細胞指標物)，IL-6的表現。Poly (I:C)也會增加NF-κB p65蛋白進入細胞核，然而Poly (I:C)會抑制IL-10的表現。在BPE作用下，會抑制Poly (I:C)所增加的CD11b和IL-6的表現，阻止NF-κB p65蛋白進入細胞核，增加IL-10的表現。綜合上述的動物實驗證實，BPE能有效抑制Poly (I:C)所造成的肺部炎症傷害。

BPE第四季成果報告: BPE在TGF-β誘發纖維化模式的抗纖維化的能力

1. BPE在纖維母細胞分化成肌肉纖維細胞的作用

TGF-β1會抑制抗纖維化因子(MMP1和Decorin)的基因表現，增加促纖維化因子COL1A1和αSMA(肌肉纖維細胞指標) 的基因表現。而同時在處理BPE後，會增加MMP1和Decorin的基因表現，抑制COL1A1和αSMA的基因表現，顯示BPE能有效阻止肌纖維細胞的分化。

2. BPE在纖維母細胞移動能力的作用

纖維母細胞細胞受到TGF-β1刺激24小時後，細胞移動能力明顯增，傷口癒合的面積明顯下降且細胞移動速率增加。然而分別處理1/6000及1/2000濃度的BPE後，增加細胞傷口的面積及降低細胞移動的速率，顯示BPE能減緩TGF-β1所增加細胞的移動能力。

3. BPE在細胞外基質生成與機轉的作用

在肺纖維化過程中，肺泡外的細胞外基質蛋白因TGF-β1/active β-catenin/ pSmad3的訊號通路持續反應下而大量表現。纖維母細胞細胞受到TGF-β1刺激48小時後，細胞外基質fibronectin和collagen type 1A1蛋白及有活性的β-catenin蛋白表現量增加。然而分別處理1/6000及1/2000濃度的BPE後，fibronectin和collagen type 1A1蛋白及有活性的β-catenin蛋白表現量明顯減少。另外，TGF-β1會使磷酸化Smad3 (p-Smad3)進入細胞核。然而分別處理1/6000及1/2000濃度的BPE，p-Smad3的表現量下降。綜合以上的結果顯示，BPE能透過抑制TGF-β1/active β-catenin/ pSmad3路徑減少細胞外基質蛋白的表現。

4. BPE在發炎所誘發PAI1(Plasminogen activator inhibitor-1)表現的作用

PAI1(Plasminogen activator inhibitor-1,纖溶酶原激活物抑製劑-1)的生理功能與血栓形成有關。有文獻指出TGF-β透過氧化壓力活化PAI1的表現來降低細胞外基質蛋白被分解，使纖維化程度更惡化。在Poly (I:C)誘發小鼠肺急性發炎實驗發現，小鼠肺組織在發炎時PAI-1會明顯增加，可能會傾向肺泡微血管栓塞或增加肺纖維化的風險，然而在BPE作用下能抑制Poly (I:C)所誘發PAI-1的表現，顯示BPE可降低肺纖維化的能力。未來會進一步以bleomycin(博來黴素)誘發肺纖維化動物實驗來加以印証。

產學合作計畫

蕉科植物萃取物(Banana Plant Extracts, BPE)應用於抑制發炎與癌症之效用與分子機轉 (專案捐款W363-19)

June. 2020 - May. 2022

萬芳癌症中心 癌症轉譯研究室

研究方向

1. 抑制Poly (I:C)誘發小鼠肺炎的動物與細胞實驗成果

2. 評估BPE抗肺纖維化能力: TGF-β誘發纖維化模式

3. 專利申請與商品開發

研究方向

1. 抑制Poly (I:C)誘發小鼠肺炎的動物與細胞實驗成果

2. 評估BPE抗肺纖維化能力: TGF-β誘發纖維化模式

3. 專利申請與商品開發

萬芳醫院BPE產學合作成果:預計2篇國際文章和1項專例

文章發表

1. Banana plant extracts Inhibit the Inflammatory Response in a Mouse Model of Polyinosinic–Polycytidylic Acid-induced Acute Lung Injury

2. Antifibrotic effects of Banana plant extracts on TGF-β–treated lung fibroblasts via repressing TGF-β/smad3/β-Catenin patheay

專利申請

Banana plant extract (BPE)抑制促纖維化因子PAI-1之用途-臺北醫學大學審查中

作者群暫定：Chien-Huang Liao, Flank Liu, Gi-Ming Lai*, Chih-Jung Yao*

BFE抗發炎實驗：仿RNA病毒感染肺細胞實驗

雙股RNA病毒裡RNA的結構

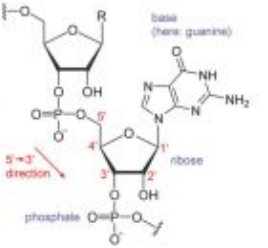

Poly (I:C)的結構

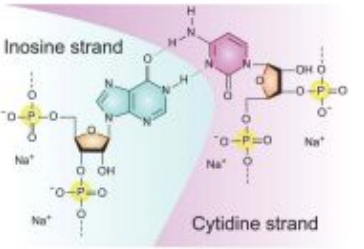

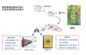
Poly (I:C)
BPE

BPE抗發炎機轉

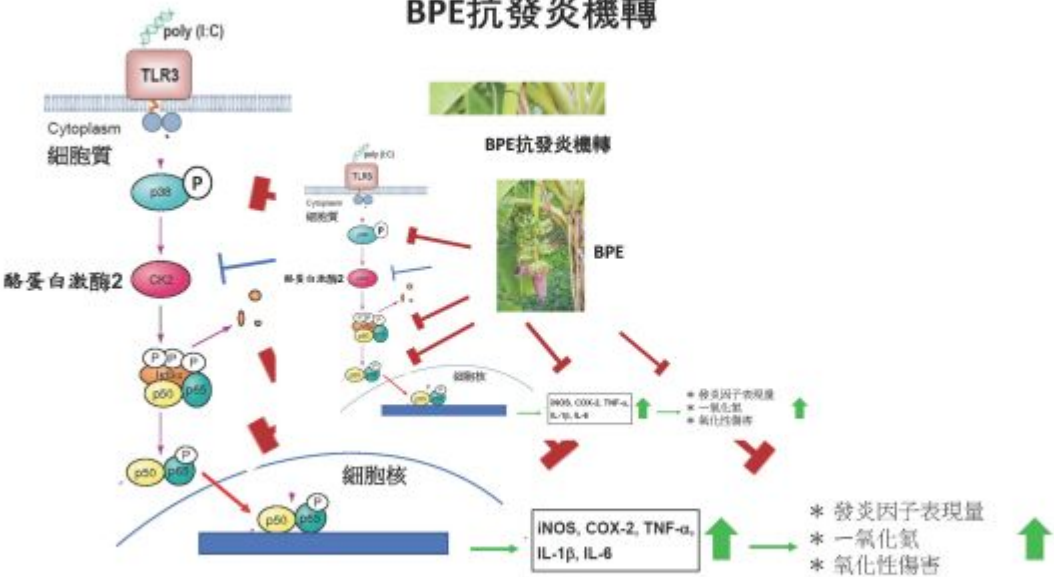
poly (I:C)
TLR3
Cytoplasm
細胞質
p38
P
酪蛋白激酶2
CK2
p50
p65
細胞核
BPE抗發炎機轉
BPE
iNOS, COX-2, TNF-α,
IL-1β, IL-6
＊發炎因子表現量
＊一氧化氮
＊氧化性傷害

BPE成果報告: BPE抑制Poly (I:C)誘發小鼠肺炎的動物實驗

1. 肺部沖洗液的免疫細胞

在小鼠的肺部沖洗液中發現，Poly (I:C)在作用 3 天後免疫細胞如白血球，嗜中性球細胞和淋巴球細胞的數目明顯增加，而處理不同濃度BPE的組別後，小鼠肺部沖洗液中的白血球，嗜中性球細胞和淋巴球細胞的數目明顯減少，尤其在600倍與200倍稀釋濃度的BPE組別都有統計上的差異。

2. 肺部沖洗液的細胞激素表現

利用ELISA微矩陣晶片分析小鼠肺部沖洗液中細胞激素的差異。結果發現，Poly (I:C)在誘發的20個細胞激素中IL-6表現量最高(增加4000倍)。而抗發炎因子IL-10則下降2倍。而在BPE作用後，IL-6的表現量隨著BPE的濃度增加而下降，呈現劑量依賴關係。另外，BPE會增加IL-10的表現，顯示BPE處理後能有效降低Poly (I:C)所誘發的急性肺部的發炎。

3. 小鼠肺部病理切片

以H&E染色(hematoxylin and eosin stain)及半定量分析後發現，Poly (I:C)明顯地增加免疫細胞浸潤到肺泡周圍，而在不同濃度的BPE作用下，明顯地阻止免疫細胞浸潤到肺泡，以600倍稀釋濃度的效果最好。利用組織免疫染色法發現，Poly (I:C)會增加CD11b(巨噬細胞指標物)，IL-6的表現。Poly (I:C)也會增加NF-κB p65蛋白進入細胞核，然而Poly (I:C)會抑制IL-10的表現。在BPE作用下，會抑制Poly (I:C)所增加的CD11b和IL-6的表現，阻止NF-κB p65蛋白進入細胞核，增加IL-10的表現。綜合上述的動物實驗證實，BPE能有效抑制Poly (I:C)所造成的肺部炎症傷害。

研究方向

1. 抑制Poly (I:C)誘發小鼠肺炎的動物與細胞實驗成果

2. 評估BPE抗肺纖維化能力: TGF-β誘發纖維化模式

3. 專利申請與商品開發

BPE抑制TGF-β的作用來降低肺纖維化程度的惡化.

BPE第四季成果報告: BPE在TGF-β誘發纖維化模式的抗纖維化的能力

1. BPE在纖維母細胞分化成肌肉纖維細胞的作用

TGF-β1會抑制抗纖維化因子(MMP1和Decorin)的基因表現，增加促纖維化因子COL1A1和αSMA(肌肉纖維細胞指標) 的基因表現。而同時在處理BPE後，會增加MMP1和Decorin的基因表現，抑制COL1A1和αSMA的基因表現，顯示BPE能有效阻止肌纖維細胞的分化。

2. BPE在纖維母細胞移動能力的作用

纖維母細胞細胞受到TGF-β1刺激24小時後，細胞移動能力明顯增，傷口癒合的面積明顯下降且細胞移動速率增加。然而分別處理1/6000及1/2000濃度的BPE後，增加細胞傷口的面積及降低細胞移動的速率，顯示BPE能減緩TGF-β1所增加細胞的移動能力。

3. BPE在細胞外基質生成與機轉的作用

在肺纖維化過程中，肺泡外的細胞外基質蛋白因TGF-β1/active β-catenin/ pSmad3的訊號通路持續反應下而大量表現。纖維母細胞細胞受到TGF-β1刺激48小時後，細胞外基質fibronectin和collagen type 1A1蛋白及有活性的β-catenin蛋白表現量增加。然而分別處理1/6000及1/2000濃度的BPE後，fibronectin和collagen type 1A1蛋白及有活性的β-catenin蛋白表現量明顯減少。另外，TGF-β1會使磷酸化Smad3 (p-Smad3)進入細胞核。然而分別處理1/6000及1/2000濃度的BPE，p-Smad3的表現量下降。綜合以上的結果顯示，BPE能透過抑制TGF-β1/active β-catenin/ pSmad3路徑減少細胞外基質蛋白的表現。

4. BPE在發炎所誘發PAI1(Plasminogen activator inhibitor-1)表現的作用

PAI1(Plasminogen activator inhibitor-1,纖溶酶原激活物抑製劑-1)的生理功能與血栓形成有關。有文獻指出TGF-β透過氧化壓力活化PAI1的表現來降低細胞外基質蛋白被分解，使纖維化程度更惡化。在Poly (I:C)誘發小鼠肺急性發炎實驗發現，小鼠肺組織在發炎時PAI-1會明顯增加，可能會傾向肺泡微血管栓塞或增加肺纖維化的風險，然而在BPE作用下能抑制Poly (I:C)所誘發PAI-1的表現，顯示BPE可降低肺纖維化的能力。未來會進一步以bleomycin(博來黴素)誘發肺纖維化動物實驗來加以印証。

研究方向

1. 抑制Poly (I:C)誘發小鼠肺炎的動物與細胞實驗成果

2. 評估BPE抗肺纖維化能力: TGF-β誘發纖維化模式

3. 專利申請與商品開發

專利申請方向

PAI1抑制劑：涵蓋抗血栓及抗纖維化(TGF-β/pSmad3/β-catenin與TGF-β/PAI1)

第二期BPE產學計畫第一年期末進度報告

1. BPE論文與專利進度說明
2. BPE抑制肝細胞纖維化與發炎
3. BPE於抗藥性癌細胞株(胰臟癌)的化療增敏作用
4. BPE植物新泌體的開發

第二期BPE產學計畫第一年期末進度報告

1. **BPE論文與專利進度說明**
2. BPE抑制肝細胞纖維化與發炎
3. BPE於抗藥性癌細胞株(胰臟癌)的化療增敏作用
4. BPE植物新泌體的開發

BPE第一期的研究成果已投稿於MDPI出版社的pharmaceutics (IF: 6.52)

Gmail

[redacted]

[Pharmaceutics] Manuscript ID: pharmaceutics-2120346 - Declined for Publication - Encourage Resubmission after Revisions

1 封郵件

Pharmaceutics Editorial Office <pharmaceutics@mdpi.com> 2023年2月1日 上午8:35

回覆: kimberly.foo@mdpi.com

收件者: Chih-Jung Yao <yaochihjung@gmail.com>

副本: Chien-Huang Liao <106122@w.tmu.edu.tw>, Yu-Yin Lin <iamyuying@yahoo.com.tw>, Yi-Chun Liao <yichunliao0109@gmail.com>, Gi-Ming Lai <gminlai@canceraway.org.tw>, Tzeon-Jye Chiou <108178@w.tmu.edu.tw>, Frank Liu <gftfrank@ms22.hinet.net>, Tien-Hua Chu <tienhuachu@cmr-biosci.com>, Szu-Yao Wu <szuyao@cmr-biosci.com>, Jacqueline Whang-Peng <jqwpeng@nhri.org.tw>, Tung-Yuan Lai <lai96917@gmail.com>, Chih-Jung Yao <yao0928@tmu.edu.tw>, Pharmaceutics Editorial Office <pharmaceutics@mdpi.com>, Zora Zhou <zora.zhou@mdpi.com>

Dear Dr. Yao,

I am writing to you concerning the manuscript you recently submitted to Pharmaceutics. Based on the review reports, the manuscript is not suitable for publication in Pharmaceutics in its present format. Significant revisions or new data are required in the manuscript to warrant further consideration for publication of this manuscript in Pharmaceutics.

Manuscript ID: pharmaceutics-2120346
Type of manuscript: Article
Title: Inhibition of Poly (I:C)-Induced Acute Pulmonary Inflammation and NF-κB Activation in Mice by a Banana Plant Extract
Authors: Chien-Huang Liao, Yu-Yin Lin, Yi-Chun Liao, Gi-Ming Lai, Tzeon-Jye

審查意見只剩下reviewer對BPE萃取方法之異議，為避免此項爭議，將改投Archives of Medical Science (IF: 3.7)

不同批次的BPE產品在抗發炎的生物功效能力相似

1. 利用RAW264.7細胞分析不同批次的BPE產品抑制Poly (I:C) 所增加的IL-6基因表現。以Q-PCR實驗結果發現，三個不同批次生產的BPE皆能有效抑制Poly (I:C) 所增加的IL-6基因表現。
2. 由上述的結果發現，不同批次生產的BPE之抑制IL-6(發炎細胞激素)基因表現的功效穩定。

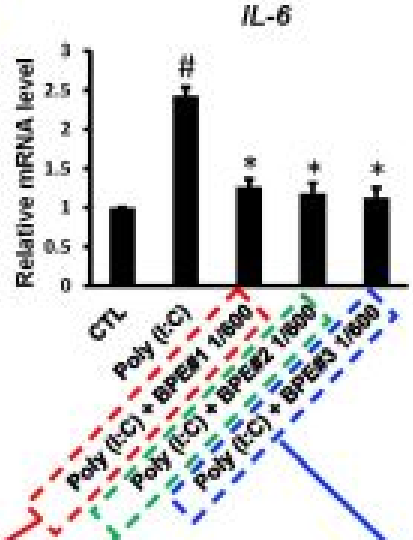

#p < 0.05, compared with the control (CTL) group. *p < 0.05, compared with poly (I:C)-stimulated group.

BPE專利申請進度說明

Fwd: 【請核稿】台灣發明專利說明書-實施例/圖式核稿事宜 (Ref：NP-35957)

Yao, chihjung

Chih-Jung Yao, Ph.D. Medical Research F

2023年4月18日 下午5:33

hw.peng@mail.saint-island.com.tw

2023年6月6日 下午2:02

收信 yao0928、我、hfchang

施博士您好，

於此檢附修稿後說明書供知悉審閱，有勞再就紅字部分進行確認與回覆，謝謝!

聖島國際專利商標聯合事務所
專利師 高玉駿 敬上
聯絡人 台北所 彭信維
TEL:(02)7702-8299 ext.272
FAX:(02)7702-8289
MOB:0930-133554
E-MAIL：hw.peng@mail.saint-island.com.tw

已修改專利事務所的建議事項後再次送審給事務所核稿

From: 彭信維
Sent: Wednesday, May 17, 2023 5:57 PM
To: Yao, chihjung <yao0928@tmu.edu.tw>
Cc: 106122@w.tmu.edu.tw; hfchang@tmu.edu.tw

第二期BPE產學計畫第一年期末進度報告

1. BPE論文與專利進度說明
2. **BPE抑制肝細胞纖維化與發炎**
3. BPE於抗藥性癌細胞株(胰臟癌)的化療增敏作用
4. BPE植物新泌體的開發

第一年的期中報告已初步發現在肝星狀細胞株(LX-2 cells)中，BPE能透過抑制TGF-β/SMAD3路徑來降低TGF-β所誘發纖維化蛋白Col1A1與α-SMA的表現。

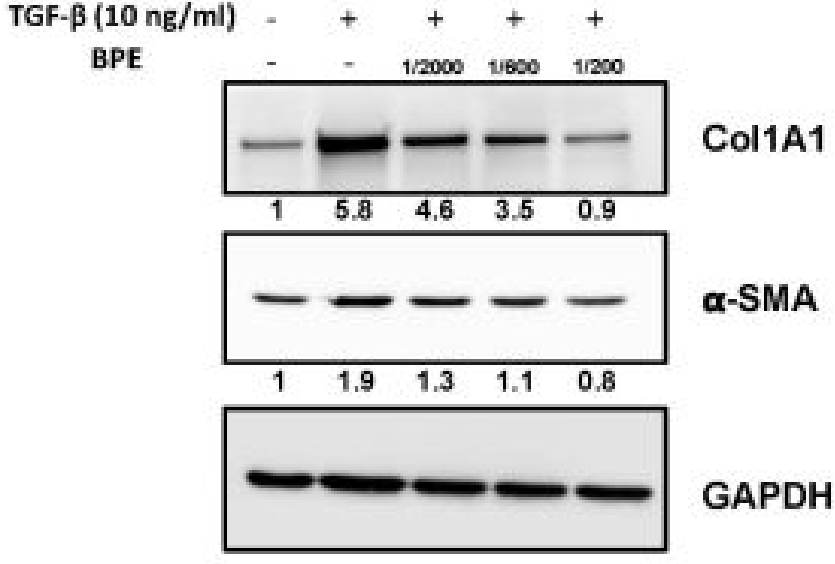

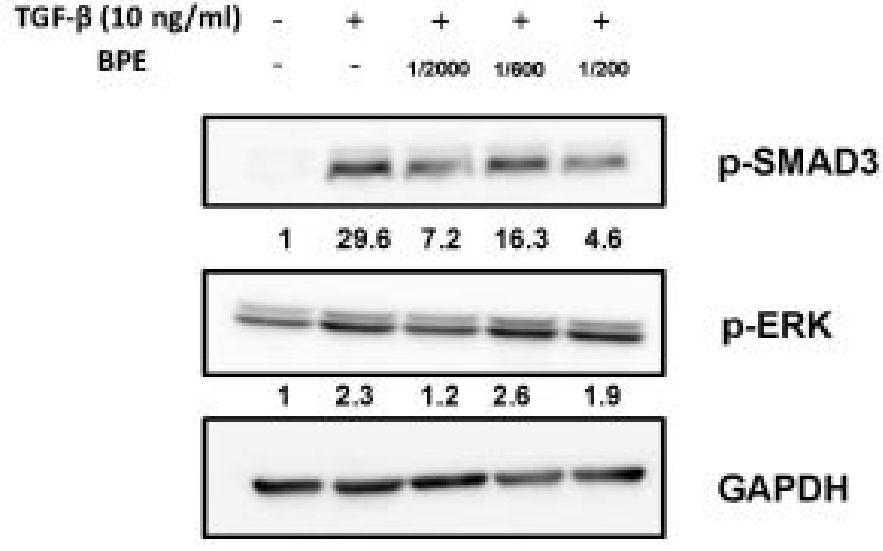

hepatic stellate cells LX2

肝纖維化病理生成

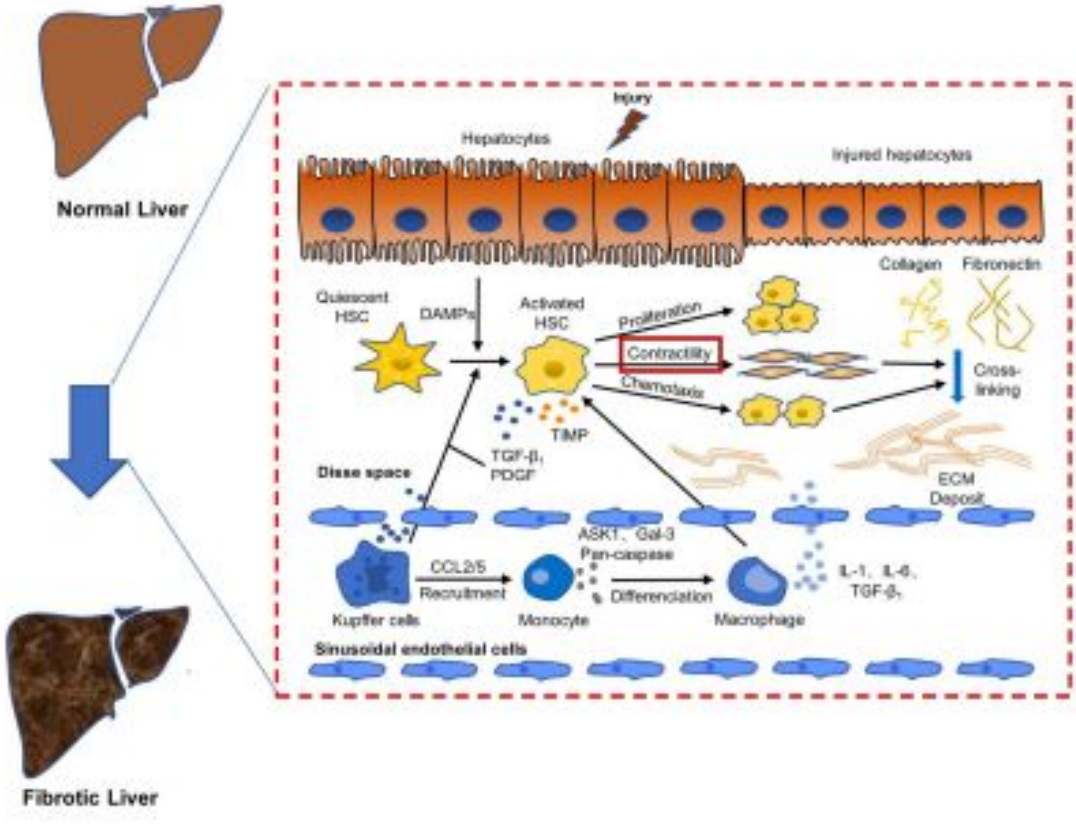

肝纖維化主要是肝臟微環境失去平衡，包括

(1). 肝細胞受損

(2). 肝星狀細胞：休眠傾向活化

(3). 肝免疫細胞(庫佛細胞): 原生態分化成巨噬細胞

其中活化態的肝星狀細胞具有多種細胞特性如細胞收縮(Contractility)，生成纖維化蛋白(Collagen)並使細胞外基質(ECM)大量累積。

阻止肝星狀細胞收縮能降低ECM的累積，減緩肝纖維化的病理生成

Front. Cell Dev. Biol.2021, 9:730176.

BPE抑制TGF-β誘發肝星狀細胞株(LX-2 cells)的細胞收縮(cell contractility)形態改變

1. 將LX-2細胞以高密度($9*10^5$/孔)種植在12 孔盤後加入TGF-β 24小時，結果發現細胞收縮而在培養皿上形成許多空洞形態。
2. 有處理不同濃度的BPE，因降低細胞收縮而減小空洞的面積，同時也增加空洞間的間距(紅色箭頭)，其中1/200稀釋的BPE阻止細胞收縮的效果顯著，該組細胞的形態幾乎與控制組相似。

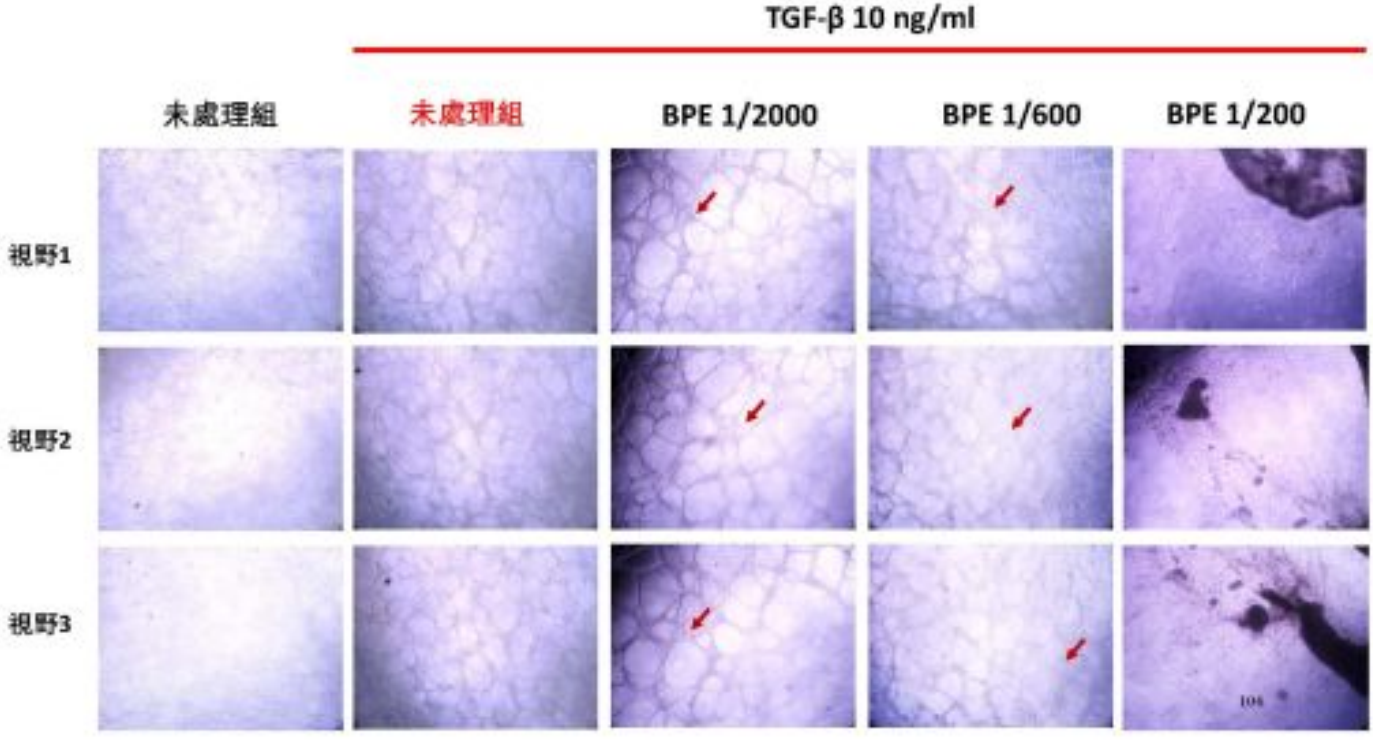

BPE抑制TGF-β誘發肝星狀細胞株(LX-2 cells)的細胞收縮(cell contractility)形態改變 (局部視野放大

紅色箭頭:
空洞間距變寬(意指細胞減緩收縮反應)。

CTL (control)

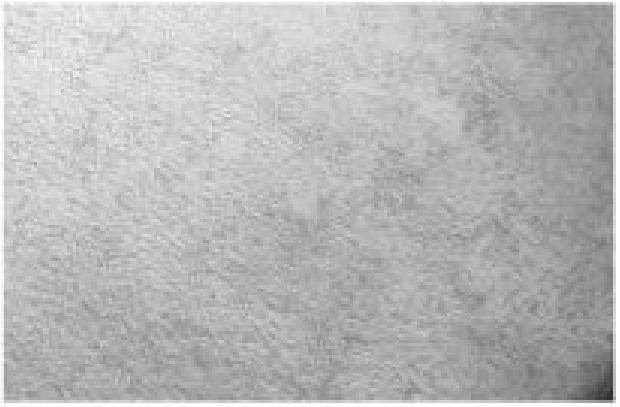

TGF-β 10 ng/ml

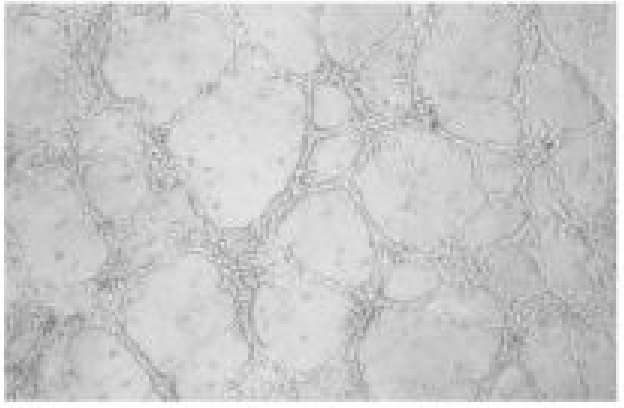

TGF-β 10 ng/ml+BPE 1/2000

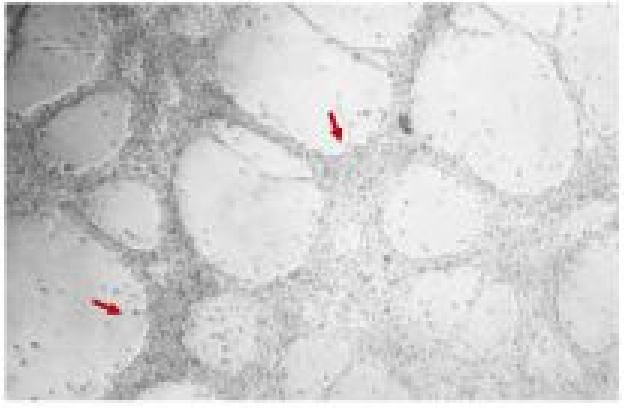

TGF-β 10 ng/ml+BPE 1/600

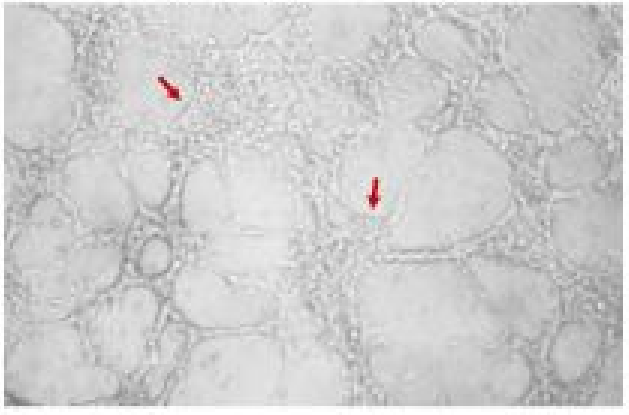

TGF-β 10 ng/ml+BPE 1/200

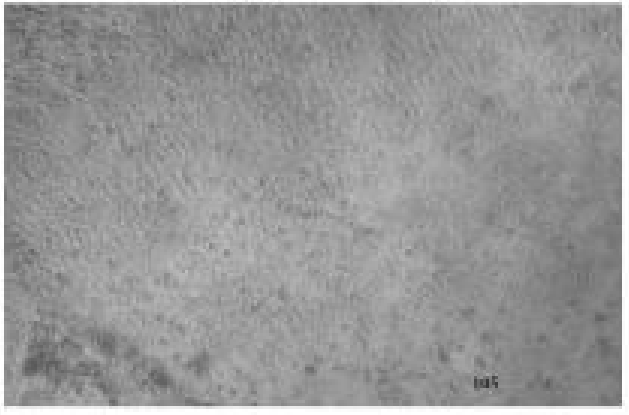

BPE降低TGF-β誘發的LX-2細胞內皮素(endothelin-1; ET-1)基因表現

Research Article

EASL JOURNAL OF HEPATOLOGY

Journal of Hepatology 2011 vol. 54 | 521–528

TGF-β1 mediated activation of Rho kinase induces TGF-β2 and endothelin-1 expression in human hepatic stellate cells

Hideaki Shimada, Nicholas R. Staten, Lakshman E. Rajagopalan*

Inflammation Research Unit, Pfizer Global Research and Development, Pfizer Inc., 700 Chesterfield Parkway West, Chesterfield, MO 63017, USA

Minireview *Highlight article*

Experimental Biology and Medicine 2020; 245: 1504–1512.

Endothelin-1 in portal hypertension: The intricate role of hepatic stellate cells

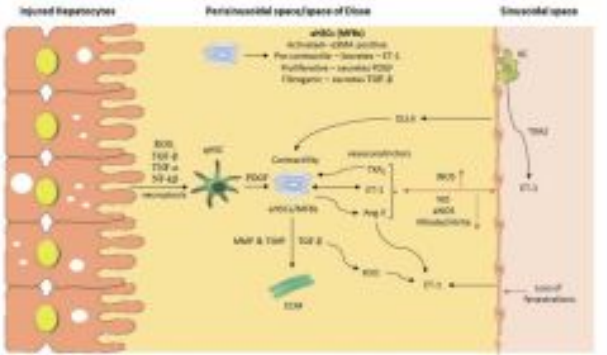

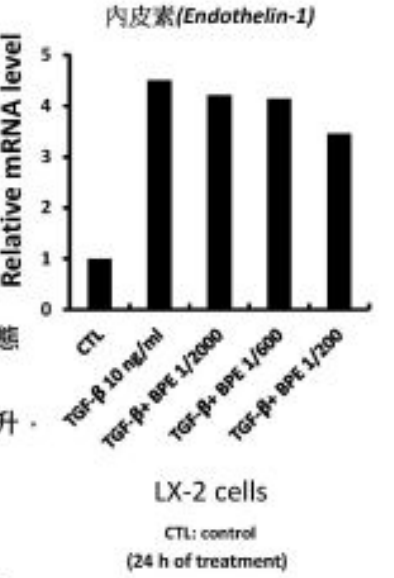

1. 活化態的肝星狀細胞產生細胞收縮形態時會增加內皮素基因的表現。
2. 在肝纖維化過程中內皮素表現量會上升，造成肝門靜脈高壓 (portal hypertension)，引發胃食道靜脈曲張出血及肝腦病變等併發症。
3. BPE能抑制LX-2細胞收縮所誘發的內皮素基因表現，顯示其降低肝纖維化併發症的潛力。

BPE 改善H_2O_2 (1 mM)作用後之肝細胞株(L02 cells)的存活率

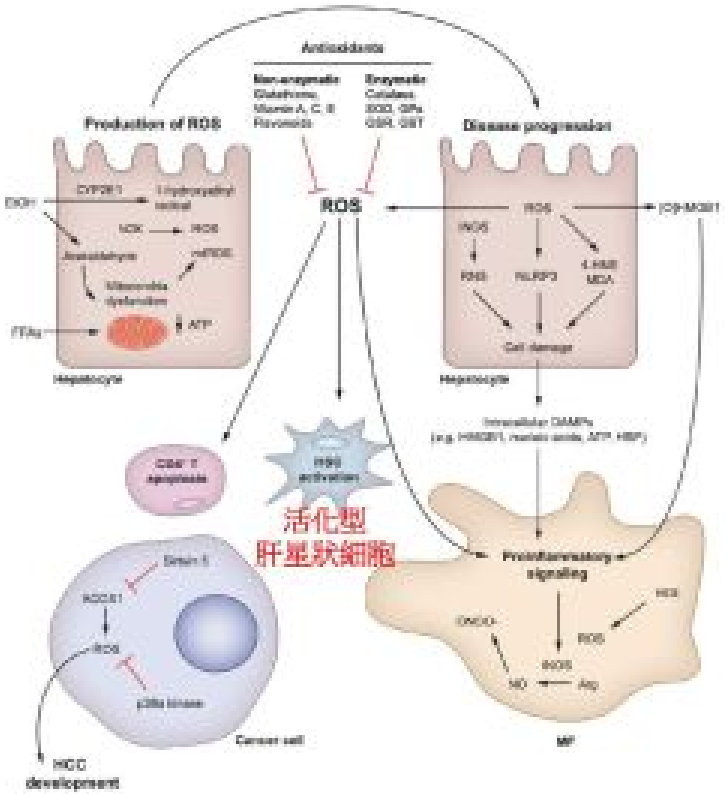

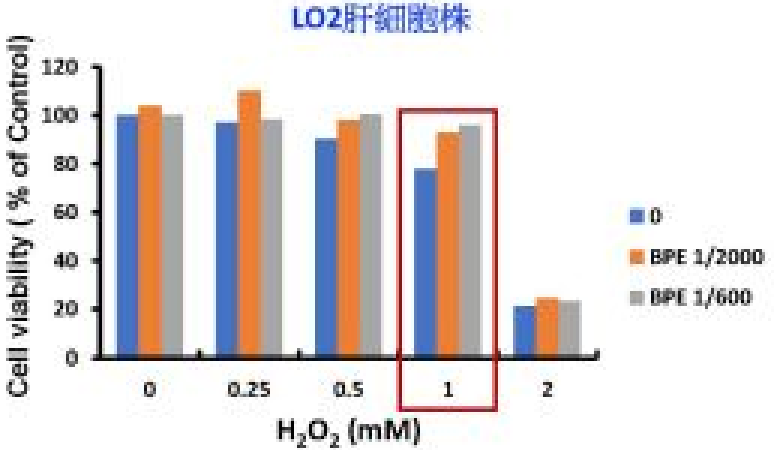

1. 肝細胞會代謝有害物質並產生氧化性物質如ROS使肝細胞受損。
2. 實驗發現，處理1 mM H_2O_2 24小時後會抑制L02細胞存活率至77%，而有同時處理1/2000 或 1/600稀釋濃度BPE的組別，其存活率會分別改善至92%和95%。
3. 由ROS造成的受損肝細胞會產生損傷相關分子模式(Damage-associated molecular patterns, DAMPs)激活化肝星狀細胞與免疫細胞，誘發纖維化的病程，因此BPE降低氧化性傷害有助於減少DAMPs產生。

BPE抑制細菌內毒素(Lipopolysaccharide, LPS)誘發肝細胞發炎、氧化壓力與肝細胞受損的效用

Inducible nitric oxide synthase (iNOS): 誘發reactive nitrogen species (RNS)
Nicotinamide adenine dinucleotide phosphate oxidase 1 (NOX1): 誘發reactive oxygen species (ROS)

1. LPS會誘發肝細胞株(L02 cells)發炎因子基因 (TNF-α, IL-6和TGF-β)、氧化基因(iNOS和NOX1)和肝細胞受損指標(GPT)的表現。

2. 右圖不同稀釋濃度的BPE皆能抑制LPS誘發的發炎基因 (TNF-α, IL-6和TGF-β)、氧化基因(iNOS和NOX1)和肝細胞受損指標(GPT)的表現。

3. 1/6000、1/2000稀釋的BPE能增加抗發炎因子IL-10基因表現。

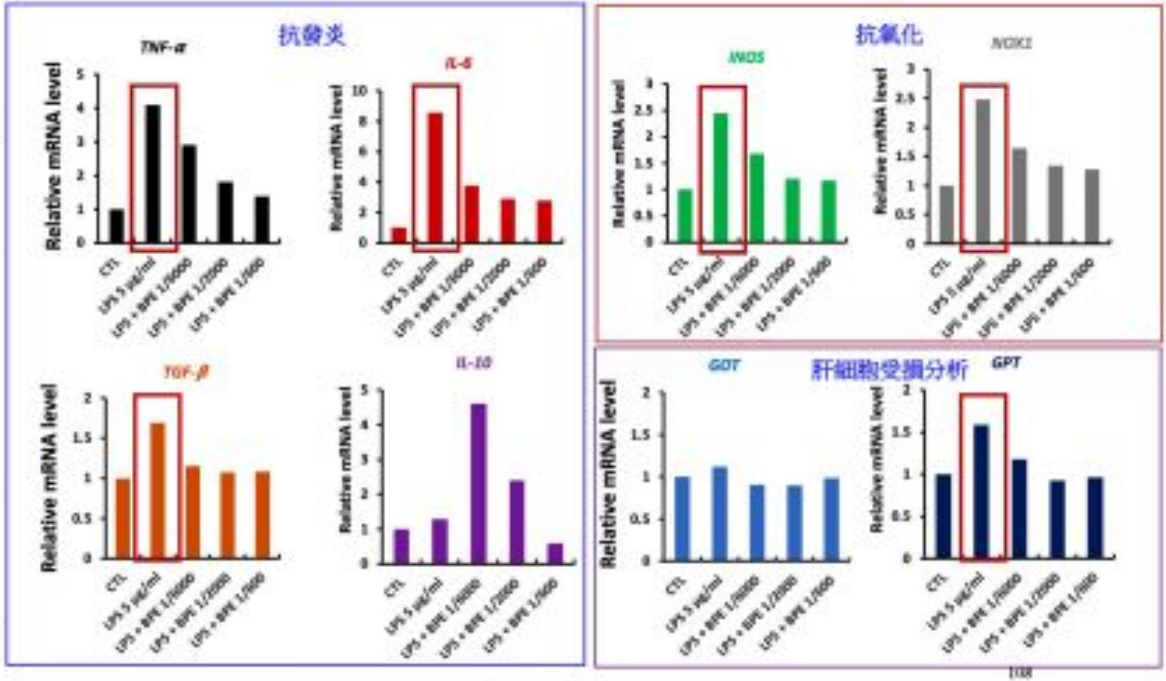

CTL: control

(24 h of treatment)

受損的肝細胞會分泌damage-associated molecular patterns, DAMPs (如HMGB1, OPN和HSP90等)與相對的受器(如RAGE, Integrin αVβ3和TLRs)結合後透過PI3K/pAKT/NFκB路徑來活化肝星狀細胞並生成肝纖維化蛋白collagen 1

Table 2. DAMPs are involved in chronic liver injury and restoration of homeostasis.

DAMP	Receptor(s)	Effect(s)	Reference(s)
ALD			
mtDNA	TLR9	Proinflammatory; Profibrogenic	
Uric acid	NLR	Proinflammatory	
ATP	P2RX7	Proinflammatory	
HSP90		Oxidative stress; Proteotoxic; Proinflammatory	
HMGB1	RAGE/TLR4	Proteotoxic	
Hyaluronic acid	TLR4	Profibrogenic	
LCN2	LCN2R	Proinflammatory	
PGE2	PGE2 receptor	Immunosuppression; Proteotoxic	
NASH			
mtDNA	TLR9	Proteotoxic; Profibrogenic	
miRNA	TLR7	Monocyte-derived macrophage activation; IFNγ and TNFα production; T cell recruitment	
AGE	RAGE	Increase during NASH progression	
mtROS	NLRP3	Proteotoxic; Profibrogenic	
Biglycan	TLR2/4	Increase during NASH progression	
Galectin-3	TLR2/4	Promote fibrosis and hepatocyte ballooning	
Fibrinogen	TLR4	Form deposits to promote fatty liver disease	
Cholesterol crystals	NLRP3	Proteotoxic	
Fibrosis			
HMGB1	RAGE	Hepatic stellate cell activation; Collagen type I production; Endoplasmic reticulum stress	
OPN	Integrin $\alpha V\beta_3$	Increases HMGB1; HSC activation via PI3K/pAkt/NF-κB; Ductular reaction	
HSP90	TLR2/TLR4	HSC activation	
HSP47	TLRs	Profibrogenic	
IL-33	IL-33R	Profibrogenic via NF-κB and MAPKs; Proinflammatory (Th2 cytokines)	
ATP adenosine	P2rx7, A2AR, A2BR	MF release of IL1β and HMGB1; Profibrogenic	
HCC			
HMGB1	RAGE, TLR9	Tumour initiation and progression	
OPN	Integrins, CD44	Tumour growth, metastasis and immune escape	
S100A1	RAGE	Increases in HCC and correlates with poor survival	
S100A4	RAGE	Tumour growth and metastasis	
S100A8	RAGE	Tumour growth and metastasis	
S100A9	RAGE	Tumour initiation and progression	
mtDNA	TLR9	HMGB1 binding to TLR9	
Extracellular ATP	P2	HCC cell migration	
Calreticulin	N/A	Tumour growth and invasion	
Histones	TLR4	HCC metastasis	

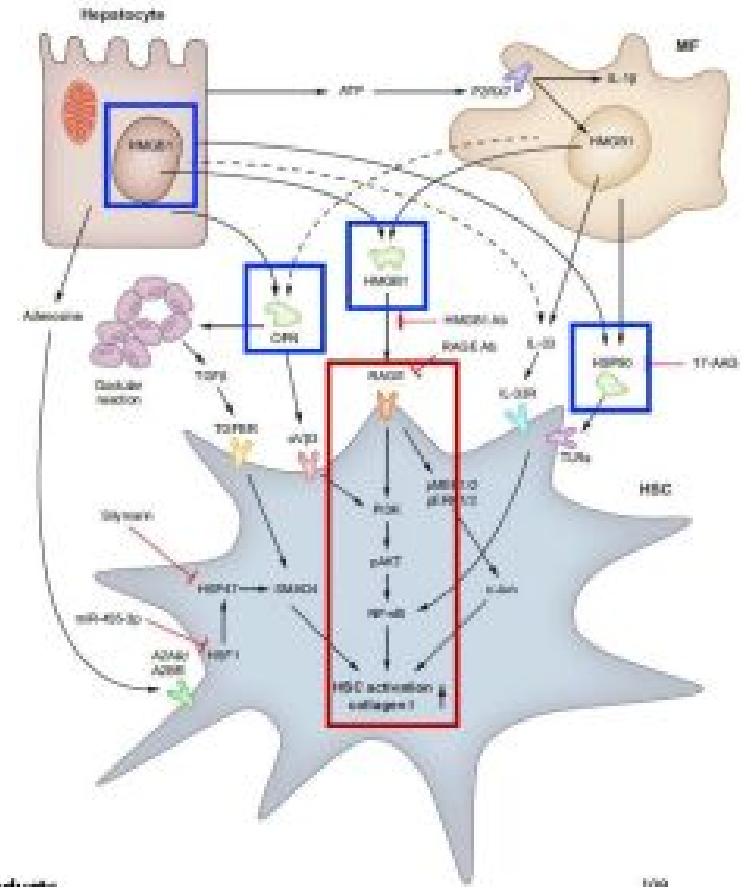

HMGB1, high-mobility group box-1

OPN, osteopontin

RAGE, receptor for advanced glycation end-products

Journal of Hepatology 2020 vol. 73 :933–951

BPE降低DAMPs的受器RAGE基因的表現進而抑制纖維化因子Col1A1和αSMA基因表現

1. BPE在LPS誘導肝細胞株(L02 cells)受損模式中會抑制osteopontin (OPN)基因的表現。
2. 在TGF-β誘導肝星狀細胞株(LX-2 cells)活化過程中，BPE會抑制TGF-β 所增加之RAGE和HSP47(會促進 Col1A1表現)基因的表現。
3. 外加TGF-β於LX-2細胞發現會增加TGF-β基因表現，顯示TGF-β會呈獻正回饋作用而持續放大TGF-β下游訊號，而處理BPE後則會抑制TGF-β基因表現而阻斷TGF-β正回饋作用。
4. LPS (5 μg/ml) 對HMGB1基因表現的影響不明顯，但其受器RAGE基因表現被TGF-β提升時，可被BPE所降低，BPE也同時抑制了RAGE調控的下游促纖維化因子(Col1A1和αSMA)基因表現，顯示DAMPs所誘發肝星狀細胞株活化路徑可被BPE所抑制。
5. 另外，TGF-β會提升另一個促纖維化因子TIMP1基因的表現，並抑制抗纖維化因子(Decorin)基因表現，而這些TGF-β的作用可被BPE逆轉。

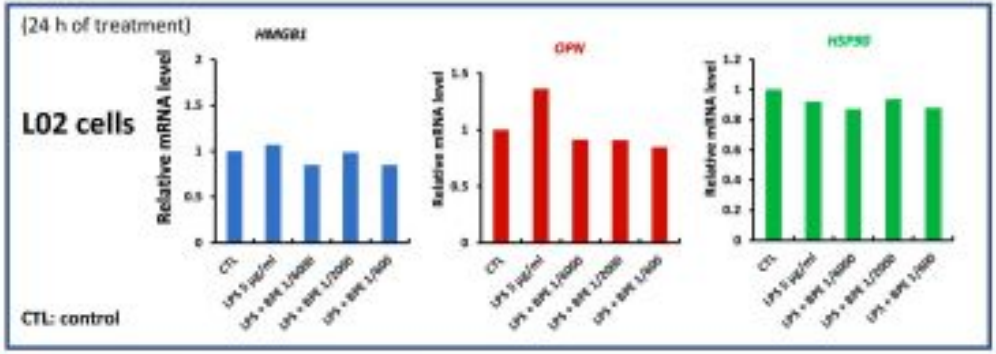

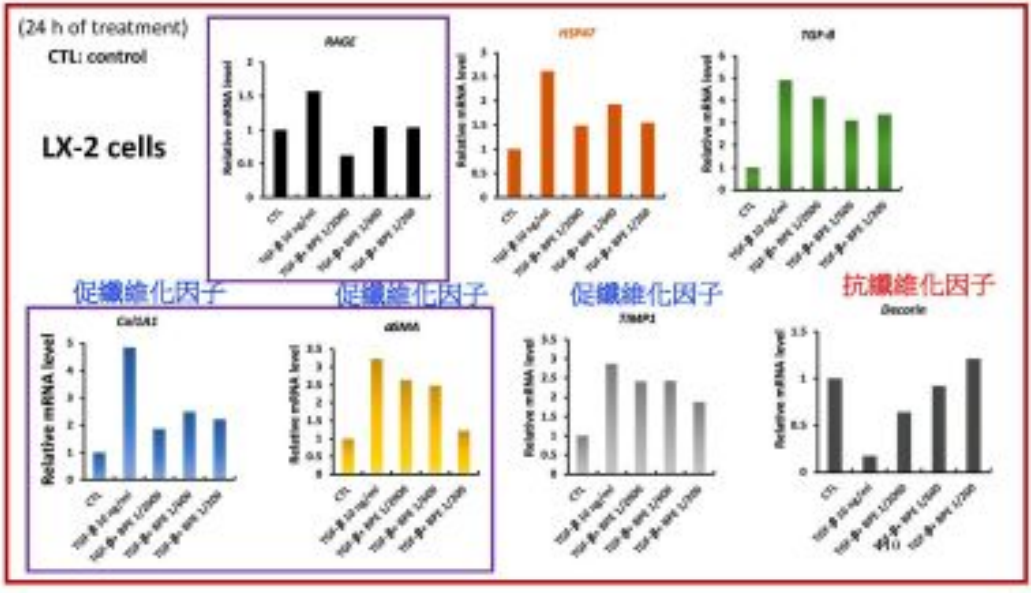

結論(一)

1. BPE抑制TGF-β誘發肝星狀細胞株(LX-2 cells)的細胞收縮(cell contractility)形態改變。
2. BPE降低TGF-β誘發LX-2細胞的內皮素(endothelin-1; ET-1)基因表現，顯示BPE有降低肝纖維引發之併發症的潛力。
3. BPE 逆轉H_2O_2對肝細胞株(L02 cells)的生存率抑制，顯示BPE可降低氧化性傷害。
4. BPE抑制細菌內毒素(Lipopolysaccharide, LPS)誘發之肝細胞株發炎，氧化壓力與肝細胞株受損。
5. BPE阻止TGF-β誘導之RAGE基因 (Damage-associated molecular patterns, DAMPs 的受器) 的表現，並抑制下游纖維化因子Col1A1和αSMA基因表現。
6. 目前正以Thioacetamide(TAA)誘發慢性肝纖維化模式，進行BPE抗肝纖維化功效評估，結果將於下次報告說明。

第二期BPE產學計畫第一年期末進度報告

1. BPE論文與專利進度說明
2. BPE抑制肝細胞纖維化與發炎
3. **BPE於抗藥性癌細胞株(胰臟癌)的化療增敏作用**
4. BPE植物新泌體的開發

第一年的期中報告已初步發現BPE能逆轉抗藥株(Panc-1 Gem 50 μM) cells對化療藥gemcitabine和Oxaliplatin的抗藥性。

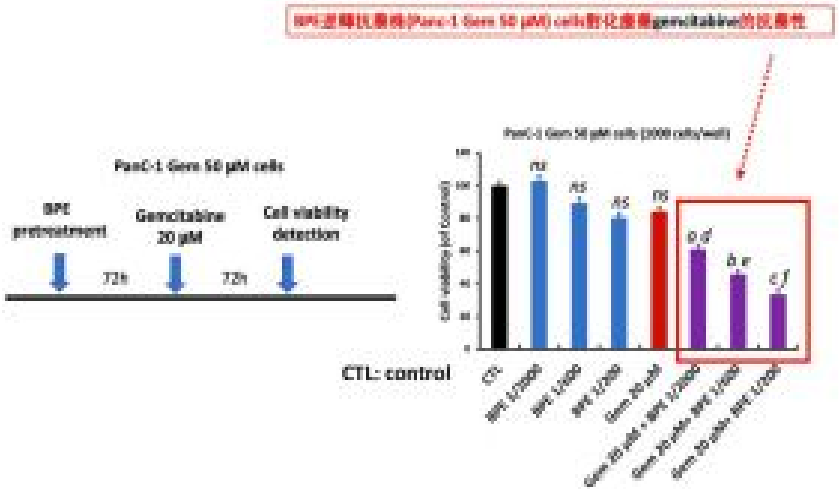

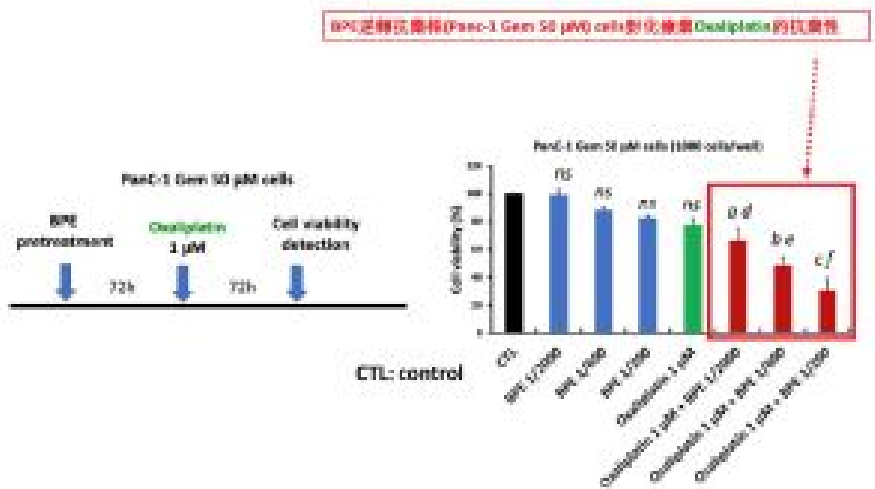

抗癌藥物引起的老化，有促進癌症惡化的風險。

A growing number of studies have convincingly demonstrated a paradoxical role for spontaneous senescence and therapy-induced senescence (TIS), that senescence may involve both cancer prevention and cancer aggressiveness.
---Front Cell Dev Biol. 2021;9:722205.

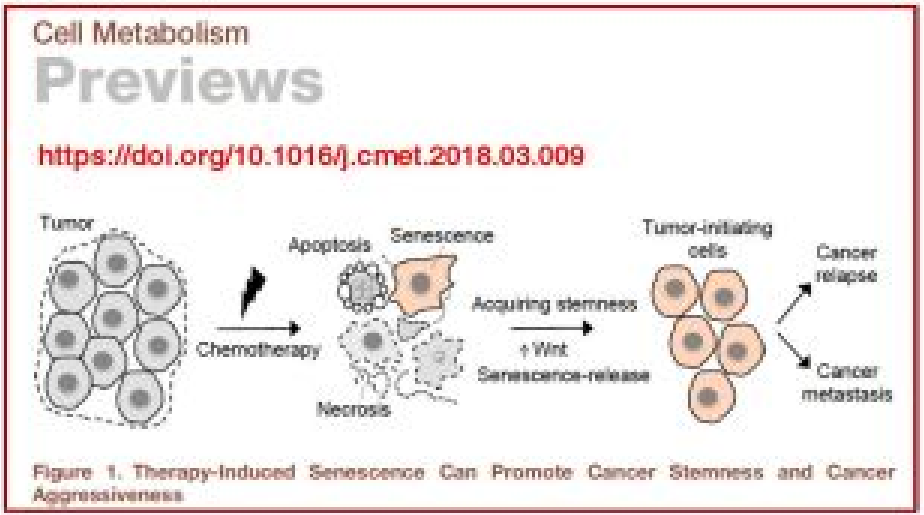

近幾年有研究發現，抗癌化學藥物在治療過程中會使癌細胞產生老化現象，稱為TIS。老化的癌細胞會分泌Senescence associated secretory phenotype (SASP)，會誘發癌細胞產生幹細胞特性並使癌症更惡性。因此，降低TIS發生可阻止癌症惡化。

BPE抑制化療藥引起胰臟癌抗藥性細胞(Panc-1 Gem 50 μM cells)的老化(senescence)反應

1. 化療藥物Gemcitabine與Oxaliplatin 於胰臟癌抗藥性細胞株(Panc-1 Gem 50 μM cells)作用72小時後，以SA-β-galactosidase試劑染色後，發現呈現藍色反應的衰老癌細胞 (紅色箭頭指示)。

2. 而有前處理BPE 72小時後再分別處理Gemcitabine或Oxaliplatin的組別經 SA-β-galactosidase試劑染色後，並無發現呈現藍色反應的衰老癌細胞，顯示BPE能抑制上述化療藥物引起的癌細胞老化反應。

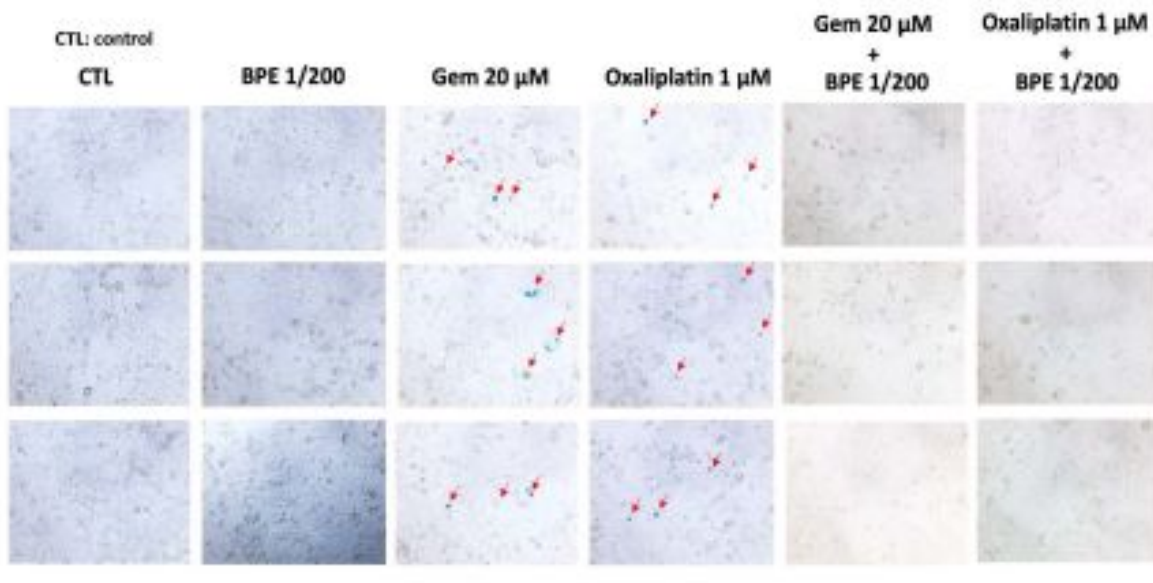

Gem: Gemcitabine

Panc-1 Gem 50 μM cells

BPE抑制化療藥引起胰臟癌(Panc-1)細胞的老化(senescence)反應

1. 化療藥物Gemcitabine與 Oxaliplatin於胰臟癌細胞株(Panc-1) 作用72小時後，以SA-β-galactosidase試劑染色後，發現呈現藍色反應的衰老癌細胞 (紅色箭頭指示)。

2. 而併用BPE+Gemcitabine或BPE+Oxaliplatin 72 h的組別經 SA-β-galactosidase試劑染色後，並無發現呈現藍色反應的衰老癌細胞，顯示BPE能抑制上述化療藥物引起的癌細胞老化反應。

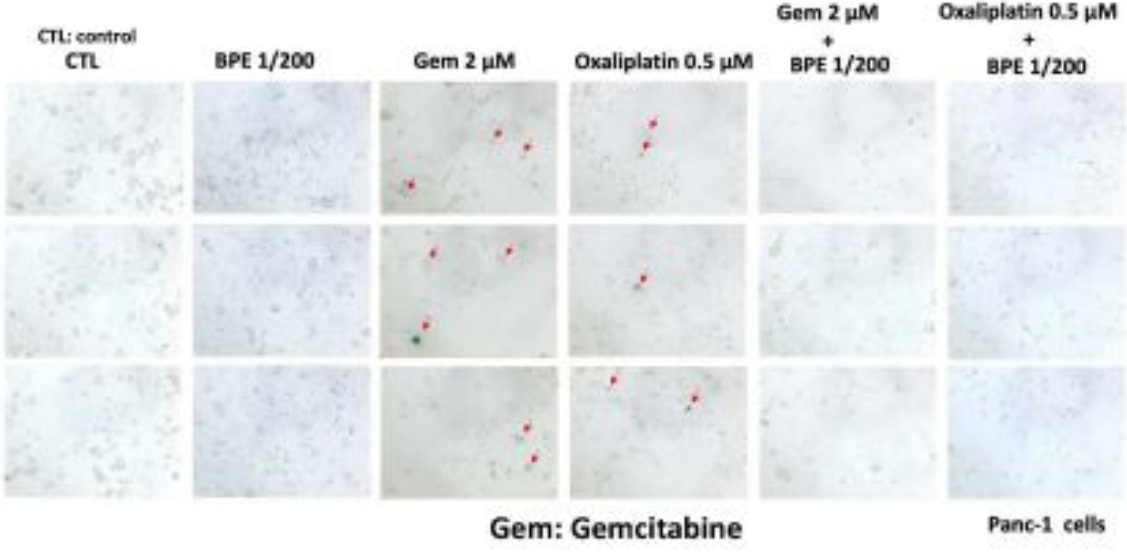

化療藥品樂拿舒(Asparaginase)於實體腫瘤的運用開發

1. 樂拿舒(Asparaginase, 衛署藥輸字第021032號)目前是抗血癌的臨床用藥，主要藥理為Asparaginase能分解血液中的L-Asparagine，使需要L-Asparagine的癌細胞缺乏營養而達到其抗癌作用。
2. 目前已有臨床前研究，探討Asparaginase 對直腸癌與胰臟癌等實體腫瘤的抑制作用。這些研究發現，併用GSK-3α抑制劑能增強低濃度Asparaginase對直腸癌細胞的抑制作用。而併用 glutamine synthetase抑制劑則可增進Asparaginase對胰臟癌細胞的抑制作用。
3. 目前胰臟癌治療上仍是嚴峻，開發 Asparaginase合併療法將有望增強低劑量Asparaginase的藥效且能降低其藥物衍生的副作用。

併用BPE能增強低劑量化療藥物樂拿舒(Asparaginase)對Panc-1胰臟癌細胞與Panc-1 Gem 50 μM抗藥性胰臟癌細胞的生長抑制效用

1. 0.5, 1和5 U/ml的asparaginase 皆能有效抑制Panc-1與抗藥性 Panc-1 Gem 50 μM胰臟癌細胞的生長，而低劑量0.1 U/ml asparaginase則無作用。
2. 單獨處理0.025 U/ml asparaginase對Panc-1胰臟癌細胞抑制作用微小(生存率97%)，然而併用1/600和1/200 稀釋濃度的BPE後，可使生存率分別降至50%和45%。
3. 單獨處理0.2 U/ml asparaginase對Panc-1 Gem 50 μM抗藥性胰臟癌細胞的抑制作用微小(生存率90%)，然而併用1/600和1/200 稀釋濃度的BPE後，可使生存率分別降至40%和48%。

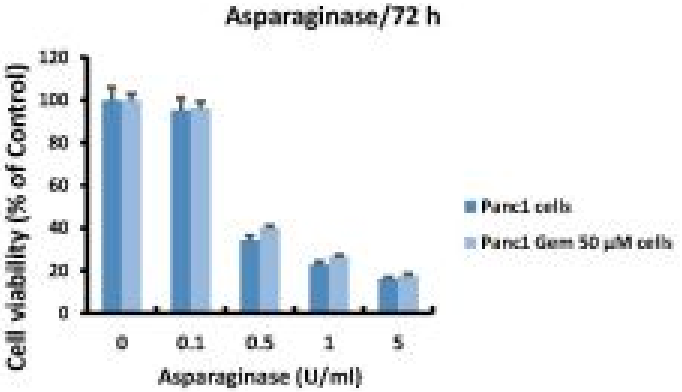

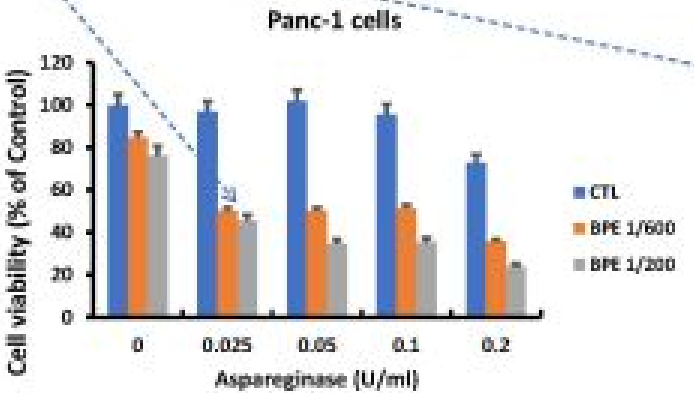

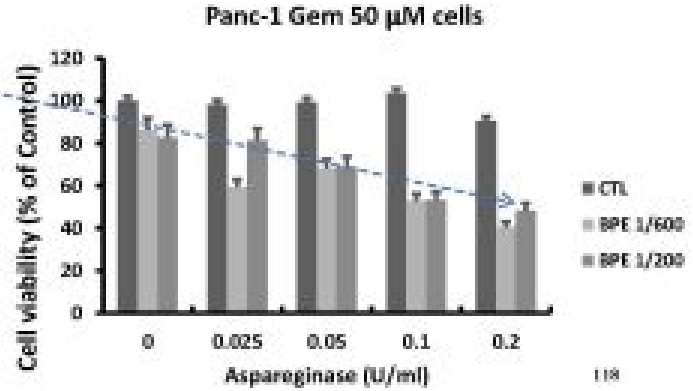

結論(二)

1. 抗癌藥物引起的癌細胞老化，有促進癌症惡化的風險。
2. 預先處理BPE可降低化療藥(gemcitabine, oxaliplatin)在Panc-1胰臟癌細胞及其抗藥株(Panc-1 Gem 50 μM cells)引起的老化(senescence)反應，且可增強化療藥(gemcitabine, oxaliplatin)對胰臟癌抗藥株細胞(Panc-1 Gem 50 μM cells)的抑制作用。
3. 已有臨床前研究，探討Asparaginase 對直腸癌與胰臟癌等實體腫瘤的抑制作用，並指出合併療法的策略。
4. 併用BPE能增強低劑量化療藥物樂拿舒(Asparaginase)對Panc-1胰臟癌細胞與其抗藥株Panc-1 Gem 50 μM cells的生長抑制作用。

第二期BPE產學計畫第一年期末進度報告

1. BPE論文與專利進度說明
2. BPE抑制肝細胞纖維化與發炎
3. BPE於抗藥性癌細胞株(胰臟癌)的化療增敏作用
4. **BPE植物新泌體的開發**

利用粒徑分析儀偵測出BPE成分中有類似植物新泌體的成分

1. BPE曾委託中國南京大學細胞生物學教授(劉人豪 博士提供)以NanoSight儀器偵測出BPE懸浮液有奈米顆粒物質，平均大小為277 nm，顯示可能有植物新泌體的物質存在。

2. 動物細胞外泌體近幾年來已廣泛被研究，並應用在商業產品，然而植物組織衍生的外泌體卻仍處於基礎研究上。有鑑於此，BPE衍生的新泌體功效值得去開發研究。

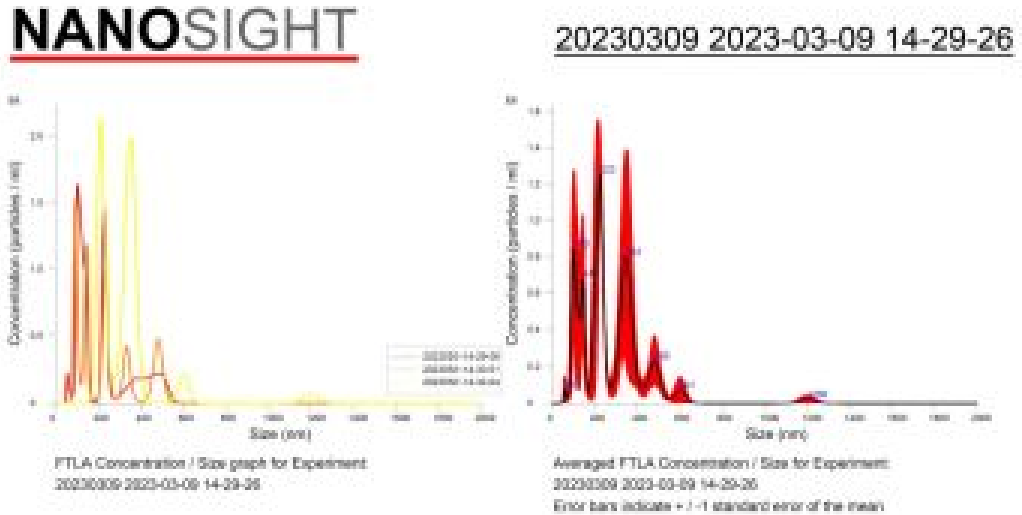

植物新泌體的優勢

傳統植物提取物與植物新泌體的對比

傳統植物提取物	植物新泌體	優勢
多用有機溶劑萃取	通過細胞培養與低溫下差速離心法直接獲取，無染質引入，更安全	更安全
一般只包含單一或幾種活性物	包含植物所有次級代謝產物，以及多種RNA、蛋白質、脂質等	更多活性
活性物質直接與空氣接觸，易氧化變質	有磷脂雙分子層保護，穩定性更高	更高穩定性
一般無法直接進入細胞內部起作用	作為信號分子，可以直接進入細胞內部起作用	作用更精準

目前文獻上尚未有蕉科植物相關新泌體的文章發表

植物新泌體的主要成分

1. 植物新泌體主要成分與動物細胞分泌的新泌體相似主要包含蛋白質，脂質，非編碼RNA，而植物新泌體額外有次級代謝物的成分。

2. 目前已有人參和綠茶 (*Applied Biological Chemistry (2022) 65:8)* 與生薑 (Biomaterials. 2016 Sep;101: 321-40.)發現其衍生的植物新泌體分別具有改善皮膚機能與抗癌的功效，且活性比傳統萃取方式更好。

3. 植物新泌體包含植物完整的生物活性，因此BPE所衍生新泌體值得開發。

Cell Communication and Signaling (2022) 20:69

BPE新泌體萃取方法：超高速離心分離

Step 1

取1 mL BPE以以 10,000 X g ，40 分鐘進行離心 ， 去除雜質。

Step 2

取上清液再用離心機低溫下以 150,000 X g ，2小時進行離心 ， 移除上清液用0.2 mL PBS 回溶(可用超音波均勻分布)。

MLA-130, Max 1,019,000 x g

Step 4

利用細胞實驗來分析傳統萃取法與BPE植物新泌體之間的差異，評估BPE植物新泌體生物活性是否優於傳統萃取法。

Step 3

將已過溶的液體先進行細胞活性測試。若有生物活性，再進行粒徑分析儀偵測新泌體大小與濃度。

結論：BPE植物新泌體未來可應用的產業

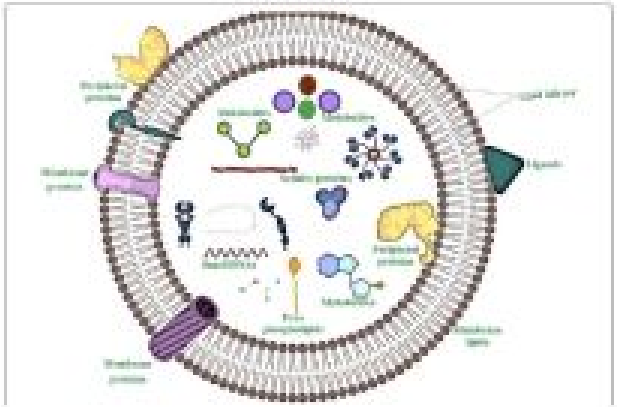

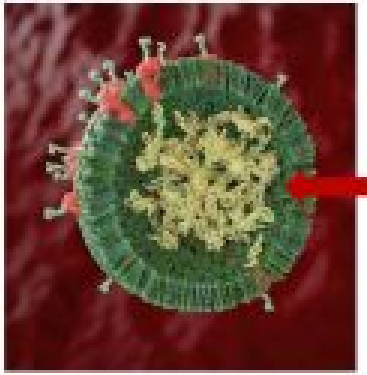

可將藥物包埋在新泌體裡，增加治療效果

醫美市場

(皮膚保養品)

醫療產業

1. 保肝
2. 抗老化
3. 逆轉化療抗藥性

生醫材料

藥物載體系統如作為化療藥Gemcitabine的藥物載體

芭蕉科植物萃取物 (BPE) 應用於抑制第一型纖維蛋白溶酶原活化抑制物 Plasminogen activator inhibitor-1 (PAI-1)

Scientific Reports volume 11,Article number: 1580 (2021)

Plasma tissue plasminogen activator and plasminogen activator inhibitor-1 in hospitalized COVID-19 patients

Yu Zuo[1], Mark Warnock[1], Alyssa Harbaugh[1], Srilakshmi Yalavarthi[1], Kelsey Gockman[1], Melanie Zuo[3], Jacqueline A. Madison[1], Jason S. Knight[1], Yogendra Kanthi[2,4] & Daniel A. Lawrence[2]

新冠肺炎病人PAI-1升高，升越高，發炎越嚴重，呼吸狀況越差

Patients with coronavirus disease-19 (COVID-19) are at high risk for thrombotic arterial and venous occlusions. However, bleeding complications have also been observed in some patients. Understanding the balance between coagulation and fibrinolysis will help inform optimal approaches to thrombosis prophylaxis and potential utility of fibrinolytic-targeted therapies. 118 hospitalized COVID-19 patients and 30 healthy controls were included in the study. We measured plasma antigen levels of tissue-type plasminogen activator (tPA) and plasminogen activator inhibitor-1 (PAI-1) and performed spontaneous clot-lysis assays. We found markedly elevated tPA and PAI-1 levels in patients hospitalized with COVID-19. Both factors demonstrated strong correlations with neutrophil counts and markers of neutrophil activation. High levels of tPA and PAI-1 were associated with worse respiratory status. High levels of tPA, in particular, were strongly correlated with mortality and a significant enhancement in spontaneous ex vivo clot-lysis. While both tPA and PAI-1 are elevated among COVID-19 patients, extremely high levels of tPA enhance spontaneous fibrinolysis and are significantly associated with mortality in some patients. These data indicate that fibrinolytic homeostasis in COVID-19 is complex with a subset of patients expressing a balance of factors that may favor fibrinolysis. Further study of tPA as a biomarker is warranted.

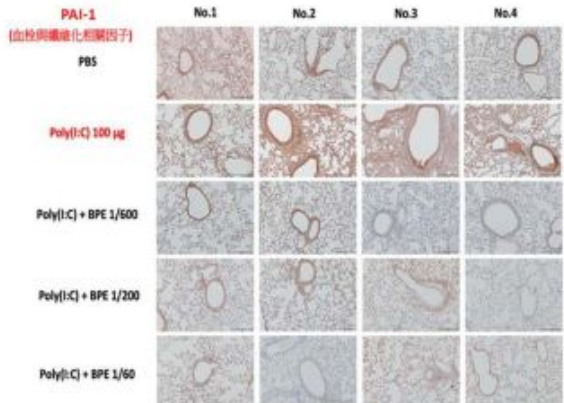

BPE抑制Poly(I:C)在小鼠肺部所增加PAI-1表現，利用組織免疫染色法分析小鼠肺部組織PAI-1蛋白的表現。

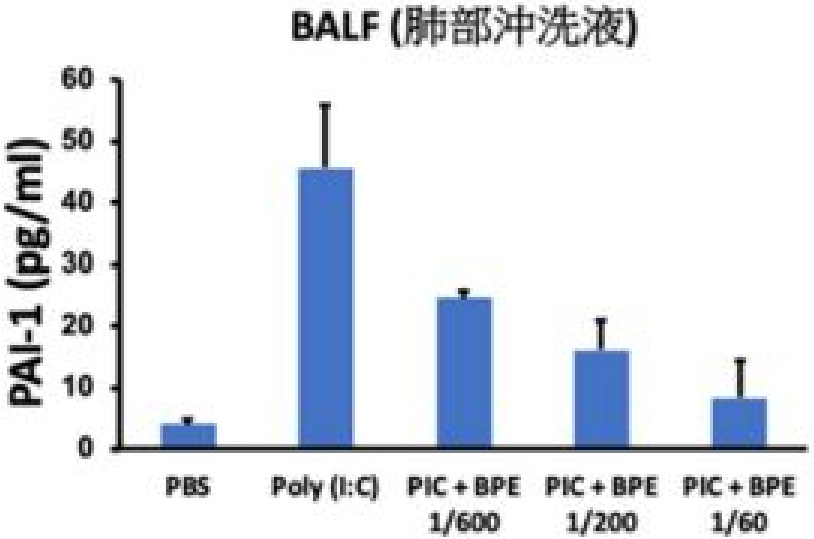

BPE抑制Poly(I:C)誘發小鼠肺部沖洗液中PAI-1的表現量，利用酵素結合免疫吸附法分析小鼠肺部沖洗液中PAI-1蛋白的表現。

BPE第一期的研究成果已在2024年1月發表於International Journal of Medical Sciences

IVYSPRING INTERNATIONAL PUBLISHER

International Journal of Medical Sciences

2024; 21(1): 107-122. doi: 10.7150/ijms.88748

Research Paper

Inhibition of Polyinosinic-Polycytidylic Acid-Induced Acute Pulmonary Inflammation and NF-κB Activation in Mice by a Banana Plant Extract

Chien-Huang Liao[1,#], Tung-Yuan Lai[2,3,#], Yu-Ying Lin[1], Yi-Chun Liao[4], Gi-Ming Lai[1,5], Tien-Hua Chu[6], Szu-Yao Wu[6], Wei-Lun Tsai[1], Jacqueline Whang-Peng[1,5], Frank Liu[7], Tzeon-Jye Chiou[1,5,✉], Chih-Jung Yao[8,9,✉]

1. Cancer Center, Wan Fang Hospital, Taipei Medical University, Taipei 11696, Taiwan.
2. Department of Chinese Medicine, Hualien Tzu Chi Hospital, Buddhist Tzu Chi Medical Foundation, Hualien 97002, Taiwan.
3. Traditional Chinese Medicine Cancer Center, Hualien Tzu Chi Hospital, Hualien 97002, Taiwan.
4. Institute of Biomedical Sciences, Academia Sinica, Taipei, 11529, Taiwan.
5. Division of Hematology and Medical Oncology, Department of Internal Medicine, Wan Fang Hospital, Taipei Medical University, Taipei 11696, Taiwan.
6. Chimera Biosciences Inc., No. 18 Siyuan St., Zhongzheng Dist., Taipei 10087, Taiwan.
7. Department of Research and Development, Natural Well Technical Company, Guishan, Taoyuan 33377, Taiwan.
8. Department of Medical Education and Research, Wan Fang Hospital, Taipei Medical University, Taipei 11696, Taiwan.
9. Department of Internal Medicine, School of Medicine, College of Medicine, Taipei Medical University, Taipei 11031, Taiwan.

文獻報導，**抑制PAI-1可增強化療與免疫治療對胰臟癌的效果** (Sci. Adv. 2020; 6 : eabb9200)。與此相符，預先處理BPE可增強gemcitabine等化療藥對胰臟癌抗藥細胞的抑制效果。

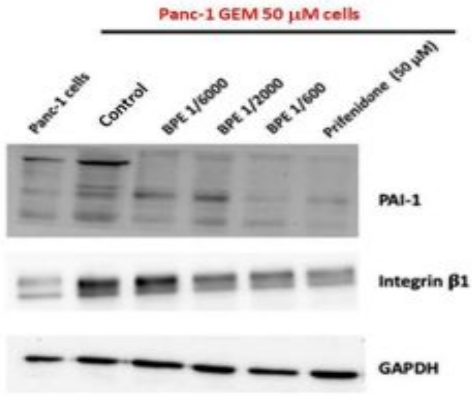

GEM: gemcitabine

BPE抑制抗藥性胰臟癌細胞 (Panc-1 GEM 50 μM) cells 之PAI-1與Integrin β1蛋白量，(Panc-1 GEM 50 μM) cells (2×10^5 cells/10 cm-dish) 貼盤24 h後，分別處理BPE (1/6000、1/2000和1/600稀釋濃度) 或 Pirfenidone (50 μM) 72小時，利用Western blot方法分析PAI-1與Integrin β1的蛋白量。

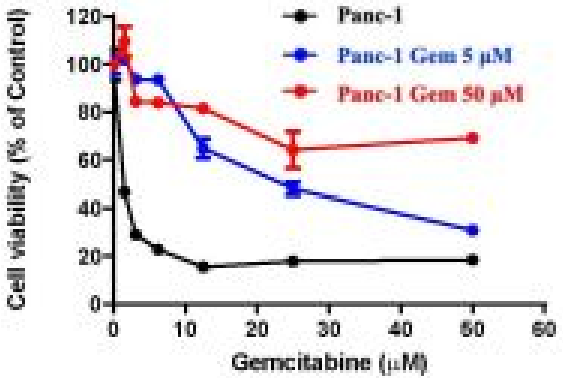
Panc-1
Panc-1 Gem 5 μM
Panc-1 Gem 50 μM
Cell viability (% of Control)
120
100
80
60
40
20
0
0
10
20
30
40
50
60
Gemcitabine (μM)

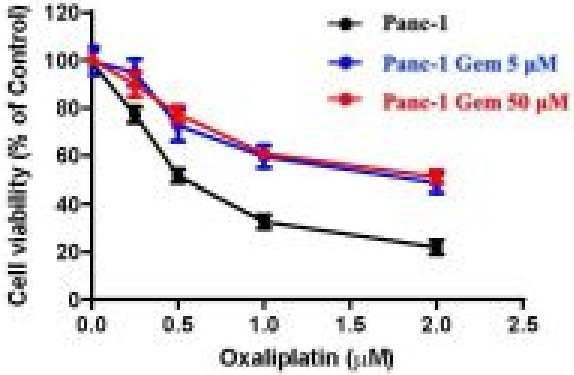
Panc-1
Panc-1 Gem 5 μM
Panc-1 Gem 50 μM
Cell viability (% of Control)
120
100
80
60
40
20
0
0.0
0.5
1.0
1.5
2.0
2.5
Oxaliplatin (μM)

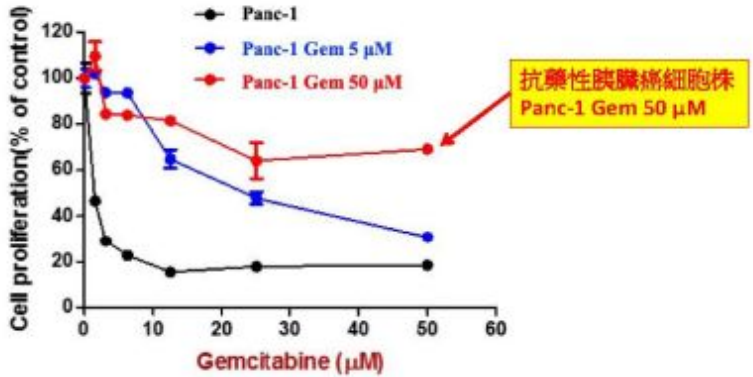

Panc-1與抗藥性胰臟癌細胞株Panc-1 Gem 5 μM和Panc-1 Gem 50 μM對gemcitabine的敏感度，將(Panc-1)、(Panc-1 Gem 5 μM)和(Panc-1 Gem 50 μM)三株細胞種於96-well plate (2×10^3 cells/well) 貼盤24 h後，加入不同濃度的gemcitabine (1.56, 3.12, 6.25, 12.5, 25, 50 μM)，72 h後以sulforhodamine B (SRB) assay測細胞生存率。

BPE增加抗藥性(Panc-1 GEM 50 μM) cells 對化療藥gemcitabine的敏感性：Panc-1 GEM 50 μM cells (1×10^3 cells/well/96-well plate) 貼盤24 h後，處理不同濃度的BPE (1/2000、1/600和1/200稀釋) 72小時後，再處理20μM gemcitabine (臨床可達濃度) 72小時，以sulforhodamine B (SRB) assay測細胞生存率。

111/06/14

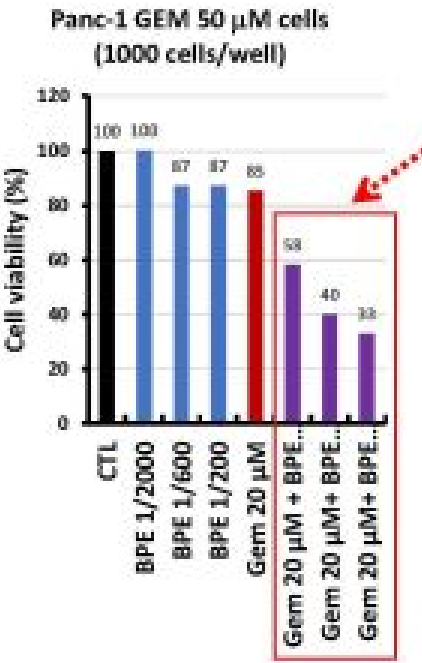

111/06/20

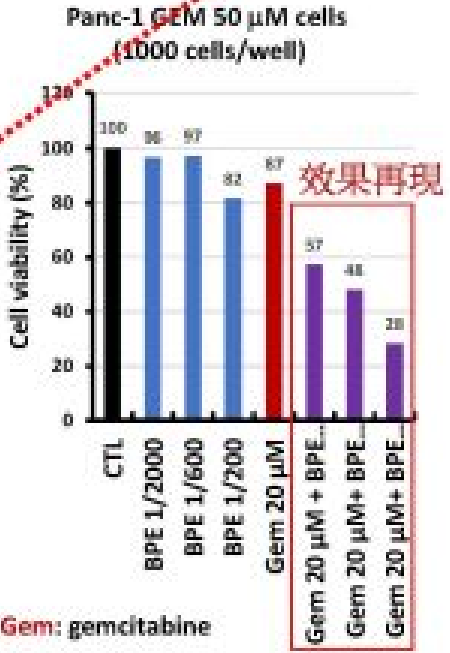

111/06/27

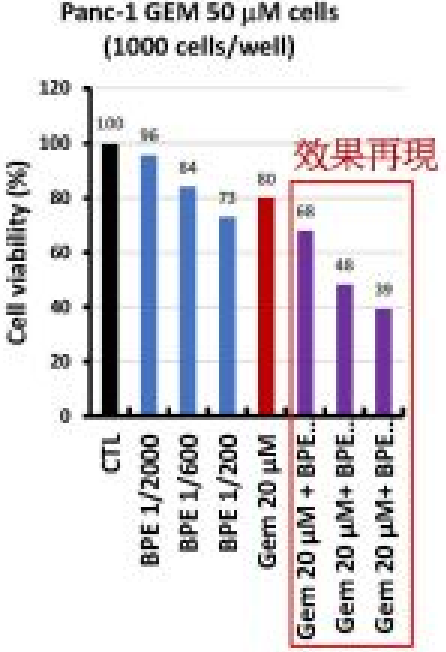

BPE增加抗藥性(Panc-1 GEM 50 μM) cells 對化療藥Oxalipatin的敏感性，Panc-1 GEM 50 μM cells (1×10^3 cells/well/96-well plate) 貼盤24 h後，處理不同濃度的BPE (1/2000、1/600和1/200稀釋) 72小時後，再處理 **Oxalipatin 1 μM** 72小時，以sulforhodamine B (SRB) assay測細胞生存率。

111/07/01

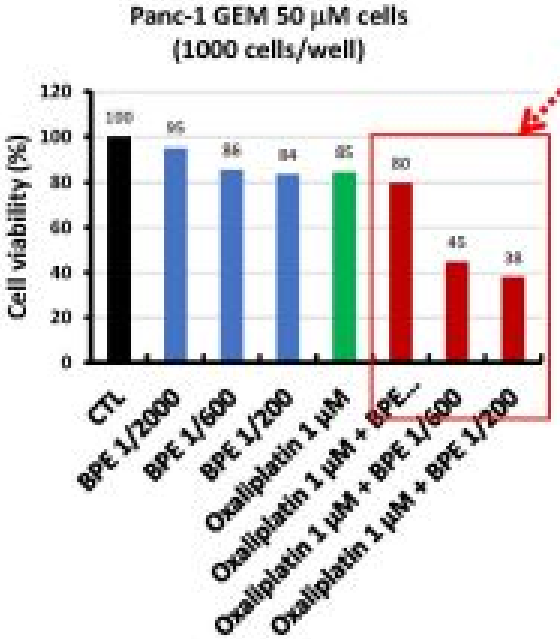

111/07/12

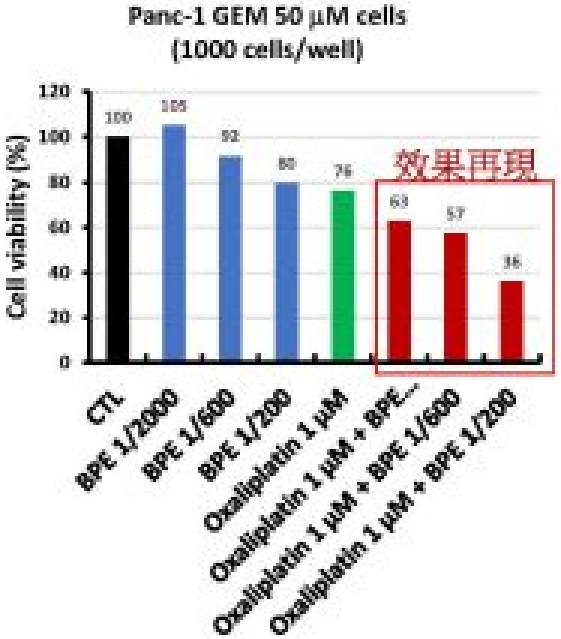

BPE增加抗藥性(Panc-1 GEM 50 μM) cells 對化療藥5-FU的敏感性，Panc-1 GEM 50 μM cells (1×10^3 cells/well/96-well plate) 貼盤24 h後，處理不同濃度的BPE (1/2000、1/600和1/200稀釋) 72小時後，再處理**5-FU 2 μM** 72小時。以 sulforhodamine B (SRB) assay測細胞生存率。

111/07/12

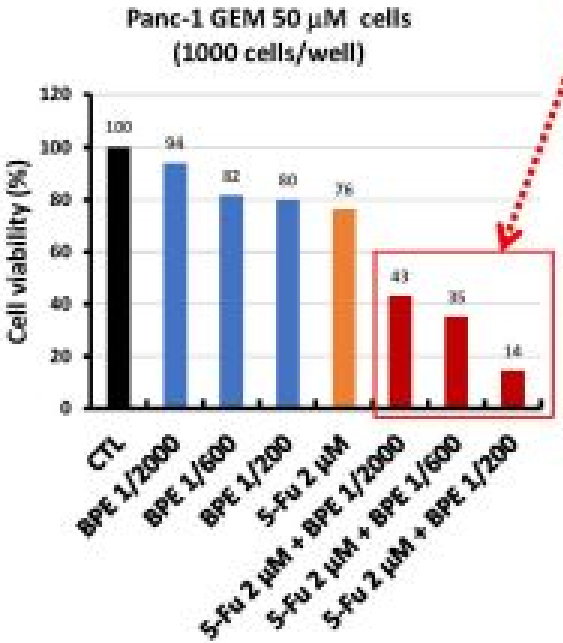

*****請特別注意***** 本次通知之應辦理事項其法定期限如下，因辦理費時，請 貴公司/台端於辦理時，務必在本通知函建議期限前早些通知本所，以免影響權益。		寄送	234 新北市中和區圓通路 301 號 4 樓 (雙和校區生醫科技大樓) 臺北醫學大學 事業處技轉中心 莊沈薇專員 鈞啟
法定期限	2024/7/11 (年/月/日)		

應辦事項	領證及繳年費	通知日期	2024/4/12

主　　旨：為通知 貴公司／台端委由本所代為辦理之下列案件進度狀況，敬請查照辦理為荷。

國別種類：中華民國 專利　　案 性：發明　　本 所 編 號：NP-35957

案件名稱：香蕉萃取物在提高癌細胞對抗癌藥物的敏感性上的用途　　貴 方 卷 號：

貴方商品號：

申 請 日：2023/8/8	申請案號：112129719	公 告 日：	優先權日：
改 請 日：	改請案號：	專利權號數：	母案本所編號
公 開 日：	公開號數：	專利權迄日：	相關案件編號

本通知事項回覆期限：	2024/4/30	應繳費年次：	
費　　用：	本所服務費 3000 元，政府規費依照所決定繳納年次的年費而定		
本次通知事項：	核准審定：准予發明專利		

(一) 恭賀本案已核准發明專利，隨函附上核准審定書（含檢索報告）影本一份，敬請查收。

(二) 本案依法必須於本函左上角所載法定期限之前，繳納領證費及第 1 年年費，否則將被視為放棄取得專利權。

(三) 發明專利權自領證後公告日起專有，但自申請日起算二十年屆滿。
※請注意，本案領證後隨時會因公告而喪失先申請國外專利資格之虞，且申請國外專利處理較費時，貴公司／台端如欲申請國外專利，宜儘早辦理以免喪失權益。
□本案需提出延緩公告，請延緩公告至：　　年　　月　　日。(延緩期限，不得逾６個月)
□本案考慮申請其他國家，擬申請：□美國　□中國大陸　□

(四) 本所代辦領證所需費用如下：上開服務費＋證書規費 1000 元＋專利年費規費。
其中專利年費如下所列，可單年繳或一次繳數年或一次全部繳清：
※第 1- 3 年每 1 年年費 2500 元　　※第 4- 6 年每 1 年年費 5000 元
※第 7- 9 年每 1 年年費 8000 元　　※第 10 年以上，每年年費 16000 元
※自 112 年 1 月 1 日起，領證時可選擇領取電子證書或紙本證書，選電子證書者，可視需要另行申請核發紙本副本。

(五) 依「專利年費減免辦法」，專利權人如為自然人、學校、中小企業者，其第 1 至 3 年年費每年可減收 800 元，第 4 至 6 年年費每年可減收 1200 元，中小企業必須符合「中小企業認定標準」所定之事業。

(六) 依專利法第５２條：第１年年費，得於逾限後６個月內，加倍補繳。
依專利法第９４條：第２年以後的年費，得於期滿後６個月內，以比率方式加繳，每逾一個月加繳百分之二十，最高加繳至依規定之專利年費加倍之數額；其逾繳期間在一日以上一個月以內者，以一個月論。
依專利法規定第二年以後之專利年費未於補繳期限屆滿前繳納者，自原繳費期限屆滿後消滅。
尚須注意，未在第二年以後專利年費繳納期限屆滿後６個月內補繳專利年費，得於補繳期限屆滿後一年內申請回復專利權，並繳納「三」倍專利年費。

(七) 本案若有美國、馬來西亞、法國（發明）、印度之相對申請案，應注意是否須將檢索報告中影響專利性的相關資訊陳報給各國專利局（簡稱ＩＤＳ<Information Disclosure Statement>陳報），若隱瞞不陳報影響專利性的相關資訊，有可能導致相對申請案無法獲准或行使專利權。

(八) 倘若本案為歐洲專利申請案之優先權基礎案，則必須向歐洲專利局陳報此檢索報告，否則歐洲專利申請案將被視為撤回。

Accelerated Skin Wound Healing in Plasminogen Activator Inhibitor-1-Deficient Mice

Am J Pathol. 2001 Nov; 159(5): 1681–1688.

傷口大小

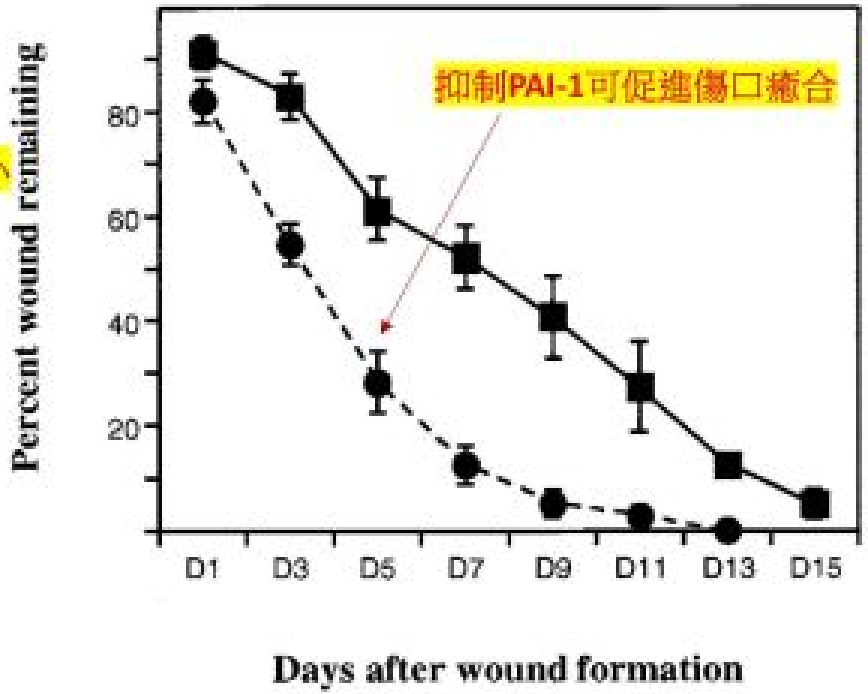

Figure 1. Kinetics of skin wound healing in *PAI-1*$^{-/-}$ and *WT* mice. The percentage area of the wound (width × length) remaining as a function of time after skin incision in *PAI-1*$^{-/-}$ (●) and *WT* (■) mice. At least 4 mice/genotype/time point are graphically represented and expressed as the average ± SE. *P* values at days 3–9 < 0.05.

EXPERT OPINION

業界發展各種PAI-1抑制劑，濃度與毒性是一大瓶頸

Plasminogen activator inhibitor-1 inhibitors: a patent review (2006 – present)

Yolanda M. Fortenberry

John Hopkins University School of Medicine, Department of Pediatric, Division of Hematology, Baltimore, MD, USA

Introduction: Plasminogen activator inhibitor-1 (PAI-1), the serine protease inhibitor (serpin), binds to and inhibits the plasminogen activators—tissue-type plasminogen activator (tPA) and the urokinase-type plasminogen activator (uPA). This results in both a decrease in plasmin production and a decrease in the dissolution of fibrin clots. Elevated levels of PAI-1 are correlated with an increased risk for cardiovascular disease and have been linked to obesity and metabolic syndrome. Consequently, the pharmacological suppression of PAI-1 might prevent or treat vascular disease.

Areas covered: This article provides an overview of the patenting activity on PAI-1 inhibitors. Patents filed by pharmaceutical companies or individual research groups are described, and the biological and biochemical evaluation of the inhibitors, including *in vitro* and *in vivo* studies, is discussed. An overview of patents pertaining to using these inhibitors for treating various diseases is also included.

Expert opinion: Although there is still no PAI-1 inhibitor being evaluated in a clinical setting or approved for human therapy, research in this field has progressed, and promising new compounds have been designed. Most research has focused on improving the pharmacological profile of these compounds, which will hopefully allow them to proceed to clinical studies. Despite the need for further testing and research, the potential use of PAI-1 inhibitors for treating cardiovascular disease appears quite promising.

Keywords fibrinolysis, inhibitors, PAI-1, plasminogen, serpin

Expert Opin. Ther. Patents (2013) 23(7):801-815

Plasminogen activator inhibitor 1 inhibitors a patent review 2006 present

Expert Opin. Ther. Patents (2013) 23(7):801-815

業界發展各種PAI-1抑制劑，濃度與毒性是一大瓶頸

Article highlights.

- PAI-1 contributes to the pathophysiology of several diseases/disorders including cardiovascular disease, cancer, diabetes, and obesity.
- PAI-1 is considered a cardiovascular disease risk factor.
- PAI-1 inhibitors consist of monoclonal antibodies, peptides, low-molecular-weight compounds, and chemical suppressors.
- Several research groups are working on developing new PAI-1 inhibitors and second-generation inhibitors with improved therapeutic potential.
- To date, no PAI-1 inhibitor has been approved for use in clinical setting.
- Nevertheless, the future use of PAI-1 inhibitors for treating cardiovascular disease appears to be promising.

This box summarizes key points contained in the article.

Plasminogen Activator Inhibitor-1 in Cancer: Rationale and Insight for Future Therapeutic Testing

Cancer Res. 2015 August 1; 75(15): 2969–2974.

業界發展各種PAI-1抑制劑，濃度與毒性是一大瓶頸

- PAI-1 inhibitors, initially developed as anti-thrombotic agents, in animal models of cancer
- The development of efficacious and non-toxic PAI-1 inhibitors as anti-cancer agents
- Prolonged plasma half-life of orally available inhibitors
- Active in vitro at concentrations in the μM range represents another limitation
- Lack of activity of most inhibitors against the stable vitronectin-bound form of PAI-1 is (the predominant form of PAI-1 in vitronectin-rich tumor tissues)
- By suppressing the control that PAI-1 exerts on plasmin-mediated fibrinolysis, small molecule PAI-1 inhibitors may impair hemostasis and cause excessive spontaneous bleeding.

芭蕉科植物萃取物 (BPE) 並用Vit D3應用於抑制GSK-3的潛力

Theranostics 2016; 6(4): 571-593.

Glycogen Synthase Kinase-3 (GSK-3)-Targeted Therapy and Imaging

GSK-3抑制劑皆未獲FDA核准 (Blood. 2019;134(4):363-373)

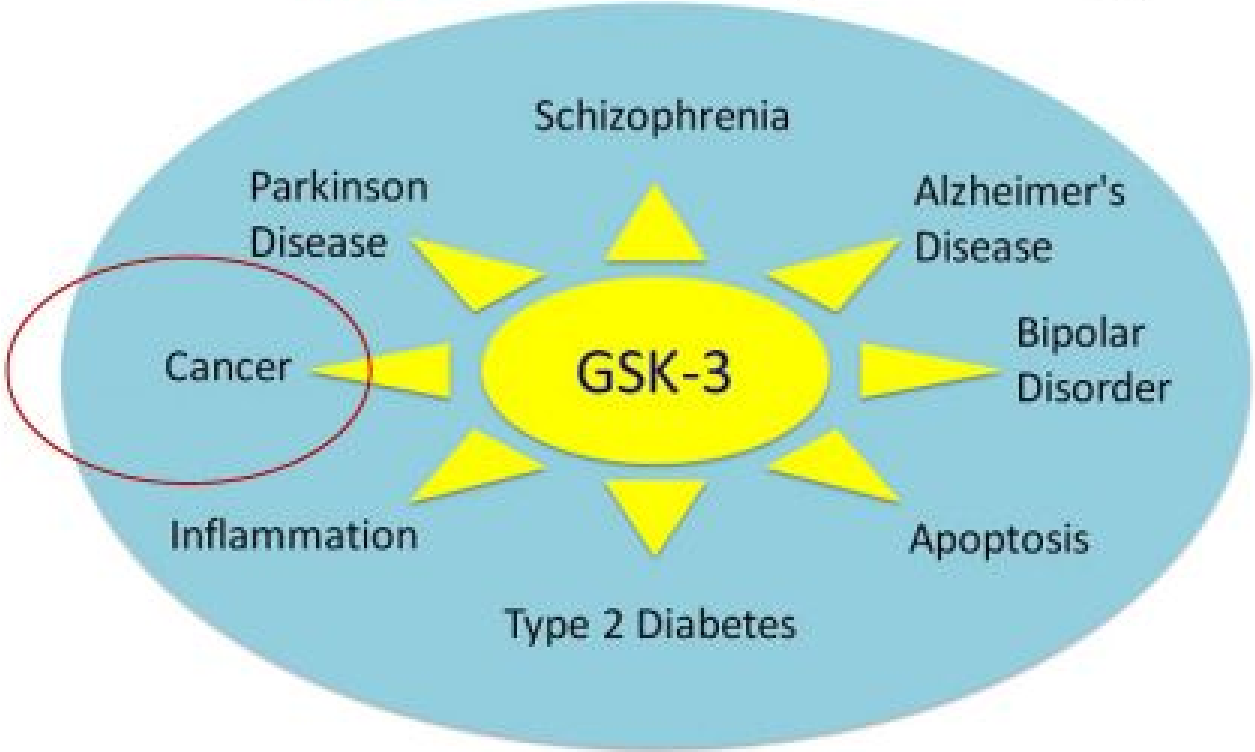

BPE併用Vit D3抑制GSK3，有潛力作為癌症治療的輔助

- Although there are many GSK3 inhibitors available to date, none are approved for cancer treatment (Blood. 2019;134(4):363-373).

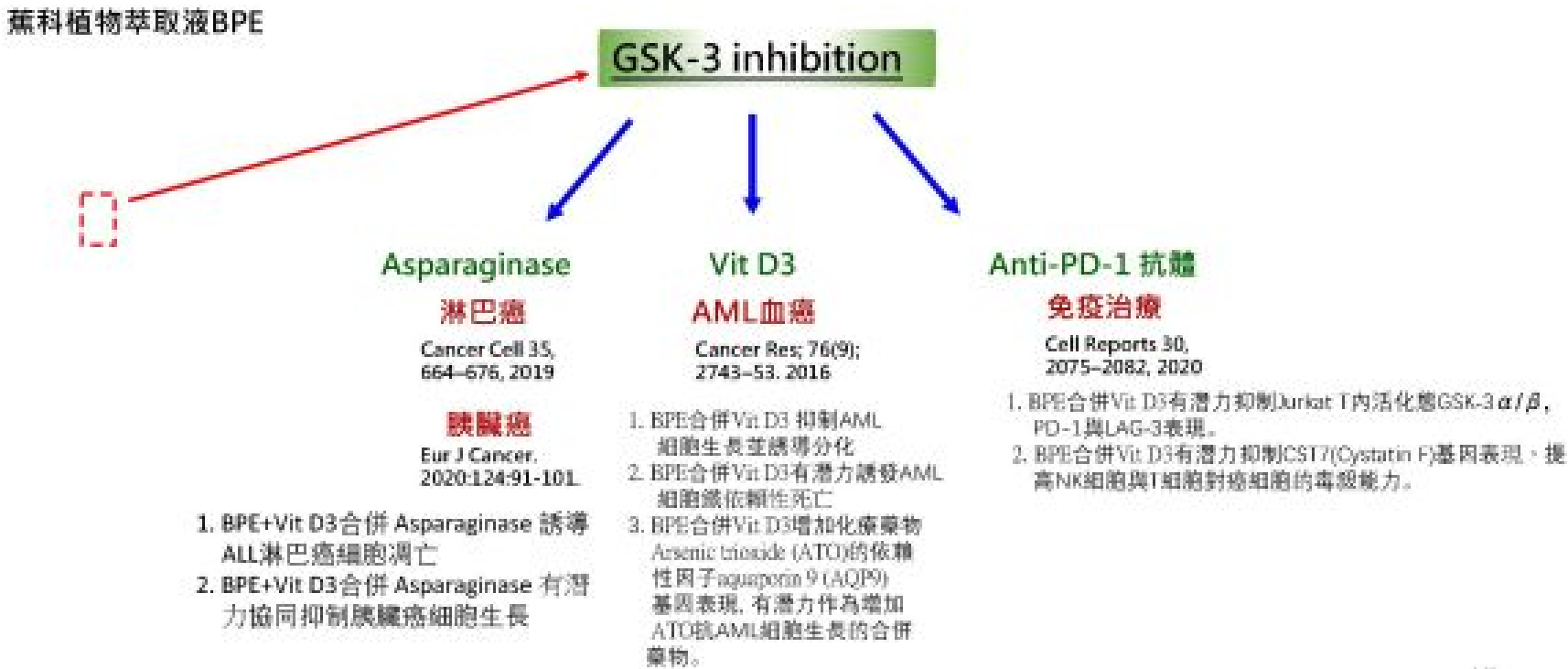

Cancer Res; 76(9); 2743–53. 2016

Therapeutics, Targets, and Chemical Biology

Cancer Research

GSK-3 Inhibition Sensitizes Acute Myeloid Leukemia Cells to 1,25D-Mediated Differentiation

Kalpana Gupta[1], Tammy Stefan[1], James Ignatz-Hoover[1], Stephen Moreton[1,2], Gary Parizher[1], Yogen Saunthararajah[3], and David N. Wald[1,2,4]

Vitamin D3: 1,25-dihydroxyvitamin

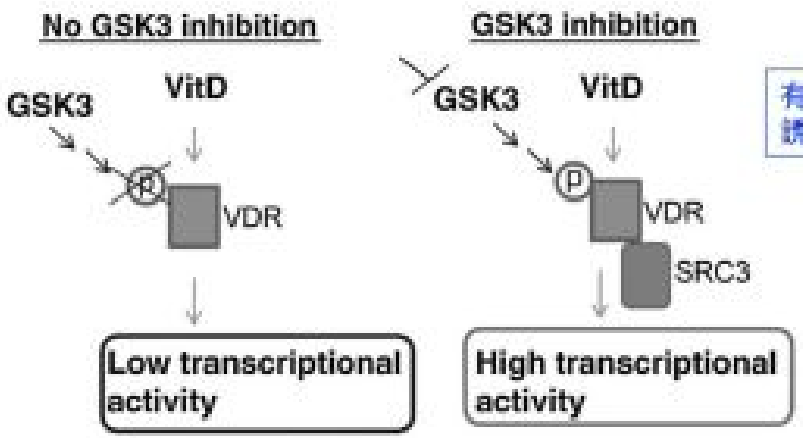

有文獻指出，抑制GSK-3可增強活性Vit D3 (active form of vitamin D3) 誘導AML血癌細胞分化的能力。

因此推測併用BPE+Vit D3 可促進AML細胞分化。

Figure 6.

Model depicting how GSK3 inhibition enhances 1,25D-mediated differentiation of AML cells.

VDR: vitamin D receptor

GSK-3: glycogen synthase kinase 3

併用BPE與活性Vit D3可協同增加AML細胞單核球分化指標CD14之基因與蛋白的表現量

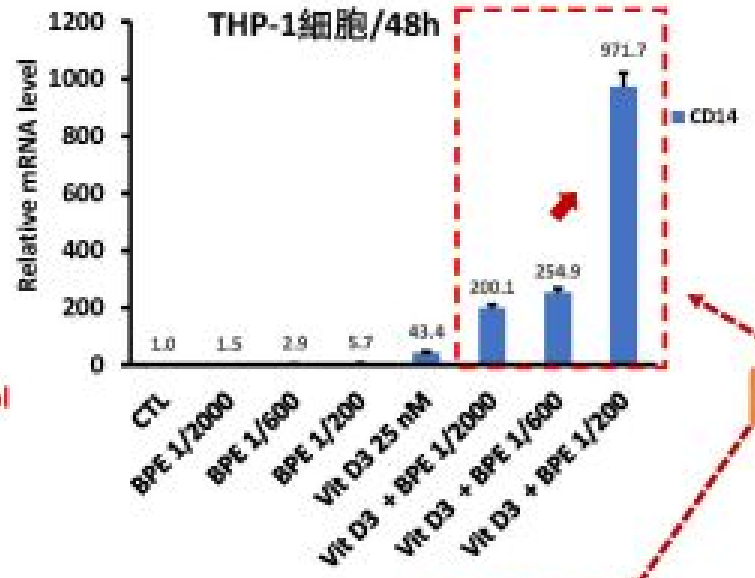

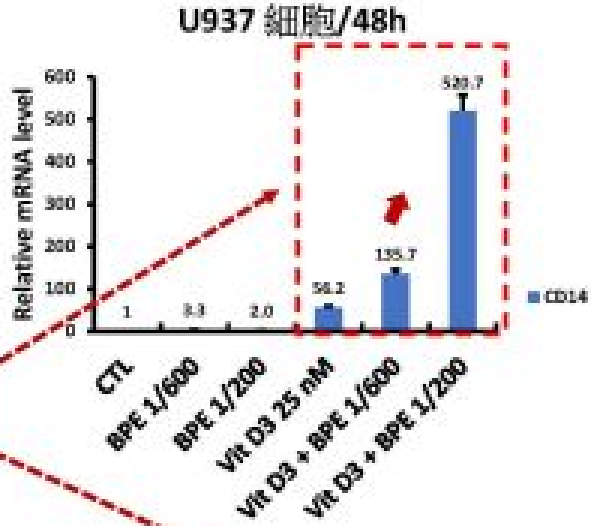

CTL: Control

BPE + Vit D3

作用72 h

作用72 h

Theranostics 2016; 6(4): 571-593.

Glycogen Synthase Kinase-3 (GSK-3)-Targeted Therapy and Imaging

GSK-3抑制劑皆未獲FDA核准 (Blood. 2019;134(4):363-373)

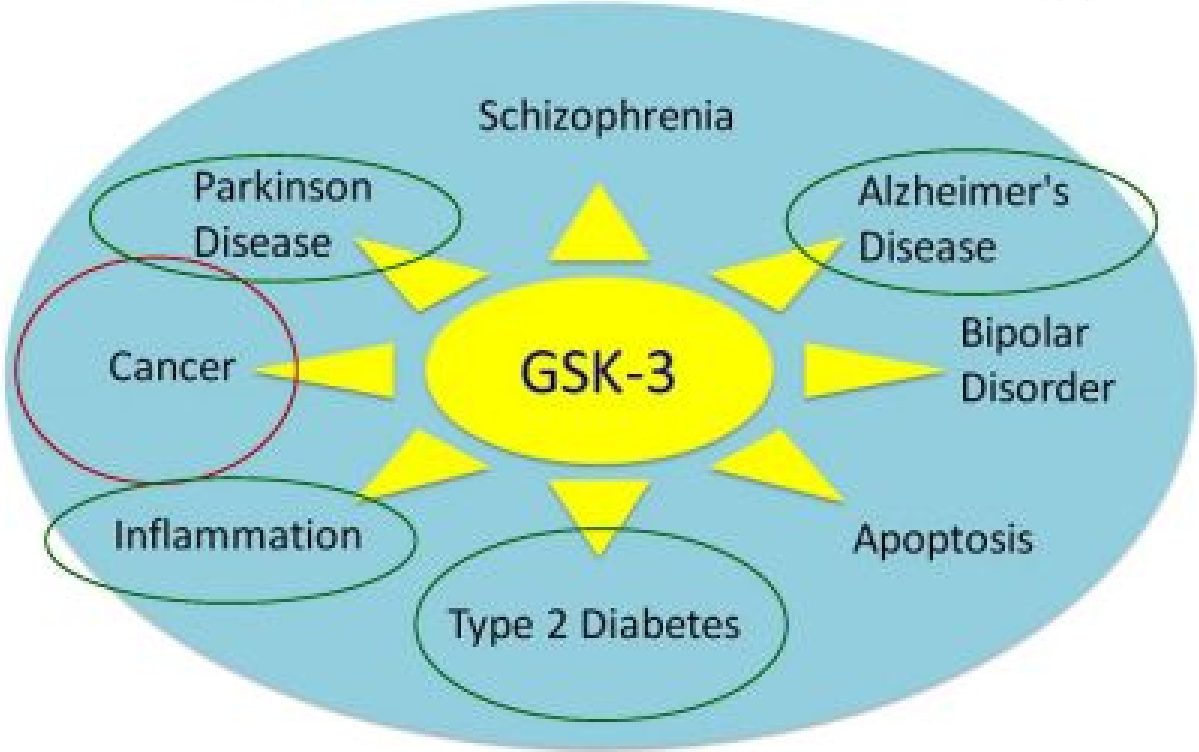

SG (Super Green) 抗癌實驗研究方向

June. 2020 - May. 2022

1. GC Mass Mass analysis (確認有效成分)
2. cGMP inhibition and Cancer Stem Cell (hepatoma) traits suppression (癌幹細胞抑制作用的機理，以肝癌為例)
3. Inhibition of IL-6 in chemotherapy-induced SASP (cancer related fatigue model，緩解癌症治療引起之發炎反應，消除癌因性疲憊症)
4. Prosurvival effect in normal and proapoptotic effect in cancer cells (降低化療對正常細胞的傷害，並增強化療對癌細胞的抑制)
5. IL-6 inhibition and PD-L1 glycosylation reduction for antitumor immunity enhancement (降低癌細胞對免疫系統的干擾)
6. Effects on Gemcitabine-resistant pancreatic cancer cells (抗藥性胰臟癌細胞的逆轉作用)
7. Synergistic effects of SG and (PG2 or Aspirin, Gemcitabine, regorafenib..與其他抗癌藥或天然物的加乘作用)
8. Targeting tumor cell-induced platelet aggregation / invasion via thromboxane A2 inhibition (對抗癌細胞凝集血小板所引起的侵犯性)

萬芳癌症中心 癌症轉譯研究團隊

姓　名	單　位	職　稱
賴基銘 醫師	萬芳醫院癌症中心	教授/顧問/主治醫師
姚智榮 博士	萬芳醫院癌症轉譯研究室	院聘醫學研究員/助理教授
廖建皇 博士	萬芳醫院癌症轉譯研究室	科聘醫學研究員

大仁科技大學

產學合作計畫

結案報告

計畫名稱: 天線元素活力滴飲抗凝血活性評估

(計畫編號：仁合102105)

委託單位: 安理科技有限公司

計畫主持人: 劉怡旻 教授

協同主持人:

劉人豪 博士 (安理科技有限公司)

鄭詠澤 醫師 (奇美醫院急診部 緊急醫療系統科)

計畫執行期限:

自民國 102 年 10 月 1 日起至 103 年 3 月 31 日止

目 錄

壹、摘要

本研究依據文獻研究抗凝血試驗之規範，將委託廠商所提供之產品「天綠元素活力滴飲」進行化學成含量檢測及對 14 天連續口服投予至 Wistar 品系大鼠體內進行抗凝血試驗評估。分別將「天綠元素活力滴液」原液(X)稀釋為 1/5000 (X/5000)、1/6000 (X/6000)、1/7000 (X/7000)與 1/8000 (X/8000)倍，經口餵食至 Wistar 大鼠(1 ml/kg)連行 14 天餵食抗凝血試驗。實驗結果得知「天綠元素活力滴液」並不會造成 Wistar 大鼠體重以及攝食與飲水量的變化。隨著「天綠元素活力滴液」作用濃度的增加可減少血小板數目。由血液凝集反應測定發現「天綠元素活力滴液」於較高濃度下具明顯抗凝血效果。進一步探討「天綠元素活力滴液」的抗凝血機轉，發現該產品主要藉由抑制血栓素的生成干擾血小板凝集，達到抗凝血的效果。

貳、實驗目的

本試驗之目的在觀察連續 14 天口服投予 Wistar 品系大鼠「天綠元素活力滴液」後，藉由血液之檢驗之分析，了解該產品抗凝血試驗作用，以做為日後開發相關保健產品之依據。

參、實驗項目與實驗方法

(一) 化學成分檢測

A. 化學成分定性檢測

1. 生物鹼類

碘化汞鉀試劑(Mayer試劑， $HgI_2 \cdot KI$)在酸性溶液中與生物鹼反應生成白色或淡黃色沉澱。利用碘化汞鉀試劑檢查待測物是否含有生物鹼。

2. 有機酸類

在有機酸的水溶液中加入氯化鈣或醋酸鉛或氫氧化鋇溶液時，能生成水不溶的鈣鹽、鉛鹽或鋇鹽的沉澱。

3. 氨基酸、蛋白質

待測物中氨基酸與蛋白質成分的存在與否可用以下方法檢查：待測物1ml，加0.2%茚三酮(ninhydrin)試液2～3滴，搖勻，在沸水浴中加熱5分鐘，如顯藍、藍紫或紫紅色為正反應。

4. 羥基蒽苷衍生物

待測物中含有羥基蒽苷衍生物與否可用以下方法檢查：待測物1ml加1%氫氧化鈉(鉀)或氫氧化銨溶液，顯紅色。此紅色加酸則色褪而復現黃色。

5. 黃酮類及黃酮

黃酮類及黃酮又稱黃鹼素類，具有C6-C3-C6的基本碳架，是廣泛存在於植物界的一類天然色素。待測物加1%三氯化鋁乙醇溶液，凡3位或5位有羥基的黃酮會因與鋁產生錯合物而顯鮮黃色。

6. 強心配醣體

利用Keller-Kiliani反應評估待測物中是否含有強心配醣體：待測物1ml溶於1m含三氯化鐵的冰醋酸液中，將溶液傾於小試管中，沿管壁徐徐加濃硫酸1ml，二液面接觸處顯示棕色環表示有強心配醣體的存在。

7. 皂素

取待測物2ml於帶塞試管中，用力振搖3分鐘，即產生持久性蜂窩狀泡沫(維持10分鐘以上)，且泡沫量不少於液體體積的1/3。

8. 醣類

取待測物2ml，加斐林(Fehling)試劑2ml，於沸水浴中加熱數分鐘，如產生紅色氧化亞銅沉澱示有還原糖存在。非還原性低聚糖與多糖須加酸水解後才顯正反應。

B. 類黃酮化合物之定量分析

以槲皮素(quercetin)作為標準品，加入2% $AlCl_3 \cdot 6H_2O$經振盪混合後，於室溫下靜置10 min 後以分光光度計檢測波長430 nm 下之吸光值，並對照標準曲線以換算每毫升樣品中所含槲皮素之含量。

(二) 抗凝血活性試驗

1. 實驗動物來源

8 週大的 Wistar 品系的雄性大鼠購自財團法人國家實驗研究院國家實驗動物中心，並飼養在本校以空調維持在室溫約 25±1℃，光照時間與黑暗時間各為 12 小時的動物室。大鼠可自由的進食與飲水。飼料(購自美國 LabDiet, Inc.)及飲水皆由本校動物中心供應。

2. 餵食的方法

為了證明劑量與作用的關係，將委託單位所提供的天線元素活力滴飲原液(X)稀釋成 5 個濃度，分別為原液(X)的 1/5000 (X/5000)、1/6000 (X/6000)、1/7000 (X/7000)與 1/8000 (X/8000)倍，經由胃管灌食測試物到實驗動物，每天於固定時間餵食兩次，連續投予 14 天。待實驗結束後以適量之 phenobartital 將實驗動物麻醉，抽取股靜脈血進行血液學檢查。

3. 血液學檢查

使用全自動血液分析儀(Sysmex F-800, Japan)，檢測項目含紅血球計數、

血紅素、血球容積、平均紅血球容積(MCV)、平均紅血球血紅素濃度(MCHC)、平均紅血球血紅素量(MCH)、血小板計數、白血球計數及分類。

4. 抗凝血活性測試

(1) 凝血酶原時間 (Prothrombin Time, PT)的測試

以Coatron M2 (Coatron M2, TECO GMBH Co. Ltd., Germany)血液凝固分析儀測量，其使用原理為凝固法，以散射光偵測凝血酶原試劑加入血漿中，加入後血漿中血纖維蛋白(Fibrin)量隨著凝血時間增加而增加，使散射光強度增加，偵測散射光強度得知50%血漿凝固所需時間做為凝血時間。取10 µl不同濃度之待測液加入50 µl的大鼠血漿，於血液凝固分析儀上37℃反應1~2 min，接著加入於血液凝固分析儀上37℃預熱至少10 min的PT 試劑 (TEClot PT,TECO GMBH Co. Ltd., Germany) 25 µl，血液凝固分析儀即會顯示出血漿凝固所需之秒數，而得知PT。以相同量之heparin取代樣品溶液做為正對照組，去離子水則為Blank 組。

(2) 活化部份凝血活酶時間 (Activated Partial Thromboplastin Time, APTT)的測試

以Coatron M2 (Coatron M2, TECO GMBH Co. Ltd., Germany)血液凝固分析儀測量，其使用原理為凝固法，以散射光偵測活化部分凝血活酶試劑加入血漿後，最後再加入Ca^{2+}後使凝血反應開始進行，血漿中血纖維蛋白(Fibrin)量隨著凝血時間增加而增加，而使散射光強度增加，偵測散射光強度得知50% 血漿凝固所需時間做為凝血時間。取10 µl不同濃度之樣品溶液加入25 µl的大鼠血漿，於血液凝固分析儀上37℃反應1~2 min，接著加入APTT試劑(TEClot APTT, TECO GMBH Co. Ltd., Germany) 25µl繼續反應3 min，最後加入於37℃預熱至少10 min 的0.025M 之$CaCl_2$(25µl)，

血液凝固分析儀即會顯示出血漿凝固所需之秒數，而得知APTT。以相同量之heparin取代樣品溶液做為正對照組，去離子水則為Blank組。

(三) 抗凝血活性機轉探討

1. 血小板凝集反應試驗

取得實驗大鼠靜脈血液，以100 mM ethylenediaminetetraacetic acid(EDTA)以1：14（v/v）的比例混合，以350g、37℃離心10分鐘，取得上層富含血小板血漿後，再以500 g、37℃離心10分鐘，將下層血小板以含有70 mg/ml bovine serum albumin(BSA)，及1.8 mg/ml glucose的Tyrode solution (NaCl 136.9 mM、KCl 2.7 mM、$MgCl_2$ 2.1 mM、NaH_2PO_4 0.4 mM、$NaHCO_3$ 11.9 mM，pH 7.4)懸浮之。以Lumi-aggregometer (Chrono-Log Co. U.S.A.)測定，將血小板加入arachidonic acid(AA; 100 μM)或是collagen(10 μg/ml)刺激後測定凝集透光度變化並觀察6分鐘。以不含血小板的Tyrode solution的吸光度作為100%的血小板凝集進行待測物引致血小板凝集程度的計算。

2. 血小板釋出TXB_2、cAMP、cGMP量之含量測定結果

在血小板凝集反應6分鐘之後，將血小板懸浮液取出倒入eppendorff tube中，以水溫100℃加熱5分鐘以終止反應。將血小板懸浮液離心(1000 rpm，5min) 後取上清液，利用ELISA kits測定血小板之thromboxane $(TX)B_2$的濃度；此外並另單獨加入藥物作用9分鐘，利用ELISA kits測定血小板中cyclic adenosine monophosphate (cAMP)、3'-5'-cyclic guanosine monophosphate (cGMP)的濃度。

(四) 統計方式

實驗所得結果以平均值±標準差(mean±S.D.)來表示。應用 One-way

ANOVA analysis 分析變異數，再以 Scheffe' s multiple range test 檢定其間差異之顯著性，凡 p 值小於 0.05 以下，則認為其差異據統計意義。

肆、結果與討論

一、 化學成分檢測

(一) 化學成分定性檢測

「天綠元素活力滴液」於胺基酸/蛋白質、羥基蒽琨衍生物、黃酮類及醣類成分等定性檢測試驗均有呈色反應；顯示「天綠元素活力滴液」含有胺基酸/蛋白質、羥基蒽琨衍生物、黃酮類及醣類等成分（表一）。

如圖一所示，「天綠元素活力滴液」與碘化汞鉀試劑反應生成白色或淡黃色沉澱，顯示該測試液含有生物鹼。

「天綠元素活力滴液」加入醋酸鉛溶液時，能生成水不溶的鉛鹽，如圖二所示，顯示該測試液中含有有機酸的成分。

「天綠元素活力滴液」放試管中激烈震搖，產生的蜂窩狀泡沫約維持20秒後即消失，如圖三所示，表示該測試液不含有皂素。

如圖四所示，「天綠元素活力滴液」溶於微量含三氯化鐵的冰醋酸液中，加濃硫酸後二液面接觸處並不顯示棕色環，表示該測試液不含有強心配醣體。

「天綠元素活力滴液」所含化學成分定性檢測結果請見表一。

(二) 類黃酮化合物之定量分析

以槲皮素作為標準品，對照標準曲線換算後得知每毫升「天綠元素活力滴液」中所含槲皮素之含量約為5.05 μg。

二、抗凝血試驗

將原液(X)的1/5000 (X/5000)、1/6000 (X/6000)、1/7000 (X/7000)與1/8000 (X/8000)倍的「天綠元素活力滴液」以每日1 ml/kg的劑量以口服方式分別投予至雄性Wistar 大鼠，以同樣方法餵食Aspirin (10 mg/kg)的雄性Wistar大鼠則為正對照組。實驗期間大鼠生長情況良好，實驗組與對照組大鼠體重與攝食、飲水的變化均於異差(表二)。

14天後餵食結束後，檢查「天綠元素活力滴液」處理組之血液，結果顯示白血球(WBC)、紅血球數(RBC)、血紅素(hemoglobin)、血球容積比(HCT)、平均紅血球體積(MCV)、平均血紅素(MCH)、平均血紅素濃度(MCHC)及等檢測項目相較於對照組之數值均介於正常值範圍內，而血小板(PLT)數值隨著「天綠元素活力滴液」處理組濃度的增加明顯地減少(表三)，表示「天綠元素活力滴液」可能會抑制血小板生成或是促進血小板代謝。

與溶劑處理組相比較，隨著「天綠元素活力滴液」作用濃度地增加，凝血酶原時間(PT)亦隨之延長，但並無統計異差(表四)。活化部份凝血活酶時間(APTT)與INR值等數值均隨著「天綠元素活力滴液」濃度增加顯著地($p<0.05$)提升(表四)，顯示「天綠元素活力滴液」確實具有抗凝血的活性。

當血小板受到各種刺激劑，如collagen等活化後，血小板表面醣蛋白會被啟動而表現到細胞表面上，並進一步與纖維蛋白質結合，使得血小板與血小板彼此凝集，形成血小板塊，此步驟被認為是血小板凝集過程中所必須的最終共同途徑。由表五所得結果可知，濃度為X/5000的「天綠元素活力滴液」對於AA或是collagen引致之血小板凝集有明顯($p<0.05$)的抑制效力，與阿斯匹靈(Aspirin)所產生的效果相當；可知「天綠元素活力滴液」具有抗血小板凝集的效果。

阿斯匹靈對照組與「天綠元素活力滴液」處理組明顯抑制血栓素之生

成，而對cAMP及cGMP皆無明顯的抑制作用（表六）；表示「天綠元素活力滴液」不影響cAMP及cGMP生成，其抑制血小板凝集與活化cAMP或cGMP無關。「天綠元素活力滴液」抑制血小板凝集及血栓形成之可能作用機轉圖請見圖五。

心血管有病的人常服用阿斯匹靈用來預防中風。阿斯匹靈的可能副作用，包括增加出血時間，特別是每天喝三杯以上的酒精飲料，或是已有出血問題，如腸胃道出血、活動性潰瘍。阿斯匹靈是藉由抑制cyclooxygenase之活性，進而抑制血栓素之形成，所以抑制了血小板凝集及血栓之形成。「天綠元素活力滴液」抑制血小板凝集及血栓之形成之作用與可能引致的副作用是否與阿斯匹靈相同，仍需進一步探討。

伍、結論

「天綠元素活力滴液」含有胺基酸/蛋白質、羥基蒽醌衍生物、黃酮類、酵類、生物鹼及有機酸等物質，可減少大鼠血小板的數目，並藉由抑制血栓素的生成干擾血小板凝集，達到抗凝血的效果。

(圖一) 生物鹼定性檢測。「天綠元素活力滴液」與碘化汞鉀試劑反應生成白色或淡黃色沉澱。

(圖二) 有機酸定性檢測。「天綠元素活力滴液」加入醋酸鉛溶液時，能生成水不溶的鉛鹽。

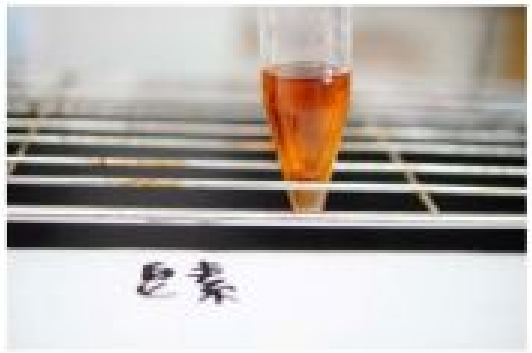

(圖三) 皂素定性檢測。「天綠元素活力滴液」放試管中激烈震搖能產生蜂窩狀泡沫 (左圖)，約維持 20 秒後泡沫即消失 (右圖)。

(圖四) 強心配醣體定性檢測。「天綠元素活力滴液」溶於微量含三氯化鐵的冰醋酸液中，加濃硫酸後二液面接觸處並不顯示棕色環。

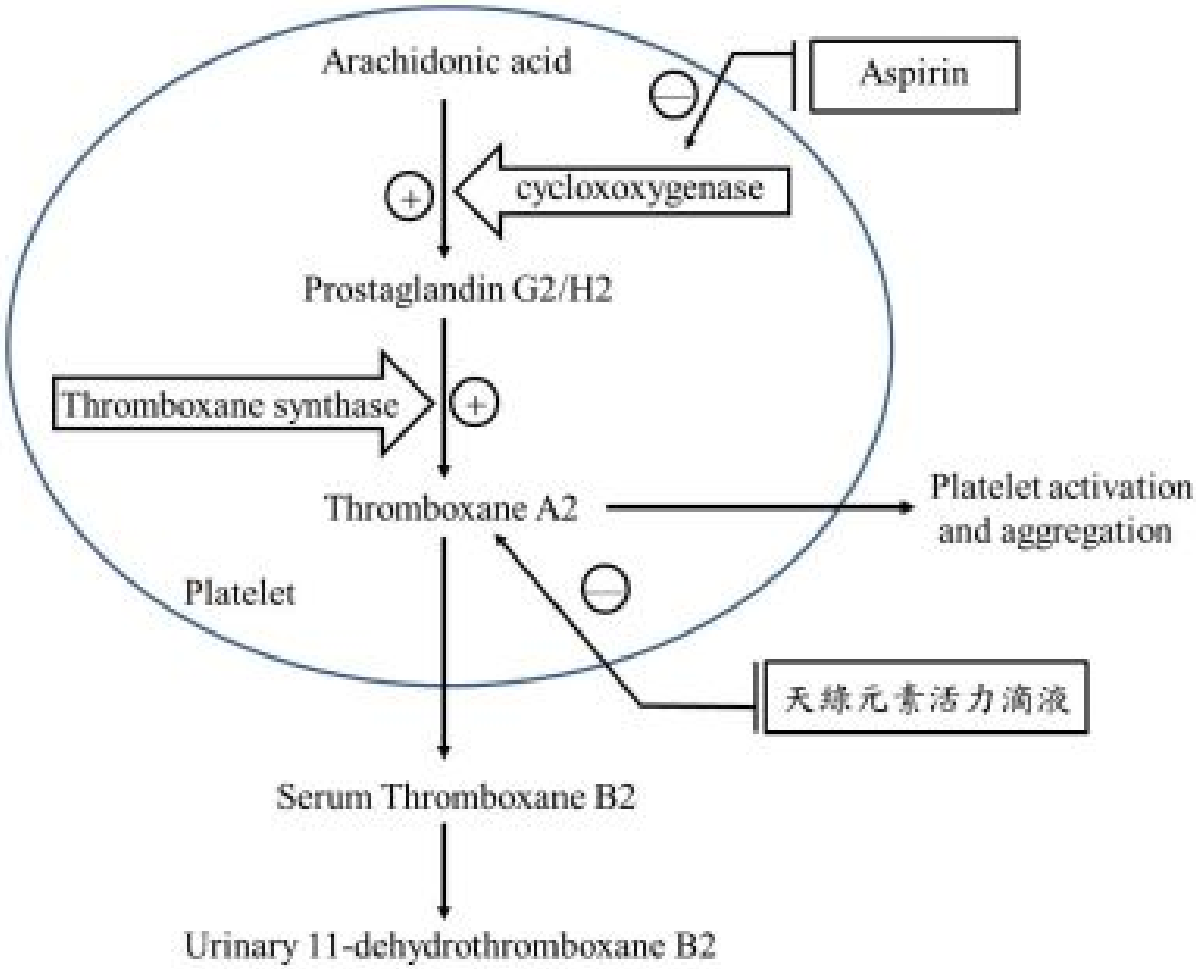

(圖五)「天绿元素活力滴液」抑制血小板凝集及血栓形成之可能作用機轉圖。

表一、天綠元素活力滴液化學成分定性檢測結果

天綠元素活力滴液							
胺基酸/蛋白質	羥基蒽醌衍生物	黃酮類	醣類	生物鹼	有機酸	皂素	強心配醣體
+	+	+	+	+	+	-	-

-:未有呈色、起泡沫或沈澱反應；+:有呈色、起泡沫或沈澱反應

表二、Wistar大鼠連續14天口服「天綠元素活力滴液」之體重與攝食、飲水的變化量

	溶劑	Asprin (10 mg/kg)	(X/5000)天綠元素活力滴液(1 ml/kg)	(X/6000)天綠元素活力滴液(1 ml/kg)	(X/7000)天綠元素活力滴液(1 ml/kg)	(X/8000)天綠元素活力滴液(1 ml/kg)
體重(g/rat)						
Week 1	315.3 ± 9.2	318.4 ± 8.7	312.4 ± 8.9	319.7 ± 9.2	319.5 ± 7.8	318.5 ± 8.8
Week 2	334.7 ± 10.3	336.9 ± 9.5	330.4 ± 9.1	339.8 ± 10.5	336.8 ± 9.4	335.4 ± 10.1
攝食量 (g/day/rat)						
Week 1	25.7 ± 3.2	26.4 ± 3.0	25.9 ± 2.8	26.2 ± 2.7	26.7 ± 3.0	26.8 ± 2.9
Week 2	29.4 ± 3.5	29.7 ± 3.1	28.8 ± 3.2	29.2 ± 3.0	30.2 ± 3.1	30.1 ± 3.2
飲水量 (ml/day/rat)						
Week 1	23.9 ± 4.1	24.1 ± 4.3	24.0 ± 3.8	24.1 ± 3.7	23.8 ± 3.9	23.9 ± 3.8
Week 2	25.2 ± 4.8	25.5 ± 4.6	25.7 ± 4.2	25.6 ± 4.0	25.5 ± 4.3	25.7 ± 4.1

溶劑處理組為口服投予1 ml/kg之RO水。

每組數據為8隻實驗動物所得結果，以mean ± S.D.表示。

天綠元素活力滴液處理組相對於溶劑處理組於同一時間點所得數據並無統計之異差。

表三、Wistar大鼠連續口服「天綠元素活力滴液」14天後之血液檢測分析值

項目	溶劑	Asprin (10 mg/kg)	(X/5000)天綠元素活力滴液(1 ml/kg)	(X/6000)天綠元素活力滴液(1 ml/kg)	(X/7000)天綠元素活力滴液(1 ml/kg)	(X/8000)天綠元素活力滴液(1 ml/kg)
RBC(10^6/μL)	7.8 ± 0.4	7.8 ± 0.4	7.7 ± 0.4	7.8 ± 0.5	7.8 ± 0.5	7.7 ± 0.4
WBC (10^3/μL)	7.6 ± 0.5	7.6 ± 0.4	7.8 ± 0.4	7.6 ± 0.5	7.7 ± 0.4	7.7 ± 0.5
Lymphocytes (10^3/μL)	7.5 ± 0.5	7.5 ± 0.5	7.4 ± 0.5	7.6 ± 0.4	7.4 ± 0.4	7.4 ± 0.5
Erythrocytes (10^6/μL)	7.4 ± 0.1	7.4 ± 0.2	7.4 ± 0.1	7.4 ± 0.1	7.4 ± 0.1	7.4 ± 0.1
HGB (g/dL)	16.3 ± 0.1	16.3 ± 0.1	16.4 ± 0.2	16.3 ± 0.2	16.4 ± 0.2	16.4 ± 0.1
Hematocrit (%)	43.2 ± 0.2	43.1 ± 0.2	43.1 ± 0.2	43.2 ± 0.3	43.4 ± 0.2	43.5 ± 0.3
MCV (fL)	52.3 ± 0.2	52.4 ± 0.3	52.3 ± 0.2	52.4 ± 0.3	52.5 ± 0.3	52.4 ± 0.2
MCH (pg)	18.4 ± 0.1	18.5 ± 0.2	18.4 ± 0.1	18.5 ± 0.1	18.6 ± 0.2	18.5 ± 0.2
MCHC (g/dL)	36.2 ± 0.2	36.1 ± 0.3	36.3 ± 0.2	36.3 ± 0.2	36.2 ± 0.3	36.2 ± 0.2
RDW (%)	12.9 ± 0.2	12.8 ± 0.3	12.7 ± 0.2	12.8 ± 0.2	12.9 ± 0.3	13.0 ± 0.3
PLT (10^3/μL)	769.6 ± 21.5	597.6 ± 21.5[b]	687.5 ± 22.5[a]	703.5 ± 23.4[a]	723.6 ± 22.8	732.6 ± 22.3
MPV (fL)	6.7 ± 0.1	6.8 ± 0.1	6.8 ± 0.1	6.7 ± 0.1	6.7 ± 0.1	6.7 ± 0.1

溶劑處理組為口服投予1 ml/kg之RO水。

每組數據為8隻實驗動物所得結果，以mean ± S.D.表示。

[a]$p<0.05$, [b]$p<0.01$相較於溶劑處理組所得數據。

表四、Wistar品系大鼠連續口服「天綠元素活力滴液」14天後之凝血數值檢測分析值

項目	溶劑	Asprin (10 mg/kg)	(X/5000)天綠元素活力滴液(1 ml/kg)	(X/6000)天綠元素活力滴液(1 ml/kg)	(X/7000)天綠元素活力滴液(1 ml/kg)	(X/8000)天綠元素活力滴液(1 ml/kg)
PT (sec)	10.32 ± 0.21	40.13 ± 0.33[b]	15.32 ± 0.14	13.62 ± 0.13	12.72 ± 0.15	11.17 ± 0.22
APTT (sec)	24.81 ± 0.52	43.21 ± 0.78[b]	39.43 ± 0.61[b]	38.45 ± 0.57[b]	37.28 ± 0.46[b]	34.56 ± 0.54[b]
INR值	0.82 ± 0.03	2.27 ± 0.63[b]	1.82 ± 0.52[b]	1.63 ± 0.4[b]	1.57 ± 0.32[a]	1.42 ± 0.37[a]

溶劑處理組為口服投予1 ml/kg之RO水。

每組數據為8隻實驗動物所得結果，以mean ± S.D.表示。

[a]$p<0.05$, [b]$p<0.01$相較於溶劑處理組所得數據。

表五、Wistar大鼠連續口服「天綠元素活力滴液」14天後對arachidonic acid(AA)或是collagen引致之血小板凝集抑制效力的評估

血小板凝集誘導劑	溶劑	Asprin (10 mg/kg)	(X/5000)天綠元素活力滴液(1 ml/kg)	(X/6000)天綠元素活力滴液(1 ml/kg)	(X/7000)天綠元素活力滴液(1 ml/kg)	(X/8000)天綠元素活力滴液(1 ml/kg)
AA（100 μM）	0[d]	89.3 ± 7.4%[b]	77.3 ± 5.7%[b]	62.4 ± 8.2%[b,c]	42.8 ± 6.7%[b,d]	36.7 ± 7.1%[b,d]
Collagen (10 μg/mL)	0[d]	92.4 ± 8.1%[b]	71.2 ± 6.3%[b,c]	59.4 ± 7.9%[b,c]	39.7 ± 5.2%[b,d]	32.4 ± 6.7%[b,d]

溶劑處理組為口服投予1 ml/kg之RO水。

每組數據為8隻實驗動物所得結果，以mean ± S.D.表示。

[a]$p<0.05$, [b]$p<0.01$相較於溶劑處理組所得數據; [c]$p<0.05$, [d]$p<0.01$相較於Asprin處理組所得數據。

表六、Wistar大鼠14天連續口服「天綠元素活力滴液」後其血小板釋出TXB_2、cAMP、cGMP之含量測定結果

分析項目	溶劑	Asprin (10 mg/kg)	(X/5000)天綠元素活力滴液(1 ml/kg)	(X/6000)天綠元素活力滴液(1 ml/kg)	(X/7000)天綠元素活力滴液(1 ml/kg)	(X/8000)天綠元素活力滴液(1 ml/kg)
TXB_2 (ng/ml)	605.5 ± 25.2^{d}	354.7 ± 22.9^{b}	$457.6 \pm 23.1^{b,c}$	$489.7 \pm 22.7^{b,c}$	578.4 ± 22.4^{d}	587.6 ± 23.2^{d}
cAMP (ng/ml)	3.2 ± 0.3	3.6 ± 0.5	3.5 ± 0.4	3.4 ± 0.2	3.3 ± 0.3	3.3 ± 0.2
cGMP (ng/ml)	2.8 ± 0.6	2.9 ± 0.4	2.8 ± 0.5	2.7 ± 0.3	2.7 ± 0.4	2.7 ± 0.4

溶劑處理組為口服投予1 ml/kg之RO水。

每組數據為8隻實驗動物所得結果，以mean ± S.D.表示。

[a]$p<0.05$, [b]$p<0.01$相較於溶劑處理組所得數據; [c]$p<0.05$, [d]$p<0.01$相較於Asprin處理組所得數據。

國立成功大學

財團法人成大研究發展基金會

研究報告

計畫名稱：「天元綠素(super green)」對於傷口癒合功效之評估

委託單位：安理科技有限公司

主　持　人：鄭瑞棠　教授

2015 年 5 月

前言

「天元綠素 (super green)」是由香蕉所抽取之產品，由安理科技公司所提供。本項液體品產品內含多種有益人體的元素，例如：鈣、鉀、鎂、等，更有微量元素的鐵、鉻、鈷、錳、等。因此，業者認為可藉由鹼性離子的提供及負離子電位的平衡來助益身體的保健。於是，推出本項產品供國人食用。

同時，業者也認為本項可能內含小分子，一些仍未解明(unknown)的物質，對於傷口修復的功能或許有所助益。於是，委託本單位先行動物的篩選評估。基於推動產學合作的理念，本單位與劉怡旻教授合作，使用了大白鼠來完成本項委託案，並將所得成果陳列於本項報告書。

壹、實驗目的

深度燒燙傷、創傷病人及糖尿病患者，其傷口特別容易遭受細菌感染，嚴重者甚至有截肢或威脅到病患生命安全之虞[1,2]。尤其老年人或糖尿病患者若遭受嚴重燒燙傷或創傷時，對其傷口的治療時，常因為組織壞死、微血管萎縮及組織灌流不足，會使傷口藥物濃度不足，以致無法控制感染的情形[1,2]。由於感染時需消耗氧氣以抑制細菌，導致組織缺氧的情形更為惡化；甚至血液循環亦受到嚴重的影響而導致糖尿病患者死亡[3]。故臨床上常以注射系統性抗生素(例如 gentamicin、penicillin 等)，並佐以局部傷口抗菌劑，以控制及治療傷口感染的情形[4]。達淨磺胺銀(silver sulfadiazine)自 1970 年上市後，至今仍是最優先選用之局部抗菌劑之一 [5]。

近年來已有報告指出以藥物誘發糖尿病之動物模式，可用來評估創傷之癒合過程與機制 [6]。使用藥物誘發動物產生糖尿病具一致性及方便性，故目前研究人員多採用此種方法，從事糖尿病及其併發症的相關研究。本試驗利用鏈佐菌素 (streptozotocin; STZ) 注射誘導的第 1 型糖尿病大鼠，採背部創

傷模式，評估廠商提供之香蕉萃取液是否有促進傷口癒合的效力，並找出最適作用濃度，冀望對糖尿病患者之創傷傷口的延遲癒合情形，能有突破性之療效。

貳、實驗材料與方法

一、實驗動物

8 週大的 Wistar 品系的雄性大鼠購自財團法人國家實驗研究院國家實驗動物中心，並飼養在本校以空調維持在室溫約 25　1℃的動物室。將部分 Wistar 雄性大鼠空腹 72 小時後，進行第 1 型糖尿病大鼠的誘導。於大鼠腹腔注射 pentobarbital 50 mg/kg，待麻醉後，經股靜脈注射 60 mg/kg streptozotocin (STZ)。於 72 小時後，抽取靜脈血，利用葡萄糖試劑，經由自動分析儀 (HITACH-7150, Japan)得知血糖值。當大鼠的血糖值大於 300 mg/dl，並有糖尿病的三多症狀出現(多吃、多喝、多尿)，即視為第 1 型糖尿病大鼠。

實驗動物之使用與操作均依據中華實驗動物學會之「實驗動物管理與使用指南」規範進行 [7]。

二、傷口癒合功效之探討

(一) 實驗敷材的配置

將廠商提供之香蕉萃取液(BE)分別稀釋成原液濃度的 1/500 (BE/500)、1/1000 (BE/1000)、1/3000 (BE/3000)與 1/6000 (BE/6000)倍。再將不同稀釋倍數的香蕉萃取液與軟膏基質(base ointment)混合製成 1%實驗軟膏。並以 4%(W/V) chlorhexidine gluconate (CG)與 1g 軟膏基質混合成軟膏製劑。另以市售 1% sulfasil (silver sulfadiazine)藥膏當為對照藥物。

(二) 傷口癒合動物實驗操作

將 STZ 糖尿病大鼠以 pentobarbital (50 mg/kg)麻醉，去除大鼠背毛，並用酒精將開傷口部位消毒，接下來在大鼠背部，分別用手術刀切除一個長及寬各 1.5 cm、厚度 0.5 cm 的皮膚；一隻大鼠開創四個傷口。

依組別貼附敷材，分別為軟膏基質、CG 軟膏、sulfasil 軟膏與不同稀釋倍數的香蕉萃取液軟膏，以繃帶包紮固定傷口，每隻大鼠均分開飼養，飼養期間供給充足的食物與水。且在皮膚切除後立即用照相機將傷口拍攝下來，之後所有的實驗鼠依組別給予治療藥物或是待評估樣品；在大鼠背部傷口開創後的第 3、7、10、15 天利用電腦軟體將傷口大小算出。

(三) 組織病理切片

術後第 15 天結束試驗，以2% Isoflurane 麻醉大鼠，經腹主動脈採血犧牲動物，取創口中心區皮膚組織之橫切面面積 0.5 cm × 2.5 cm 放入 10%的中性福馬林溶液固定 1 週，經組修及石臘包埋後製成 2 μm 厚度之組織切片，分別以蘇木精-伊紅染色（hematoxylin and eosin stain; H&E stain）及蛋白質纖維染色 (Masson's trichrome stain)方法染色，於一般光學顯微鏡下 (Opticphot-2, Nikon, Tokyo, Japan) 觀察皮膚癒合之各種組織病理變化。

H&E 染色主要判讀炎症反應(inflammation)、血管新生作用 (angiogenesis) 及表皮上皮細胞再生癒合 (re-epithelialization)等變化 [8]。蛋白質纖維染色 (Masson's trichrome stain)是一種三重的染色方式，將 collagen(膠原纖維)標的呈現為藍色，與其它組織進行區別，主要用於判讀肉芽組織形成 (granulation) 化的表現 [9]。

皮膚癒合之形態學評估項目，依據炎症反應 (inflammation) 、血管新生 (angiogenesis) 、表皮上皮細胞再生癒合(re-epithelialization)與肉芽腫 (granulation)等級予以半定量分析，請見下表 [10,11]。

(表) 大鼠皮膚創口癒合組織病理評估標準

Scores	Angiogenesis	Granulation tissue	Re-epithelialization
0, -	Absence of angiogenesis, inflammation, and hemorrhage	Absent	Absent
1, +	Altered angiogenesis (1–2 vessels per site) characterized by a edema, hemorrhage, and occasional congestion and thrombosis	Thin granular layer	Little epidermal and dermal organization
2, ++	Few newly formed capillary vessels (3–6 per site); edema and hemorrhage. Occasional congestion and intervascular fibrin deposition; absence of thrombosis	Moderate granulation layer	Moderate epidermal and dermal organization
3, +++	Newly formed capillary vessels (7–10 per site); edema and congestion.	Thick granulation layer	Complete remodeling of epidermis and dermis
4, ++++	Newly formed and well- structured capillary vessels (10 per site) vertically disposed toward the epithelium and at the wound margins.	Very thick granulation layer	

三、統計分析

實驗所得結果以平均值±標準誤差(mean ± S.E.M.)來表示，再以 analysis of variance（ANOVA）來評估兩者間差異；$P<0.05$，即為有顯著差異。

叁、結果與討論

(一) 糖尿病大鼠傷口癒合效力之探討

在 STZ 糖尿病大鼠背部傷口開創後的第 3 天，各組大鼠傷口的大小並沒有顯著的異差；如圖一所示。

相較於 sulfasil 藥膏所產生傷口癒合效力(11.4%)，在 STZ 糖尿病大鼠背部傷口開創後的第 7 天，BE/6000、BE/3000 及 BE/1000 軟膏促進傷口癒合的效力分別為 3.9、8.4 與 8.1%。BE/500 軟膏促進傷口癒合的效力甚至可達

17.6% (圖一)。

在 STZ 糖尿病大鼠背部傷口開創後的第 10 天，相較其他香蕉萃取液的稀釋組別，BE/6000 軟膏促進傷口癒合的效力最佳，達 29.3%，相當於 sulfasil 藥膏所產生的效果 (30.7%；圖一)。

在 STZ 糖尿病大鼠背部傷口開創後的第 15 天，BE/6000 軟膏促進傷口癒合的效力亦較其他香蕉萃取液的稀釋組別所產生的效果為佳，可達到 40.1%，接近 sulfasil 藥膏所產生的效果 (47.2%；圖一)。STZ 糖尿病大鼠背部傷口開創後的第 15 天其傷口大小的變化請見圖二。

由實驗結果可知，香蕉萃取液的稀釋倍數較低時於 STZ 糖尿病大鼠背部傷口開創的初期有較佳促進傷口癒合的效果；香蕉萃取液的稀釋倍數較高時於背部傷口開創的後期有較佳促進傷口癒合的效力。

在實驗期間，CG 處理的 STZ 糖尿病大鼠其背部傷口不但沒有縮小的情形，反而有惡化的趨勢；CG 並沒有促進 STZ 糖尿病大鼠背部傷口癒合的活性。

(二) 傷口組織病理切片評估

1. H&E 染色結果

在 STZ 糖尿病大鼠背部傷口開創後的第 15 天，採取傷口標本，進行 H&E 染色(100X)，結果請見圖三；各組大鼠皮膚創口組織病理半定量分析評估結果請見表一。

由 H&E 病理切片染色發現， CG 與 BE/1000 軟膏處理的傷口仍有明顯發炎的現象。相較其他香蕉萃取液的稀釋組別，BE/3000 軟膏抑制傷口發炎反應的效力最佳；sulfasil、BE/6000 與 BE/500 軟膏所產生的抗炎效力居次。

與 CG 軟膏處理的傷口相比較，sulfasil、BE/6000、BE/3000 與 BE/500 軟膏處理的傷口其血管新生的程度較為緩和，有助於發炎程度的緩解。

BE/6000 軟膏處理的傷口有表皮上皮細胞再生再生的促進作用；其他組

別的大鼠其傷口看不到有表皮上皮細胞再生的現象。

2. Masson's Trichrome 染色結果

在皮膚創傷第 15 天採取標本，進行蛋白質纖維染色，結果請見圖四；各組大鼠皮膚創口組織病理半定量分析評估結果請見表一。

因糖尿病大鼠其膠原酶較多，會分解膠原蛋白，所以糖尿病大鼠的膠原蛋白較少，以致於糖尿病大鼠受傷，傷口會延遲癒合 [12]，與其他敷膏處理的傷口相比較，BE/6000 敷膏處理的傷口有較多之膠原蛋白與肉芽腫形成組織，顯示 BE/6000 敷膏有促進傷口癒合效應。

肆、結論

香蕉萃取液稀釋製成的敷膏可降低糖尿病創傷之發炎，促進傷口膠原蛋白增生，並增進傷口癒合的發生。尤以稀釋 6000 倍的香蕉萃取液敷膏(BE/6000)處理的糖尿病大鼠，其傷口癒合表面積和上皮再生程度均優於其他組別的大鼠。顯示稀釋 6000 倍的香蕉萃取液敷膏有較佳促進糖尿病傷口癒合的效應。

伍、參考文獻

1. Jeschke MG, Finnerty CC, Shahrokhi S, Branski LK, Dibildox M. ABA Organization and Delivery ofBurn Care Committee. Wound coverage technologies in burn care: novel techniques. J Burn Care Res. 2013;34:612-20.
2. Peters EJ, Lipsky BA. Diagnosis and management of infection in the diabetic foot. Med Clin North Am. 2013;97:911-46.

3. Kim PJ, Steinberg JS. Complications of the diabetic foot. Endocrinol Metab Clin North Am. 2013;42:833-47
4. Peters EJ, Lipsky BA. Diagnosis and management of infection in the diabetic foot. Med Clin North Am. 2013 ;97:911-46.
5. Morsi NM, Abdelbary GA, Ahmed MA. Silver sulfadiazine based cubosome hydrogels for topical treatment of burns: development and in vitro/in vivo characterization. Eur J Pharm Biopharm. 2014;86:178-89.
6. Mansford KR, OPIE L. Comparison of metabolic abnormalitiesn in diabetes mellitus induced by streptozotocin or by alloxan. Lancet. 1968;1:670-1.
7. Yu J, Cheng CK, Chen BJ, Cheng MJ, Cheng HH, Chang WJ, Chen HH, Hong CC, Lee PJ, Liang SC, Sheu KS, Sung YY, Weng CN, Tsai CW, Wang CS, Wang MH, Yen LS, Yu CK, Yu YL. A Guideline for the Care and Use of Laboratory Animals. 2nd ed. Chinese Society for the Laboratory Animal Science. Taipei. 2005; 207 pp. (in Chinese)
8. Chan JK. The wonderful colors of the hematoxylin-eosin stain in diagnostic surgical pathology. Int J Surg Pathol. 2014;22:12-32.
9. Linos K, Sedivcová M, Cerna K, Sima R, Kazakov DV, Nazeer T, Glazyrin A, Valerian BT, Carlson JA. Extra nuchal-type fibroma associated with elastosis, traumatic neuroma, a rare APC gene missense mutation, and a very rare MUTYH gene polymorphism: a case report and review of the literature. J Cutan Pathol. 2011;38:911-8.
10. Altavilla D, Saitta A, Cucinotta D, Galeano M, Deodato B, Colonna M, Torre V, Russo G, Sardella A, Urna G, Campo GM, Cavallari V, Squadrito G, Squadrito F. Inhibition of lipid peroxidation restores impaired vascular endothelial growth factor expression and stimulates wound healing and angiogenesis in the genetically diabetic mouse. Diabetes. 2001;50:667-74.
11. Altavilla D, Galeano M, Bitto A, Minutoli L, Squadrito G, Seminara P, Venuti FS, Torre V, Calò M, Colonna M, Lo Cascio P, Giugliano G, Scuderi N, Mioni C,Leone S, Squadrito F. Lipid peroxidation inhibition

by raxofelast improves angiogenesis and wound healing in experimental burn wound. Shock. 2005;24: 85-91.

12. Ramamurthy NS, Kucine AJ, McClain SA, McNamara TF, Golub LM. Topically applied CMT-2 enhances wound healing in streptozotocin diabetic rat skin. Adv Dent Res. 1998;12:144-8.

(表一) 各組糖尿病大鼠皮膚創口組織病理半定量分析評估結果

Treatments	STZ-diabetic rats			
	Inflammation	Angiogenesis	Granulation	Re-epithelialization
Blank	+++	++	+	-
CG	+++	+++	+	-
sulfasil	++	+	++	-
BE/6000	++	+	++	+
BE/3000	+	+	+	-
BE/1000	+++	++	+	-
BE/500	++	+	+	-

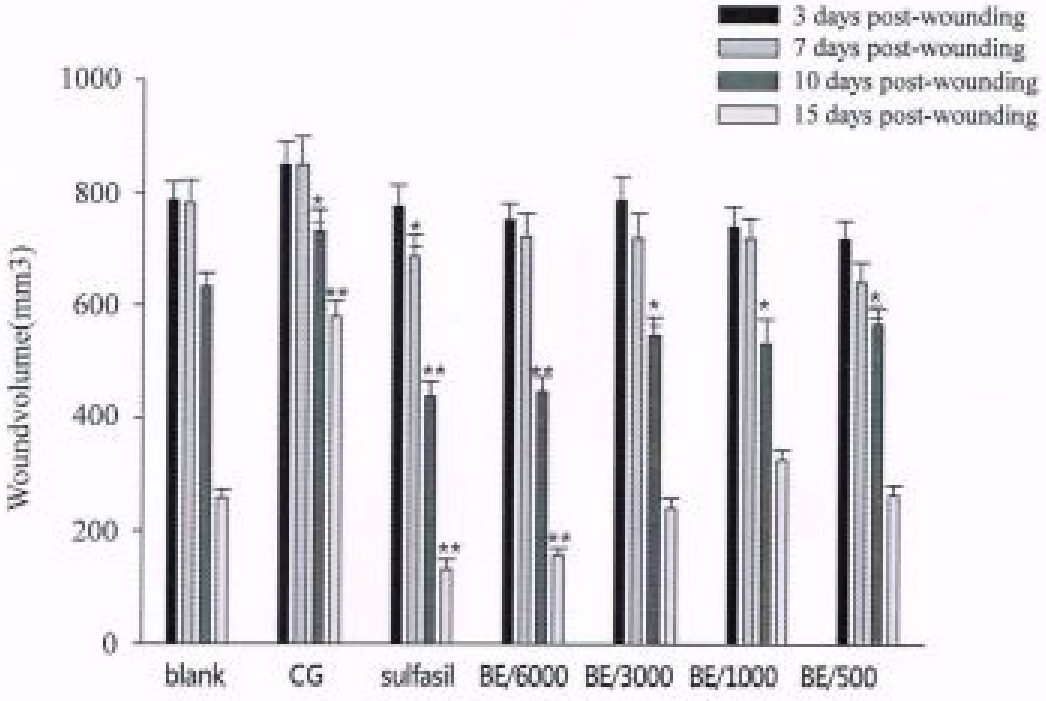

(圖一) STZ 糖尿病大鼠分別處理軟膏基質、CG 軟膏、sulfasil 軟膏與不同稀釋倍數的香蕉萃取液軟膏，於背部傷口開創後不同時間點傷口大小的變化。每組數據為 6 隻大鼠所得平均值，以 mean ± S.E.M. 表示。*P<0.05, **P<0.01 相較處理基質軟膏的動物於同一時間點所得數據 (blank)。

軟膏基質　　CG 軟膏　　sulfasil 軟膏

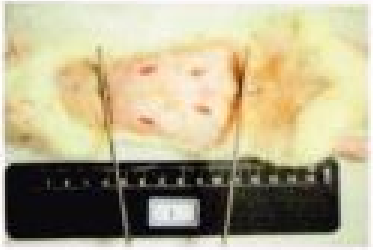

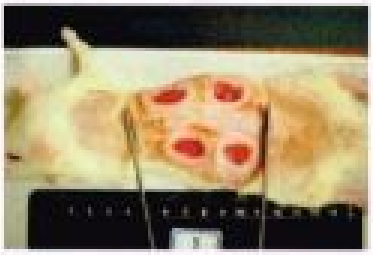

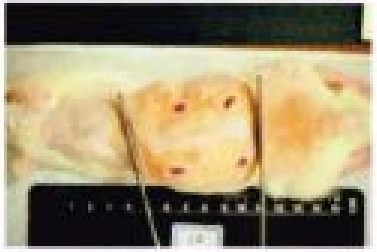

BE/6000 軟膏　　BE/3000 軟膏　　BE/1000 軟膏　　BE/500 軟膏

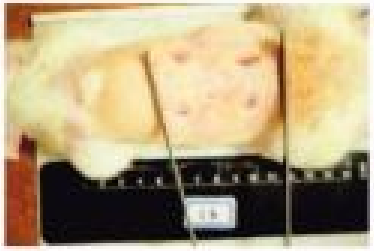

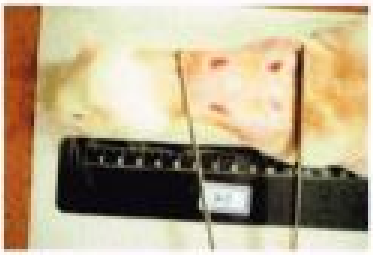

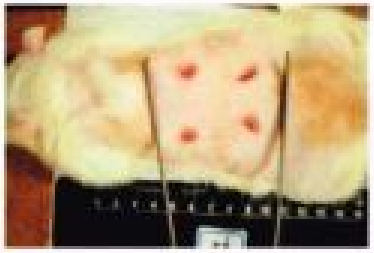

(圖二) STZ 糖尿病大鼠分別處理軟膏基質、CG 軟膏、sulfasil 軟膏與不同稀釋倍數的香蕉萃取液軟膏，於背部傷口開創後第 15 天傷口大小的變化。

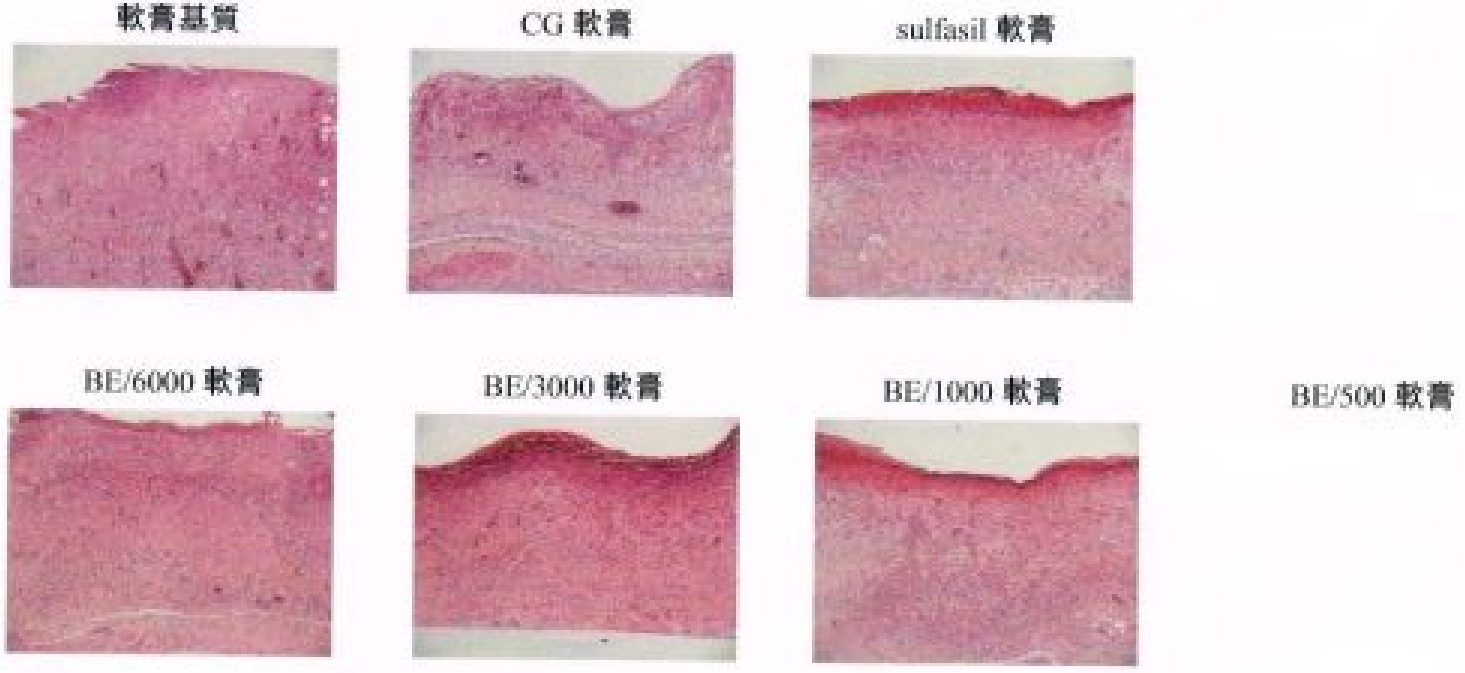

(圖三) STZ 糖尿病大鼠分別處理軟膏基質、CG 軟膏、sulfasil 軟膏與不同稀釋倍數的香蕉萃取液軟膏，於背部傷口開創後第 15 天，傷口組織進行蘇木精-伊紅染色 (100X)的結果。

軟膏基質

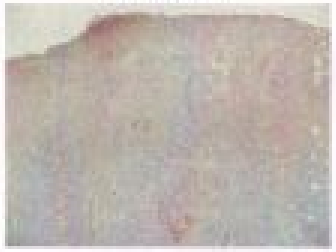

CG 軟膏

sulfasil 軟膏

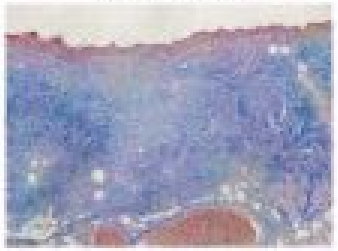

BE/6000 軟膏

BE/3000 軟膏

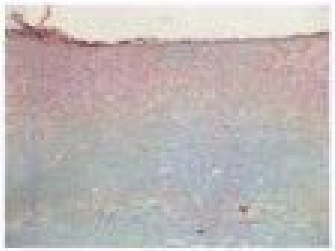

BE/1000 軟膏

BE/500 軟膏

(圖四) STZ 糖尿病大鼠分別處理軟膏基質、CG 軟膏、sulfasil 軟膏與不同稀釋倍數的香蕉萃取液軟膏，於背部傷口開創後第 15 天，創口癒合之肉芽腫形成組織病理切片圖(100X)。

四、其他

(一) 美国 Manufacturer_FDA Certification

2021

CERTIFICATE OF REGISTRATION

This certifies that:

Nutritional Supplement Manufacturers Inc
1055 Bay Blvd Ste D
Chula Vista, CA 91911-1628
United States

is registered with the U.S. Food and Drug Administration pursuant to the Federal Food Drug and Cosmetic Act, as amended by the Bioterrorism Act of 2002 and the FDA Food Safety Modernization Act, such registration having been verified as currently effective on the date hereof by Registrar Corp.

U.S. FDA Registration No.:	13686401166
U.S. Registration Agent:	**Registrar Corp** 144 Research Drive, Hampton, Virginia, 23666, USA Telephone: +1-757-224-0177 • Fax: +1-757-224-0179

This certificate affirms that the above named facility is registered with the U.S. Food and Drug Administration pursuant to the Federal Food Drug and Cosmetic Act, as amended by the Bioterrorism Act of 2002 and the FDA Food Safety Modernization Act, such registration having been verified as effective by Registrar Corp as of the date hereof, and Registrar Corp will confirm that such registration remains effective upon request and presentation of this certificate until December 31, 2021, unless such registration has been terminated after issuance of this certificate. Registrar Corp makes no other representations or warranties, nor does this certificate make any representations or warranties to any person or entity other than the named certificate holder for whose sole benefit it is issued. Registrar Corp assumes no liability to any person or entity in connection with the foregoing. The U.S. Food and Drug Administration does not issue a certificate of registration, nor does the U.S. Food and Drug Administration recognize a certificate of registration. Registrar Corp is not affiliated with the U.S. Food and Drug Administration.

Registrar Corp
144 Research Drive, Hampton, Virginia, 23666, USA
Telephone: +1-757-224-0177 • Fax: +1-757-224-0179
info@registrarcorp.com • www.registrarcorp.com

David Lashway
Executive Director
Registrar Corp
Dated: December 18, 2020

© Copyright 2001-2020 Registrar Corp

(二) 美国 Certificate Of Free Sale

Certificate Unique ID: EFA2-H7H6

October 28, 2020

TO WHOM IT MAY CONCERN:

We have reviewed correspondence on behalf of:

Super Green Biotech
19925 Stevens Creek Blvd Ste 100
Cupertino, CA 95014

concerning the status of:

Super Green High Energy Drop Drink (30ml per bottle)

This product is regulated by the Food and Drug Administration (FDA) pursuant to the requirements of the Federal Food, Drug, and Cosmetic Act (FD&C Act) and the Fair Packaging and Labeling Act (FPLA) and other related laws.

The Food and Drug Administration does not have statutory authority to approve any food or any food manufacturer or distributor of such products.

The above referenced product is under the jurisdiction of the Food and Drug Administration which has primary responsibility for the administration and enforcement of the FD&C Act and the FPLA and other related laws. We have not examined the specific product being offered for export or reviewed the label. Under the FD&C Act, such a product may be exported if:

1. It is not adulterated or misbranded and it meets the other requirements of the FD&C Act for marketing in the U.S.; or

2. It cannot be lawfully marketed in the U.S. but meets the requirements of section 801(e) of the FD&C Act (21 U.S.C. 381(e)).

Sincerely yours,

Haijing Hu, Ph.D.
Director, Regulatory Implementation Staff
Office of Dietary Supplement Programs
Center for Food Safety and Applied Nutrition
U.S. Food and Drug Administration

Certificate Unique ID: 9GKG-H2M9

CERTIFICATE OF FREE SALE

1. Pursuant to the Provisions of Rule 44 of the Federal Rules of Civil Procedure, I hereby certify that the attached letter (and product list, if applicable), as described below, is a true copy of material on file in the Food and Drug Administration, Department of Health and Human Services and is a part of the official records of said Administration and Department.

Attachment Dated
October 28, 2020
To Whom It May Concern
Regarding
Super Green High Energy Drop Drink (30ml per bottle)

Super Green Biotech, 10925 Stevens Creek Blvd Ste 100, Cupertino, CA 95014

2. In witness whereof, I have pursuant to the provisions of Title 42, United States Code, Section 3585, and the authority delegated by the Commissioner of Food and Drugs, hereto set my hand and cause the seal of the Department of Health and Human Services to be affixed this 28th day of October, 2020.

Haijing Hu, Ph.D.
Director, Regulatory Implementation Staff
Office of Dietary Supplement Programs
Center for Food Safety and Applied Nutrition
By direction of the Secretary of Health and Human Services

THIS CERTIFICATE EXPIRES: October 28, 2022.

（三）美国 MSDS-Transportation Guidelines

MSDS – Super Green Drop Drink

Identification of The Substance and Supplier

Identification of The Product	Super Green Drop Drink is a natural product prepared by the extracting freshly fruits from Musa Paradisiaca Banana Trees.
Trade Name	Super Green Drop Drink – SGDD.
References	FDA standard of identity 21 CFR 146.146 and USDA grading standard, 7 CFR 52.1551.
Type of Product and Usage	Paradisiaca Banana Extract is ready to be diluted into any beverage or liquid food as a dietary supplement.
Company Identification	Super Green Biotech Corporation 19925 Stevens Creeks Blvd, Suite 100 Cupertino, CA 95014
Emergency Telephone	North America: 800-424-9300 (Chemtrek) International: 703-527-3887 (Call Collect)
General Information Telephone	+1-415-326-9986

Hazards Identification

General	The main hazard associated with this product is its mild alkalinity, due to the content of naturally occurring potassium from banana extract.
EU Hazard Designation	Xi Irritant (Category 2B - Mild Irritant)

EU Hazard Classification	R36 Irritating to eyes.
GHS Classification	Eye irritant Category 2B.
GHS Label Elements	Signal Word: Warning. H320 – Cause eye irritation.
Prevention	P262 – Do not get in eyes. P264 – Wash thoroughly after handling. P280 – Wear eye protection.
Response	P305+P351+P338 – IF IN EYES: Immediately rinse continuously with water for several minutes. Quick but gently remove contact lenses if present. Continue rinsing.
Disposal	P501 – Dispose of contents/container in accordance with local, regional, national, and international regulations.

Composition/Information on Ingredients

Substance/Preparation **Substance**

Ingredient Name	WT%	CAS No.	EINECS No.	GHS Hazard Code
Concentrated Banana Extraction	100%	none	not listed	Xi (see also Sec. 15)

The above product is considered to be a "food" as defined in the Federal Food, Drug and Cosmetic Act (21 U.S.C. 201 (f)).

First Aid Measures

After Eye Contact	Remove any contact lenses at once. Flush eyes well with generous quantities of water for at least 5 minutes. Seek medical attention if symptoms persist.

Firefighting Measures

Extinguishing Media	Substance is nonflammable, use agent most appropriate to extinguish surrounding fire.
Special Exposure Hazards	When heated to dryness and decomposition under fire conditions, this product may release carbon monoxide, carbon dioxide, and other decomposition products of undetermined hazard.
Protect Against Fire	As with any fire situation, full face, self-contained breathing apparatus and appropriate protective clothing should be worn.

Accidental Release Measures

After Spillage / Leakage	Absorb spillage on suitable inert media and place in closed container. Safety glasses with side guards should be worn to prevent injury from flying particles and/or other eye contact with this product.
Waste Handling, Disposal	Dispose of absorbed spillage according to local regulations.
Environmental Precautions	The product is not toxic. Small spills may be easily flushed with water.

Handling and Storage

Handling	Avoid eye and skin contact. Protect against physical damage to containers. As with all semi-finished materials, prudent industrial practices should be employed to minimize contact with eyes.
Storage	Store at 2°C to 30°C (36°F – 140°F) to prevent spoilage and maintain freshness.

Exposure Controls/Personal Protection

Ingredients with Limit Values	This product does not contain any ingredients with critical values that need to be monitored in the workplace.
Personal Protection	Respiratory protection: Not required. Skin Protection: Use skin protection appropriate to the conditions of use. Hand Protection: Wear suitable gloves resistant to chemical penetration. Eye Protection: Safety glasses with side guards should be worn to prevent injury from flying droplets and/or other eye contact with this product.

Physical and Chemical Properties

Appearance	Physical state: Viscous liquid Color: Yellowish Odor: Fresh-cut mushroom
Physical Data	Initial boiling point: not applicable. Apparent Density at 20° C (kg/L): 1.3 Solubility: well soluble in water. Solution is clear and little yellowish. pH value: > 9 Flash point: not applicable.

Stability and Reactivity

Chemical Stability	Stable
Hazardous Polymerization	Will not occur.

Toxicological Information

Potential Acute Health Effects	Skin contact: No irritant effect. Eye contact: May cause eye irritation. Inhalation: No irritant effect.

Acute Toxicity	RTECS ®: Banana Extract --Not listed Irritation Data: Not available Tumorigenic Effects Data: Not available.
Over-Exposure Signs/Symptoms	Eye: Adverse symptoms: irritation, redness.

Ecological Information

Environmental Effects	No specific information or data.

Disposal Considerations

Disposal	May be harmful to the environment if released in generous quantities. Inform appropriate authorities if entry of spillage into sewers/water courses cannot be prevented. This product should be handled in accordance with instructions given under Sections 6, 7 and 8. Collect larger spills and dispose of in accordance with National and Local laws. Disposal of surplus product via a licensed waste disposal contractor only.
Disposal Precautions	No special precautions

Transportation Information

General	US DOT — Not regulated as a hazardous material.
Marine pollutant	No

Regulatory Information

Inventory Status	Not listed on TSCA , not listed EINECS/ELINCS.
U.S. Regulations	OSHA—permissible exposure limit not listed US FDA: Generally Recognized As Safe (GRAS) U.S. Superfund Amendments and Reauthorization Act (SARA) Title III: This product is not listed in SARA 313 Toxic Release Chemicals.
EU Risk(R), Safety(S)	Xi – Irritant R 36- Irritating to the eyes. S 24/25 - Avoid contact with skin and eyes. S 26 - In case of contact with eyes, rinse immediately with plenty of water and seek medical advice. S 37/39 - Wear suitable gloves and eye/face protection.

Other Information

The contents of this MSDS are written by the manufacturer, Super Green Biotech Corporation, in accordance with the UN Globally Harmonized System of Classification and Labeling of Chemicals (GHS) and with reference to the requirements of EC Commission Directive EU 1272/2008

While The Company believes that the data contained herein are factual, the data are not to be taken as a warranty or representation for which The Company assumes legal responsibility. They are offered solely for your consideration, investigation, and verification. Any of these data and information must be determined by the user to be in accordance with applicable National and Local Laws and Regulations. Super Green Biotech Corporation makes no warranty of any kind, express or implied, concerning the safe use of this material in your process or in combination with other substances.